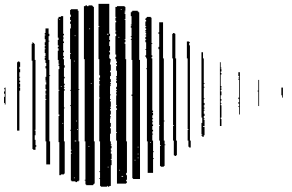

NATIONAL CENTER FOR EARTHQUAKE ENGINEERING RESEARCH

State University of New York at Buffalo

Active Bracing System: A Full Scale Implementation of Active Control

by

A. M. Reinhorn, T. T. Soong, R. C. Lin and M. A. Riley

Department of Civil Engineering
State University of New York at Buffalo
Buffalo, New York 14260

Y. P. Wang

Department of Civil Engineering
Chung-Hwa Polytechnic Institute
Hsin-Chu
Taiwan

and

S. Aizawa and M. Higashino

Technical Research Laboratory
Takenaka Corporation
2-5-14 Minamisuna Koto-Ku
Tokyo 136
Japan

Technical Report NCEER-92-0020

August 14, 1992

This research was conducted at the State University of New York at Buffalo, Chung-Hwa Polytechnic Institute, and Takenaka Corp., and was partially supported by the National Science Foundation under Grant No. BCS 90-25010 and the New York State Science and Technology Foundation under Grant No. NEC-91029.

NOTICE

This report was prepared by the State University of New York at Buffalo, Chung-Hwa Polytechnic Institute, and Takenaka Corp. as a result of research sponsored by the National Center for Earthquake Engineering Research (NCEER) through grants from the National Science Foundation, the New York State Science and Technology Foundation, and other sponsors. Neither NCEER, associates of NCEER, its sponsors, the State University of New York at Buffalo, Chung-Hwa Polytechnic Institute, and Takenaka Corp., nor any person acting on their behalf:

a. makes any warranty, express or implied, with respect to the use of any information, apparatus, method, or process disclosed in this report or that such use may not infringe upon privately owned rights; or

b. assumes any liabilities of whatsoever kind with respect to the use of, or the damage resulting from the use of, any information, apparatus, method or process disclosed in this report.

Any opinions, findings, and conclusions or recommendations expressed in this publication are those of the author(s) and do not necessarily reflect the views of the National Science Foundation, the New York State Science and Technology Foundation, or other sponsors.

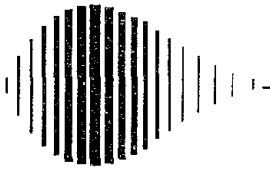

Active Bracing System:
A Full Scale Implementation of Active Control

by

A.M. Reinhorn[1], T.T. Soong[2], R.C. Lin[3], M.A. Riley[4],
Y.P. Wang[5], S. Aizawa[6] and M. Higashino[7]

August 14, 1992

Technical Report NCEER-92-0020

NCEER Project Numbers 89-2201, 90-2201 and 91-5121

NSF Master Contract Number BCS 90-25010
and
NYSSTF Grant Number NEC-91029

1 Professor, Department of Civil Engineering, State University of New York at Buffalo
2 Samuel P. Capen Professor, Department of Civil Engineering, State University of New York at Buffalo
3 Research Associate, Department of Civil Engineering, State University of New York at Buffalo
4 Graduate Research Assistant, Department of Civil Engineering, State University of New York at Buffalo
5 Associate Professor, Department of Civil Engineering, Chung-Hwa Polytechnic Institute, Hsin-Chu, Taiwan, R.O.C.
6 Senior Research Engineer, Technical Research Laboratory, Takenaka Corp., Tokyo, Japan
7 Research Engineer, Technical Research Laboratory, Takenaka Corp., Tokyo, Japan

NATIONAL CENTER FOR EARTHQUAKE ENGINEERING RESEARCH
State University of New York at Buffalo
Red Jacket Quadrangle, Buffalo, NY 14261

PREFACE

The National Center for Earthquake Engineering Research (NCEER) was established to expand and disseminate knowledge about earthquakes, improve earthquake-resistant design, and implement seismic hazard mitigation procedures to minimize loss of lives and property. The emphasis is on structures in the eastern and central United States and lifelines throughout the country that are found in zones of low, moderate, and high seismicity.

NCEER's research and implementation plan in years six through ten (1991-1996) comprises four interlocked elements, as shown in the figure below. Element I, Basic Research, is carried out to support projects in the Applied Research area. Element II, Applied Research, is the major focus of work for years six through ten. Element III, Demonstration Projects, have been planned to support Applied Research projects, and will be either case studies or regional studies. Element IV, Implementation, will result from activity in the four Applied Research projects, and from Demonstration Projects.

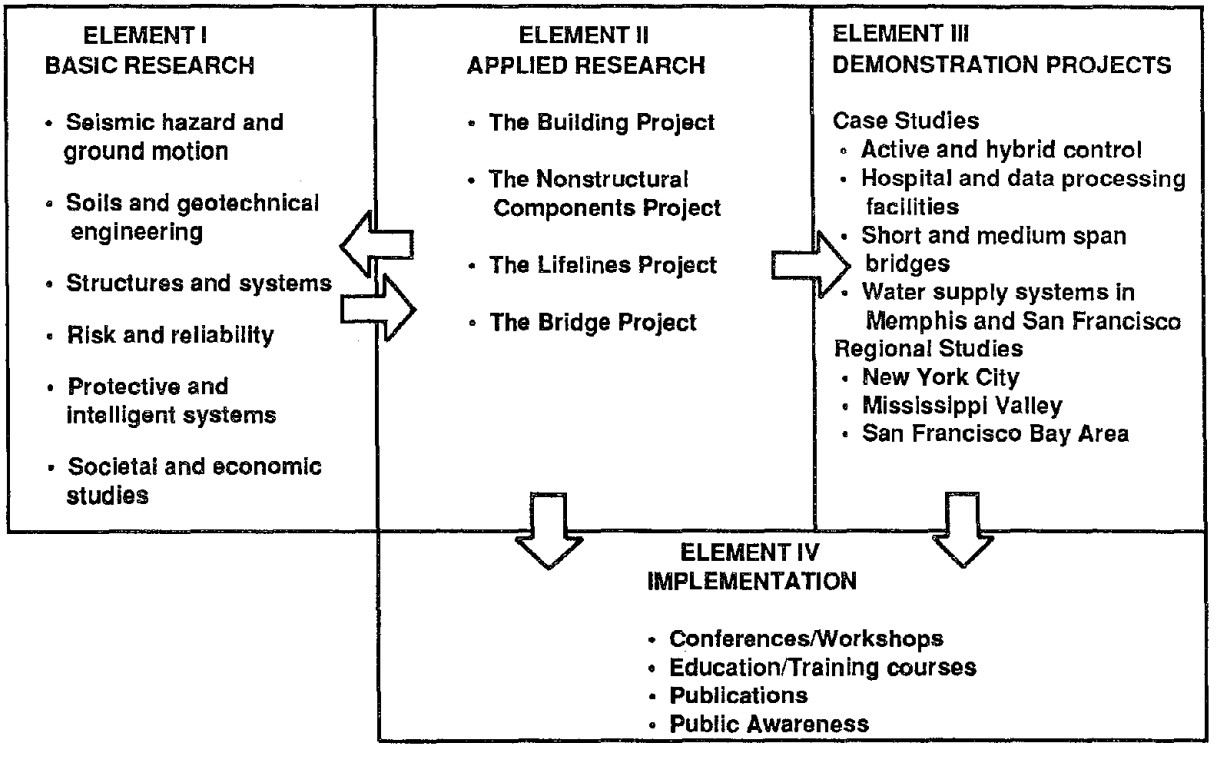

Research in the **Building Project** focuses on the evaluation and retrofit of buildings in regions of moderate seismicity. Emphasis is on lightly reinforced concrete buildings, steel semi-rigid frames, and masonry walls or infills. The research involves small- and medium-scale shake table tests and full-scale component tests at several institutions. In a parallel effort, analytical models and computer programs are being developed to aid in the prediction of the response of these buildings to various types of ground motion.

Two of the short-term products of the **Building Project** will be a monograph on the evaluation of lightly reinforced concrete buildings and a state-of-the-art report on unreinforced masonry.

The **protective and intelligent systems program** constitutes one of the important areas of research in the **Building Project**. Current tasks include the following:

1. Evaluate the performance of full-scale active bracing and active mass dampers already in place in terms of performance, power requirements, maintenance, reliability and cost.
2. Compare passive and active control strategies in terms of structural type, degree of effectiveness, cost and long-term reliability.
3. Perform fundamental studies of hybrid control.
4. Develop and test hybrid control systems.

NCEER's research efforts in the active control area has led to the development of a full-scale active bracing system, which was installed in an experimental structure in Tokyo. This report describes design, fabrication, and operational aspects of this system, together with its observed performance under three actual earthquakes and other artificial loadings. We note that, while several active mass dampers have been implemented in full-scale structures over the last few years, the active bracing system described here represents the first full-scale active system of this type developed and tested under actual ground motions. The experience gained through the development of this system can serve as an invaluable resource for the development of active structural control systems in the future.

ABSTRACT

An active bracing system has been designed, fabricated, and installed in a full-scale dedicated test structure for structural response control under seismic loads. This report presents (i) a description of the constructed system, (ii) design specifications for the control system along with simulation studies for the design earthquake, and (iii) observed performance of the system under three actual earthquakes and other artificial loadings. Detailed design and analysis of the active system are carried out with respect to hardware development, control force constraints, and power and energy requirements. It is shown that a full-scale efficient active structural control system can be developed within limits of current technology. Simulation results provide information on performance bounds that can be expected of active systems in structural control under seismic loads and under constraints imposed by practical considerations. Installation details of the system in the building structure are presented along with the selections for fail-safe shutdown operations in case of malfunctions. Also presented are the procedures for proper maintenance and self testing which ensure continuous control with minimal resources. The observed performance under artificial loadings and actual ground motions is compared with the estimated analytical response. It is shown that the performance of the active bracing system is predictable by simple analytical procedures and efficient within the design limitations.

ACKNOWLEDGEMENTS

This work is a product of a series of analytical and experimental research projects which began in 1980, funded by the National Science Foundation. This continuing support is gratefully acknowledged. The full-scale development phase was supported in part by the National Center for Earthquake Engineering Research, Grant Nos. NCEER-89-2201, NCEER-90-2201, and NCEER-91-5121.

Industrial participation and contributions were also important to the success of this research effort. It is a pleasure to acknowledge support received from the MTS Systems Corporation, the Takenaka Corporation, and Kayaba Industry, Ltd.

Special acknowledgements are due to many engineers and technicians who assisted and dedicatedly developed many components of the system. Among those it is a pleasure to acknowledge the major assistance of Mr. Mark Pitman, Mr. Daniel Walsh, Mr. Xiao-Qing Gao (SUNY/Buffalo), Mr. Niel Peterson (MTS Corp.), and Mr. Haniuda (Kayaba Industries).

TABLE OF CONTENTS

SECTION	TITLE	PAGE
1	**INTRODUCTION**	1-1
2	**TEST STRUCTURE AND ACTIVE BRACING SYSTEM**	2-1
2.1	Full-Scale Test Structure	2-1
2.2	Active Bracing System (ABS)	2-1
2.2.1	Braces	2-7
2.2.2	Hydraulic actuators	2-7
2.2.3	Hydraulic power supply	2-12
2.3	Analog/Digital Controller	2-15
2.4	Digital Microcomputer	2-15
2.5	Sensors	2-17
3	**CONTROL ALGORITHM DEVELOPMENT**	3-1
3.1	Basic Considerations	3-1
3.2	Velocity Feedback with Observer	3-4
3.3	Three-Velocity Feedback Control	3-10
3.4	Time Delay	3-12
4	**DESIGN OF ACTIVE CONTROL**	4-1
4.1	Design Earthquakes	4-1
4.2	Analysis and Design	4-1
4.2.1	Determination of weighting factor β	4-1
4.2.2	Design of passive power resource	4-3
4.3	Verification	4-5
4.4	Power and Energy	4-5
5	**EXPERIMENTAL STUDY**	5-1
5.1	Control Algorithm	5-1
5.2	Automatic Control Operation	5-1
5.3	System Reliability and Maintenance	5-2
5.4	Control Software	5-3
6	**SYSTEM PERFORMANCE**	6-1
6.1	Identification of Dynamic Properties	6-1
6.2	Free and Forced Vibration Response	6-2
6.3	Response to Earthquakes	6-2
7	**ANALYTICAL PREDICTION OF OBSERVED RESPONSE**	7-1

TABLE OF CONTENTS (cont.)

SECTION	TITLE	PAGE
8	COMPARISON OF PERFORMANCES OF ABS AND AMD	8-1
9	CONCLUDING REMARKS	9-1
10	REFERENCES	10-1
	APPENDIX I	A-1

LIST OF FIGURES

FIGURE	TITLE	PAGE
1.1	Experimental Stages of Active Bracing Control	1-2
2.1	View of Building	2-2
2.2	Configuration of Active Bracing System (a) Side View; (b) Top View	2-3
2.3	Active Brace System	2-4
2.4	Details of First Story Active Braces	2-5
2.5	Block Diagram of Control System	2-6
2.6	Member of Active Brace	2-8
2.7	Joint Configuration of Active Brace	2-9
2.8	Actuator and Connected with Brace	2-10
2.9	A Set of Actuators with a Servovalve	2-11
2.10	Details of Control System for Active Bracing System	2-13
2.11	Manifold and Accumulators	2-14
2.12	Digital Microcomputer System	2-16
2.13	Servovelocity Seismometer	2-18
2.14	LVDT Installed Actuator	2-19
3.1	Control Parameters as Functions of (β)	3-7
3.2	Structural Response Under 32% El Centro Earthquake $(\beta = 4)$	3-8

LIST OF FIGURES (cont.)

FIGURE	TITLE	PAGE
3.3	Control Requirements Under 32% El Centrol Earthquake ($\beta = 4$)	3-9
4.1	Cumulative Oil Flow During 32% El Centro Earthquake	4-4
5.1	Block Diagram of Control System Software	5-5
6.1	Typical Acceleration of AMD During Harmonic Loading Tests	6-6
6.2	Sixth Floor Response During Harmonic Loading Tests	6-7
6.3	Ground Accelerations During Earthquakes	6-8
6.4	Comparison of Controlled (Observed) vs. Uncontrolled (Estimated Responses	6-9
6.5	Acceleration Transfer Functions With and Without Active Braces	6-11
7.1	Comparison of Analytical and Observed Responses During Harmonic Loading Tests	7-2
7.2	Comparison of Analytical and Observed Responses During April 14 Earthquake	7-3
8.1	Full-Scale AMD	8-2
8.2	Observation Results of AMD	8-3
8.3	Acceleration Transfer Functions With and Without Active Mass Damper (From Aizawa et al, 1990)	8-4

LIST OF TABLES

TABLE	TITLE	PAGE
3.1	Performance Comparisons with Different Control Algorithms	3-11
4.1	Design Earthquakes	4-2
4.2	Summary of Response Analysis Under Design Earthquakes ($\beta = 4$)	4-6
5.1	Control System Software	5-6
6.1	Uncontrolled Dynamic Properties of Structure	6-2
6.2	Characteristics of Harmonic Loading Tests	6-4
6.3	Peak and RMS Response During Earthquakes	6-5
8.1	Comparison of AMD and ABS	8-1
A1	Actual Earthquakes During the Operation Period of ABS	A-1

SECTION 1

INTRODUCTION

The possible use of active control systems as a means of structural protection against seismic loads has received considerable attention in recent years. It has now reached the stage where active systems have been installed in full-scale structures (Soong 1990). The focus of this report is on the development of an active bracing system and it's implementation to a full-scale dedicated test structure whose performance could be assessed under actual ground motions.

Active control using structural braces and tendons has been one of the most studied control mechanisms. Systems of this type generally consist of a set of prestressed tendons or braces connected to a structure, their tensions being controlled by electrohydraulic servomechanisms. One of the reasons for favoring such a control mechanism has to do with the fact that tendons and braces are already existing members of many structures. Thus, active bracing control can make use of existing structural members and thus minimize extensive additions or modifications of an as-built structure. This is attractive, for example, in the case of retrofitting or strengthening an existing structure.

Active tendon control has been studied analytically in connection with control of slender structures, tall buildings, bridges and offshore structures. Early experiments involving the use of tendons were performed on a series of small-scale structural models (Roorda 1980), which included a simple cantilever beam, a king-post truss and a free-standing column while control devices varied from tendon control with manual operation to tendon control with servo-controlled actuators.

More recently, a comprehensive experimental program was designed and carried out in order to study the feasibility of active bracing control using a series of carefully calibrated structural models. As Fig. 1.1 shows, the model structures increased in weight and

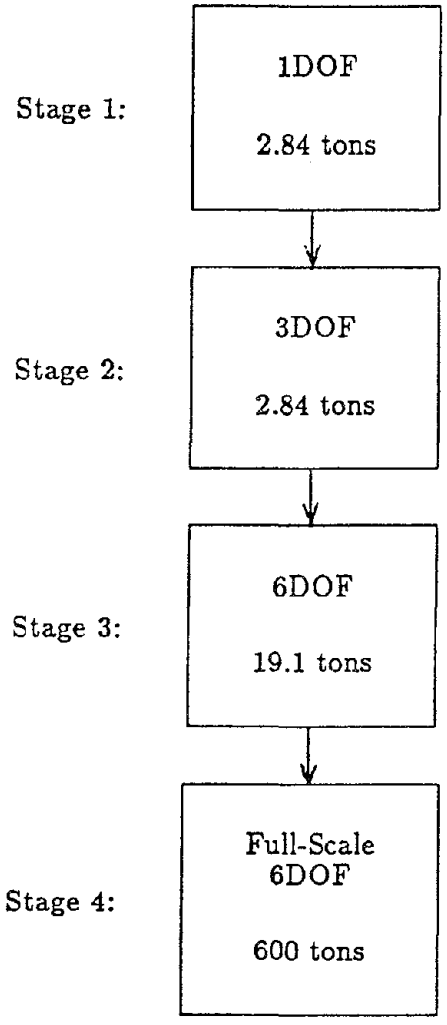

Fig. 1.1 Experimental Stages of Active Bracing Control

complexity as the experiments progressed from Stage 1 to Stage 3 so that more control features could be incorporated into the experiments. At Stages 1 and 2, the model structure was a three-story steel frame modeling a shear building by the method of mass simulation. At Stage 1, the top two floors were rigidly braced to simulate a single-degree-of-freedom system. The model was mounted on a shaking table which supplied the external load and the control force was transmitted to the structure through two sets of diagonal prestressed tendons mounted on the side frames.

Results obtained from this series of experiments are reported in (Chung et al. 1988, Chung et al. 1989). Several significant features of these experiments are noteworthy. First, they were carefully designed in order that realistic structural control situations could be investigated. Efforts made towards this goal included making the model structure dynamically similar to a real structure, working with a carefully calibrated model, using realistic base excitation, and requiring more realistic control force. Secondly, these experiments permitted a realistic comparison between analytical and experimental results, which made it possible to perform extrapolation to real structural behavior. Furthermore, important practical considerations such as time delay, robustness of control algorithms, modeling errors and structure-control system interactions could be identified and realistically assessed.

Experimental results show significant reduction of structural motion under the action of the simple tendon system. In the single-degree-of-freedom system case, for example, a reduction of over 50% of the first-floor maximum relative displacement could be achieved. This is due to the fact that the control system was able to induce damping in the system from a damping ratio of 1.24% in the uncontrolled case to 34.0% in the controlled case (Chung et al. 1988).

As a further step in this direction, a substantially larger and heavier six-story model structure was fabricated for Stage 3. It was also a welded space frame utilizing artificial mass simulation, weighing 19.1 metric tons and standing 5.5 m in height. In this series of experiments, multiple tendon control was possible and the results again show that simple tendon arrangements can produce significant motion reduction under simulated earthquake excitations (Reinhorn et al. 1989).

Another added feature at this stage was the testing of a second control system, an active mass damper, on the same model structure, thus allowing a performance comparison of these two systems. Furthermore, control requirements and control efficiencies realized in this series of experiments were extrapolated to the full-scale case, leading to a preliminary design of the full-scale active bracing system for Stage 4. The feasibility of implementation was analyzed, followed by the design and simulation study in order to assess its performance capabilities when installed in an actual structure (Soong et al. 1991).

The active bracing system has since been fabricated, installed in a full-scale test structure, tested using artificial excitations, and subjected to actual ground motions (Reinhorn et al. 1992). The objectives of the full-scale implementation are (i) to verify the complex electronic-digital-servohydraulic system under actual strong motions, (ii) to verify the capability of the system to operate or shutdown under prescribed conditions, and (iii) to validate simplified analytical procedures used to predict actual system performance. This report provides information on the detailed design and analyses of the full-scale active bracing system. The performance of the system under simulated excitations and actual ground motions is described and compared with predicted performances using simple analytical procedures.

SECTION 2

TEST STRUCTURE AND ACTIVE BRACING SYSTEM

2.1 Full-Scale Test Structure

A dedicated full-scale test structure was erected for performance verification of the active bracing system under actual seismic ground motions. Located in Tokyo, Japan, the structure is a symmetric two-bay six-story building as shown in Figs. 2.1 and 2.2. It was constructed of rigidly connected steel frames of rectangular tube columns and W-shaped beams with reinforced concrete slabs at each of the floors. Having rectangular columns, the two orthogonal directions are not structurally identical. Weighing 600 metric tons, the structure was designed as a relatively flexible structure with a fundamental period of 1.1 sec in the strong direction and 1.5 sec in the weak direction, in order to simulate a typical high-rise building. The structure was constructed without claddings except for the top story (sixth floor), which houses an experimental active mass damper (AMD) (Aizawa et al, 1990). Side access stairs were built without connection to the main structure to preserve the symmetry of the system for sake of simplicity. Due to lack of cladding and the simple connections, the structure has very low damping in the dominant modes (between 0.5% and 1% of critical).

2.2 Active Bracing System (ABS)

As shown in Figs. 2.2 and 2.3, solid diagonal tube braces were attached at the first story of the building after the main structure was constructed (see details in Fig. 2.4). The control system enables longitudinal expansion and contraction of the braces by means of hydraulic servocontrolled actuators, inserted between the brace elements and forming an internal part of the bracing system. The control system includes also a hydraulic power supply, an analog and digital controller, and analog sensors as shown schematically in Fig. 2.5.

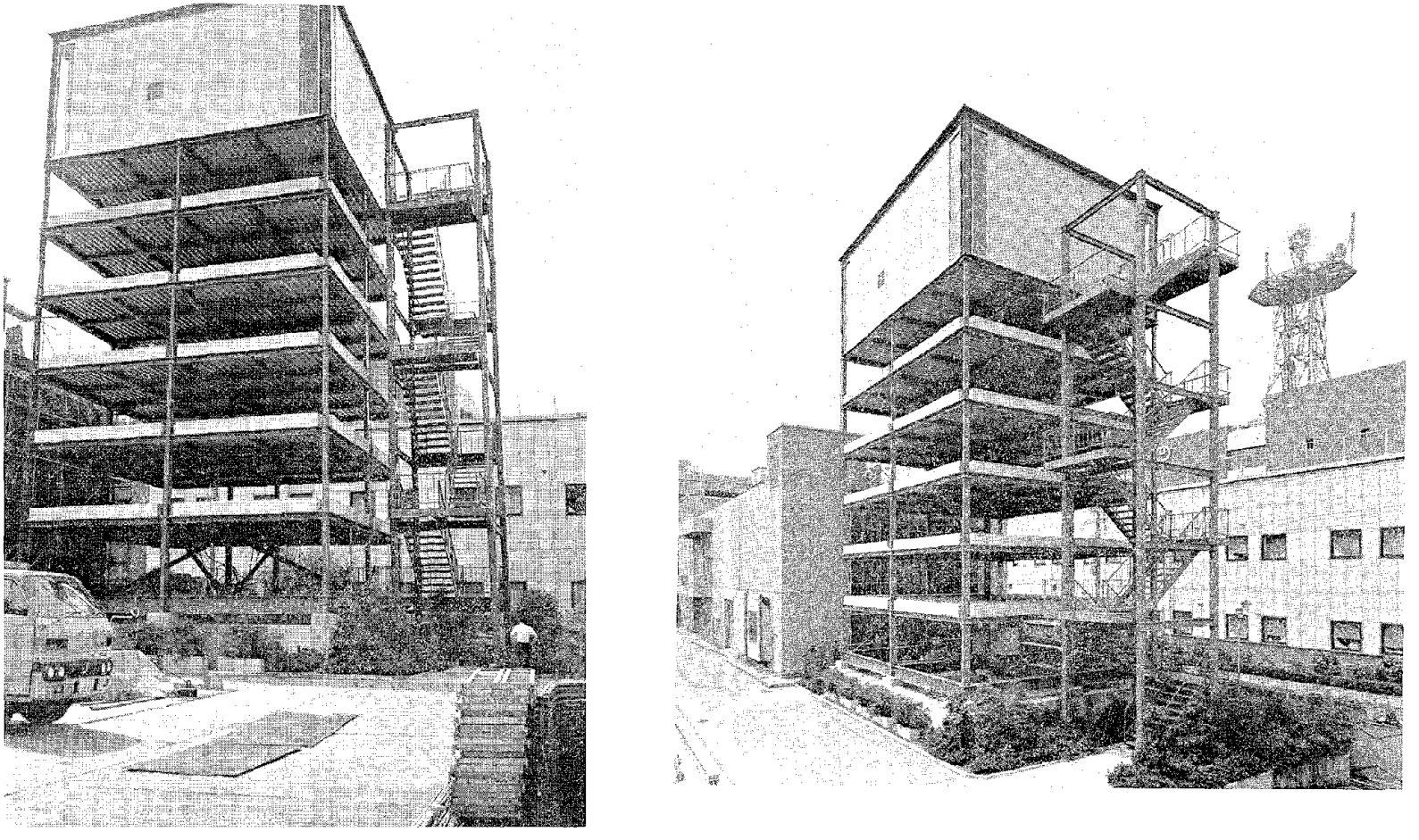

Fig. 2.1 View of Building

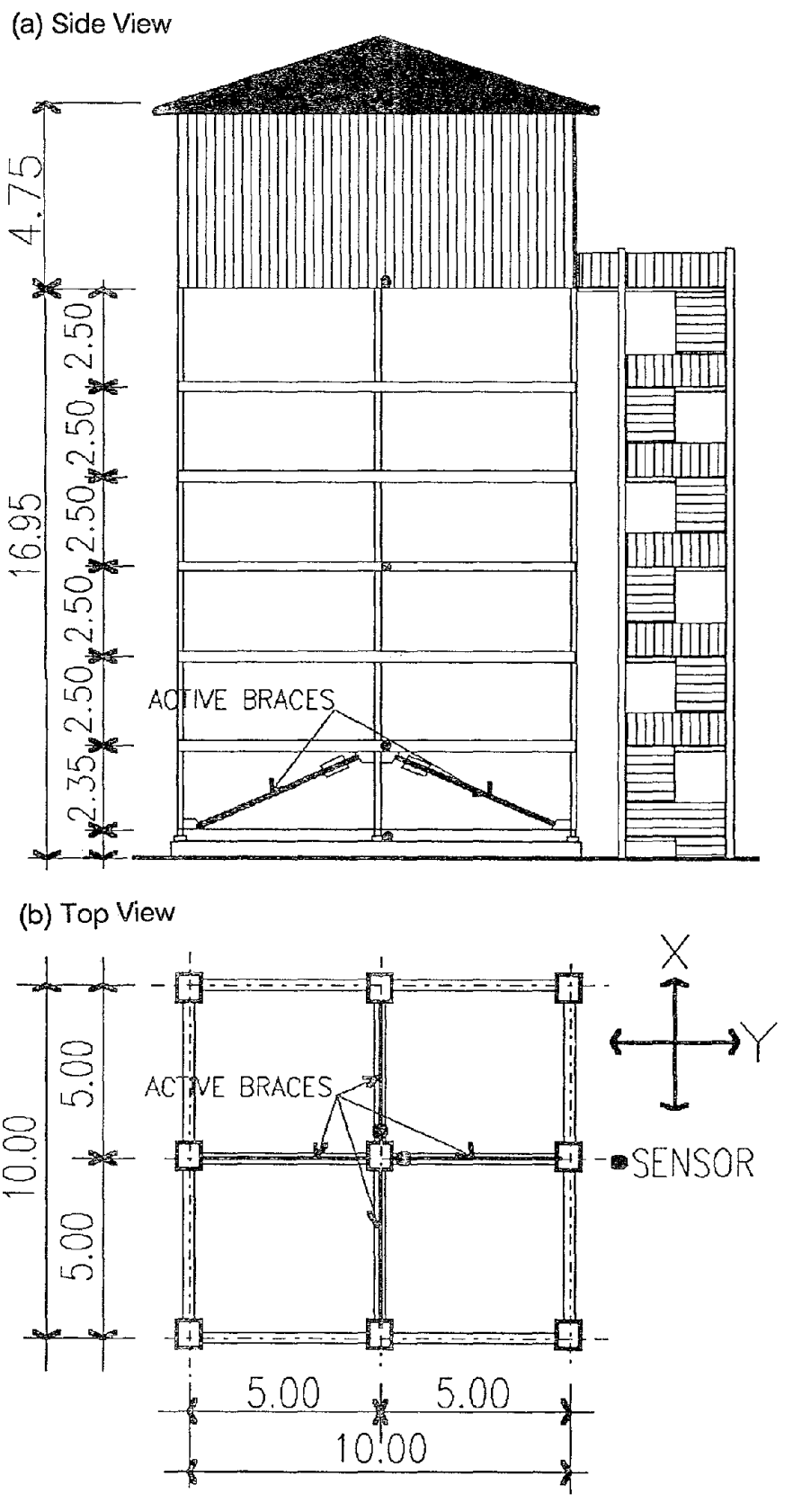

Fig. 2.2 Configuration of Active Bracing System

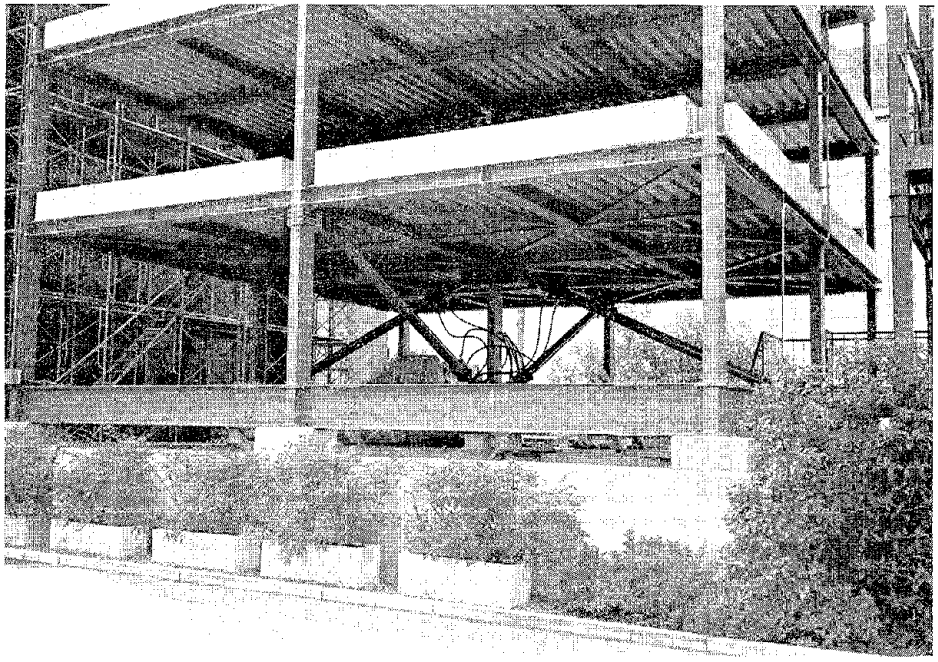

Fig. 2.3 Active Brace System

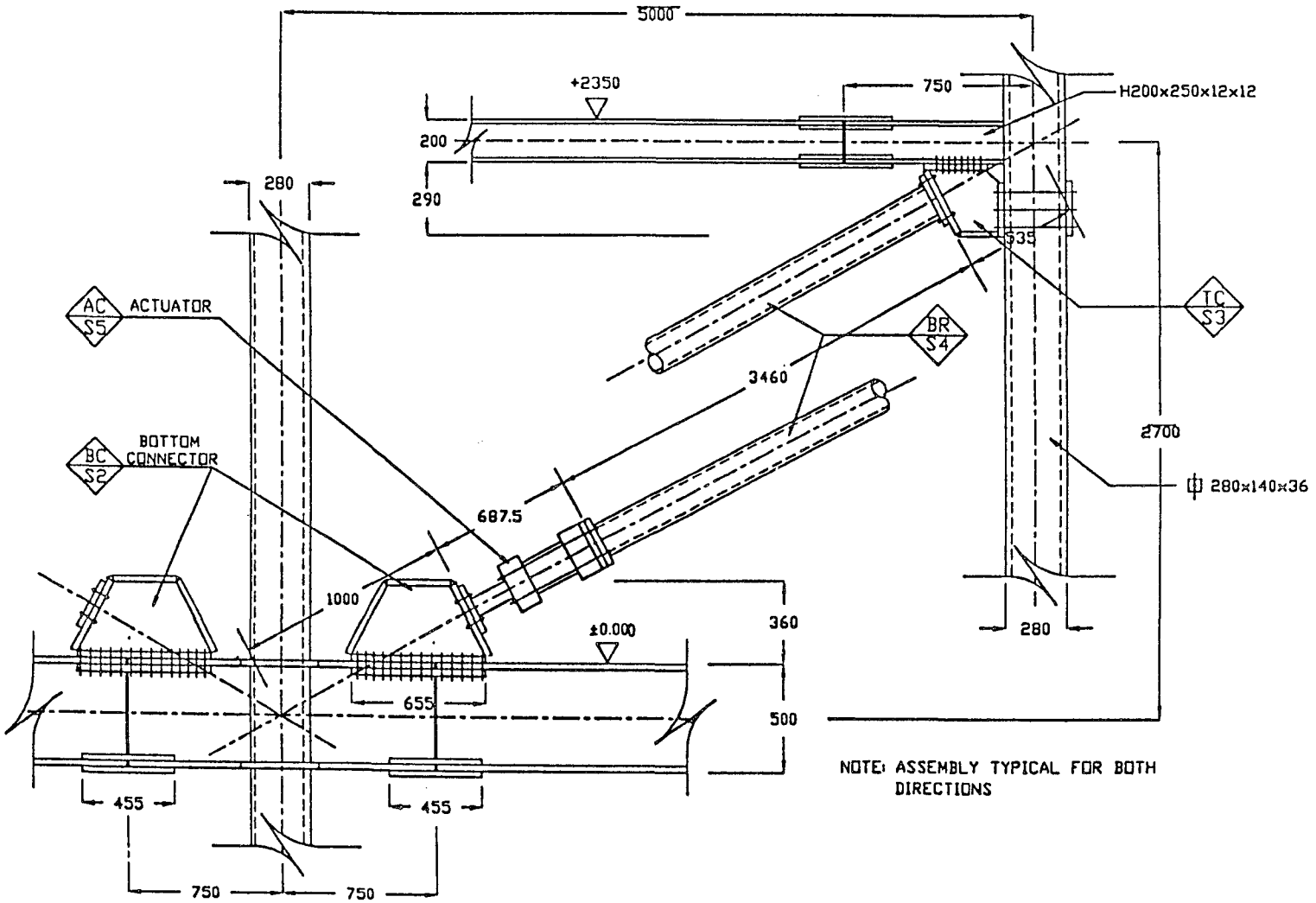

Fig. 2.4 Details of First Story Active Braces

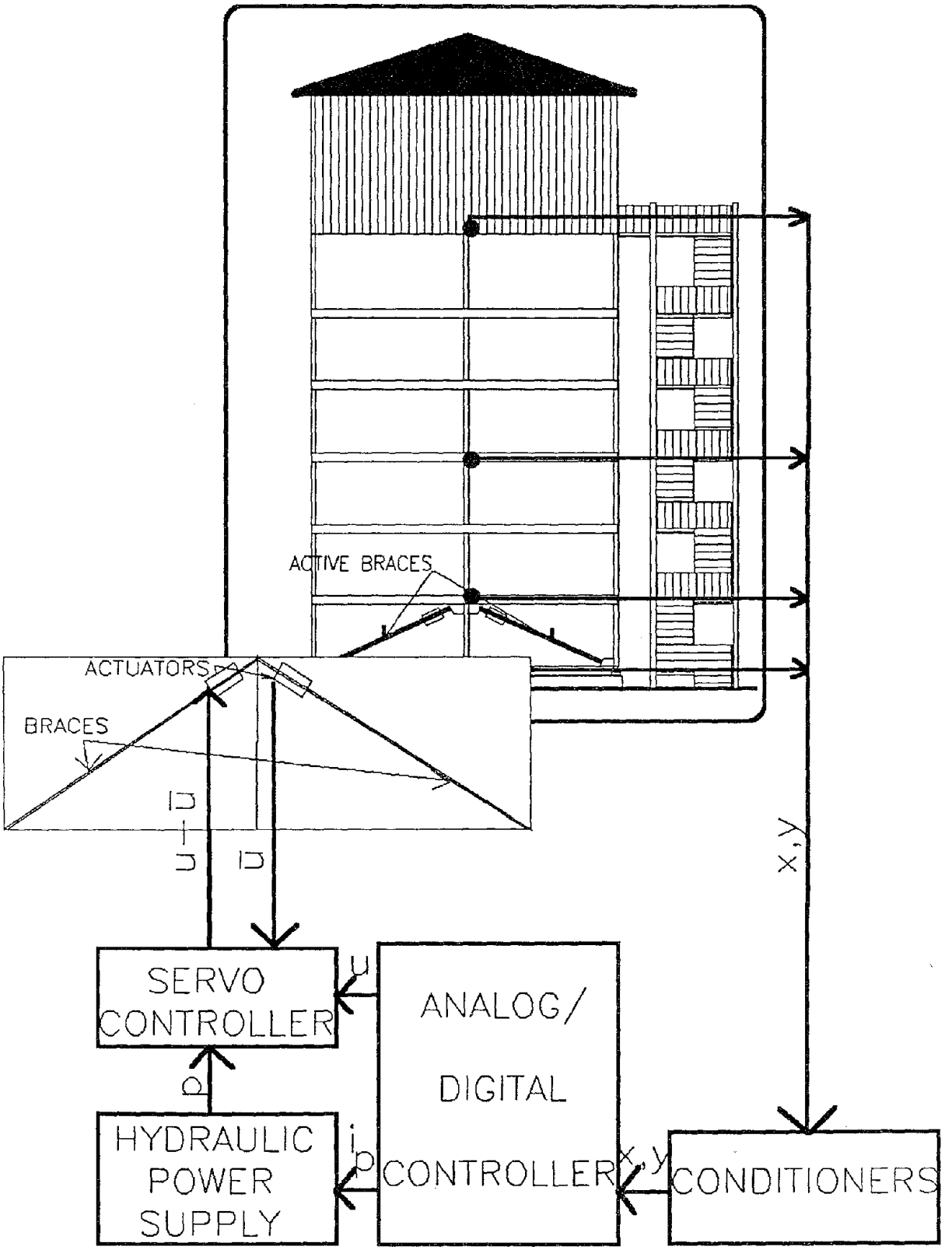

Fig. 2.5 Block Diagram of Control System

2.2.1 Braces

The design of the braces was based on the maximum control force and the anticipated stiffness with the assurance that buckling will not occur under actuator actions. The active brace and the joint configuration are shown in Figs. 2.6 and 2.7. Circular steel tubes were used as bracing members with the following specification: length = 360.5 cm, diameter = 165.2 mm, thickness = 4.5 mm, and strength = 564 kN. The measured stiffness of the braces is 98.4 kN/mm in the x-direction and 73.8 kN/mm in the y-direction.

2.2.2 Hydraulic Actuators

Four units of Parker, heavy-duty hydraulic cylinder series 2H--style TC (NFPA style Mx2) were selected as actuators with the following specifications: length = 735 mm, piston diameter = 152.4 mm, rod diameter = 63.5 mm, stroke = ± 50 mm, and average capacity = 344 kN. Figure 2.8, shows the manner in which the actuator is connected with the brace. Although the expected movement in the actuators is only ± 12 mm, larger size actuators were chosen to enable length corrections during construction. In future applications, a much shorter actuator would be sufficient.

The average capacity of the actuator is based on the working pressure [20.68 MPa (3,000 psi)] of the hydraulic oil and the average piston area, i.e., the average of the piston area on one side and the same area minus the rod area on the opposite side of the piston. The capacity can be improved by increasing the working pressure of the hydraulic oil.

Two hydraulic actuators are coupled in series in each direction and are monitored by one servovalve, which is shown in Fig. 2.9, and one servovalve-controller of type

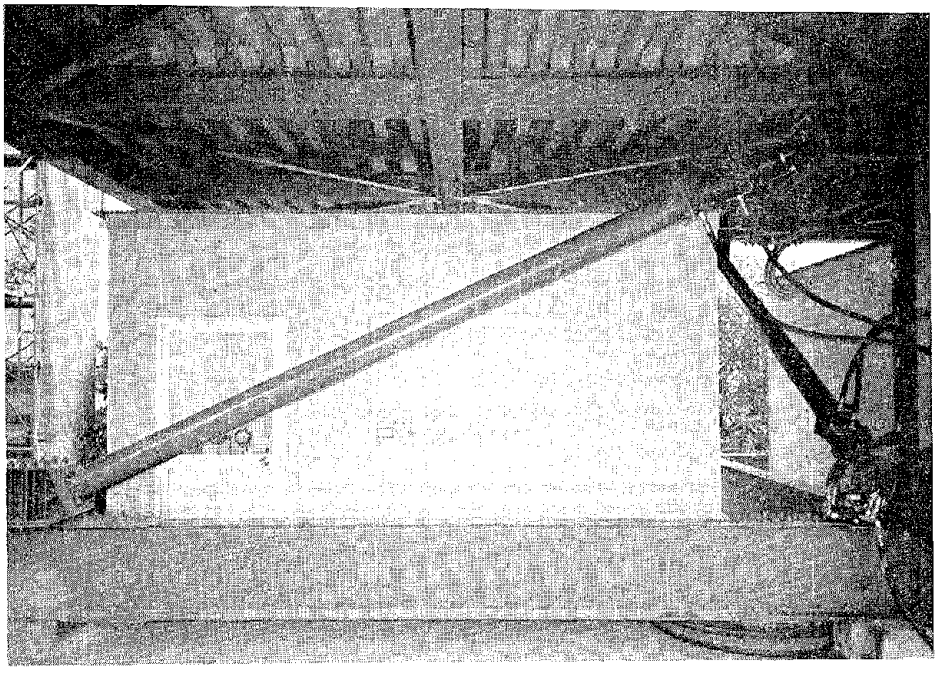

Fig. 2.6 Member of Active Brace

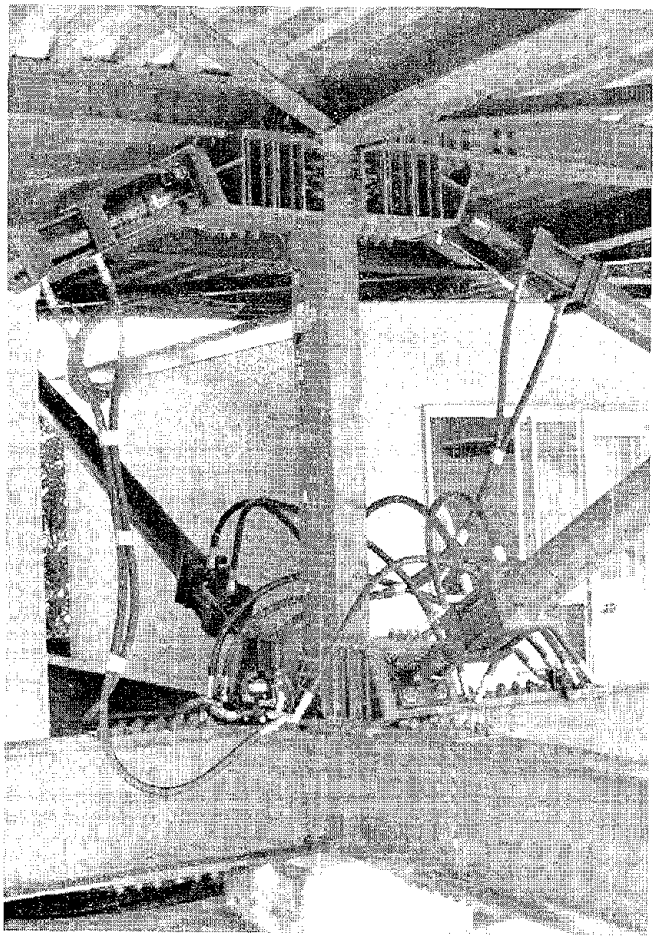

Fig. 2.7 Joint Configuration of Active Brace

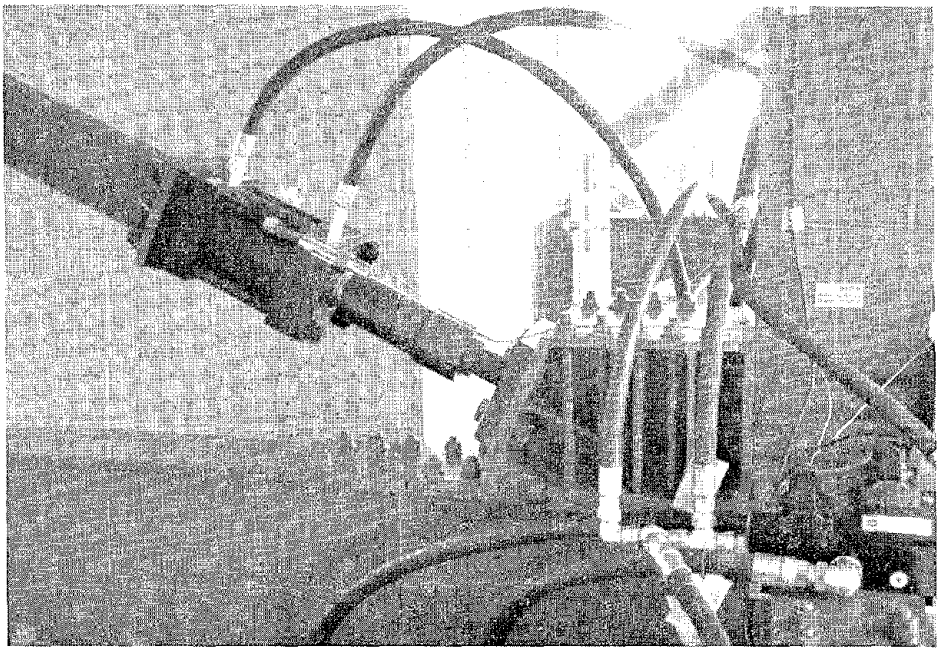

Fig. 2.8 Actuator and Connected with Brace

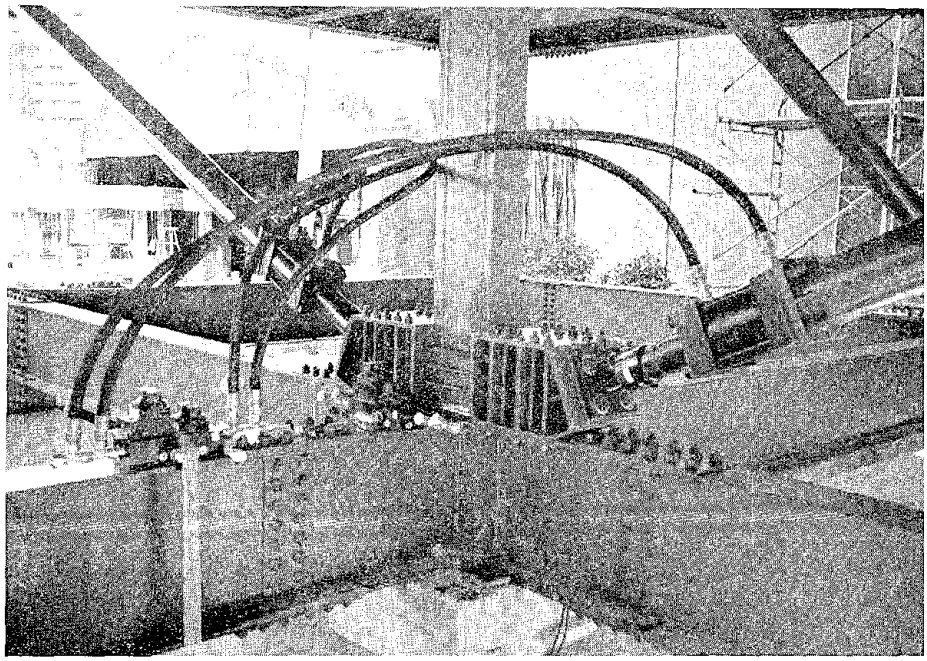

Fig. 2.9 A Set of Actuators with a Servovalve

MTS 458. The inner control loop for the hydraulic actuators is used for position feedback. The servovalve MTS252.2x can supply up to 55 liter/min (15 gpm) at a pressure drop of 6.89 MPa (1000 psi).

2.2.3 Hydraulic power supply

The final design of the hydraulic system allows the active system to remain ready for full power controlled operation, while requiring the hydraulic pump to operate for only a few seconds each hour, to keep the system fully charged. As shown in the simplified block diagram of the control system hardware (see Fig. 2.10), hydraulic accumulators, which are shown in Fig. 2.11, are placed between the pump and a hydraulic manifold, and are kept charged by the hydraulic pump. This stored power is used when the active control is first started so that full hydraulic pressure is instantly available. The accumulators can supply enough power to allow the hydraulic pump to reach full pressure operation, and can drive the actuators for approximately one minute, longer than most major earthquakes, in the event of a power failure.

The actuators use oil at pressures varying between 19 and 21 MPa (2700 - 3000 psi). The hydraulic pump with a capacity of 120 liter/min (~30 gpm) operates between the upper and lower pressure limits. The hydraulic power system was designed to operate almost passively, i.e., the accumulator battery of 38 liters (10 gallons) is inserted in the line to maintain continuous pressure and to supply the required oil for an event of up to 60 seconds. The hydraulic manifold (an electrically controlled valve) opens the hydraulic system in case of an event, while the accumulators supply the required oil. When the pressure on the hydraulic lines drops below the lower operating pressure limit, the hydraulic pump starts its operation to restore the pressure and charge the accumulators. According to this design

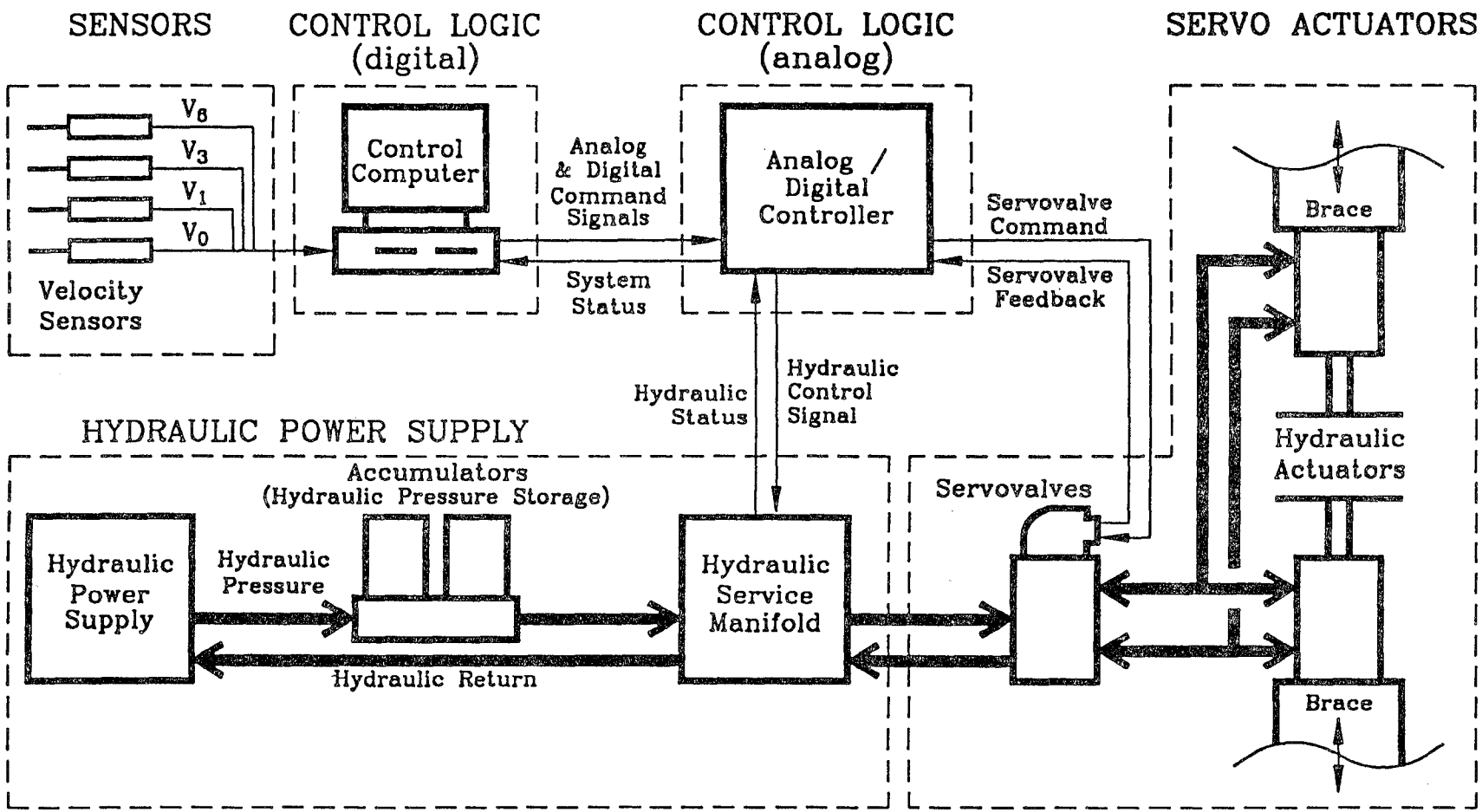

Fig. 2.10 Details of Control System for Active Bracing System

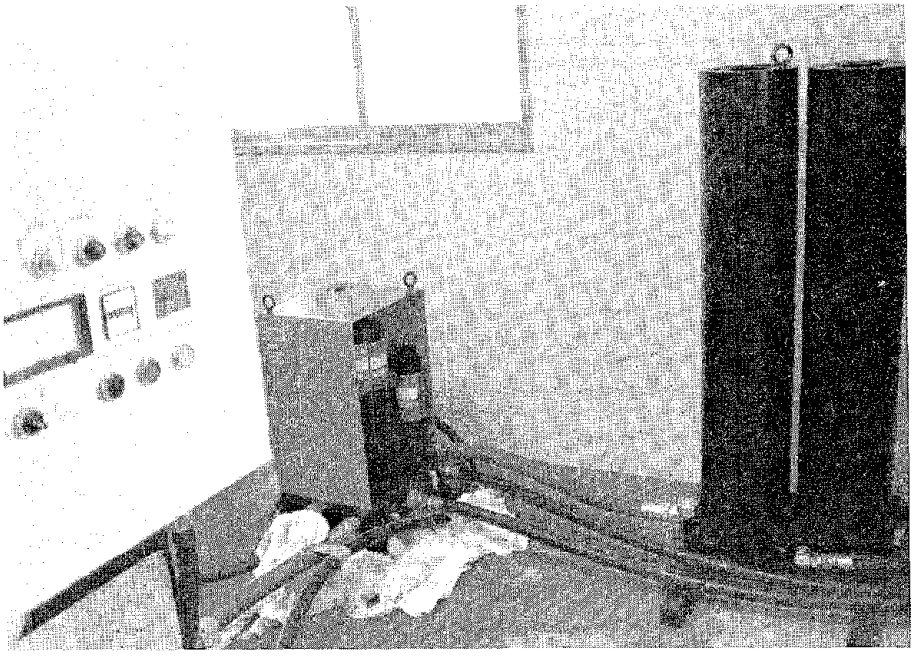

Fig. 2.11 Manifold and Accululators

it is expected to have the hydraulic pump operating only after (and not during) a seismic event. The schematic of the hydraulic system is shown in Fig. 2.10 coupled to the necessary controllers and actuators.

2.3 Analog/Digital Controller

An analog/digital controller was chosen based on the requirements that the analog controller must be compatible with the hydraulic service manifold and with the servovalves, and be capable of simultaneously controlling the two sets of servovalves. The controller is capable of fully controlling the state of the hydraulic service manifold, and driving the servovalves; moreover, the controller has a series of fail-safe circuits designed to properly shut down the entire system if any problems are detected. As built, the controller was designed to allow a digital computer to monitor the status of the controller and the hydraulic system linked to the controller, and to adjust some operating parameters of the system, including triggering the fail-safe circuits. More detailed discussion of the fail-safe system is presented in Section 5.3. To allow the computer to control all aspects of the system, a field modification was made to the digital logic circuits of the controller, which allows the hydraulic system to be remotely controlled through an external digital connection.

2.4 Digital Microcomputer

The microcomputer executes the control algorithm, monitors the status of operation of various hydraulic components and monitors the status of the structural system. The software algorithm is designed to start operation upon detection of an event or shutdown in case of malfunctions. The system consists of a PC computer with an INTEL^{TM} 80386/25 MHz processor equipped with an INTEL^{TM} 80387/25 MHz math-coprocessor, which are shown in Fig. 2.12. Two analog-to-digital (A/D) and digital-to-analog (D/A) conversion boards provide interface for up to 16 channels of differential inputs from sensors and four channels of analog outputs to controllers. In addition, 16

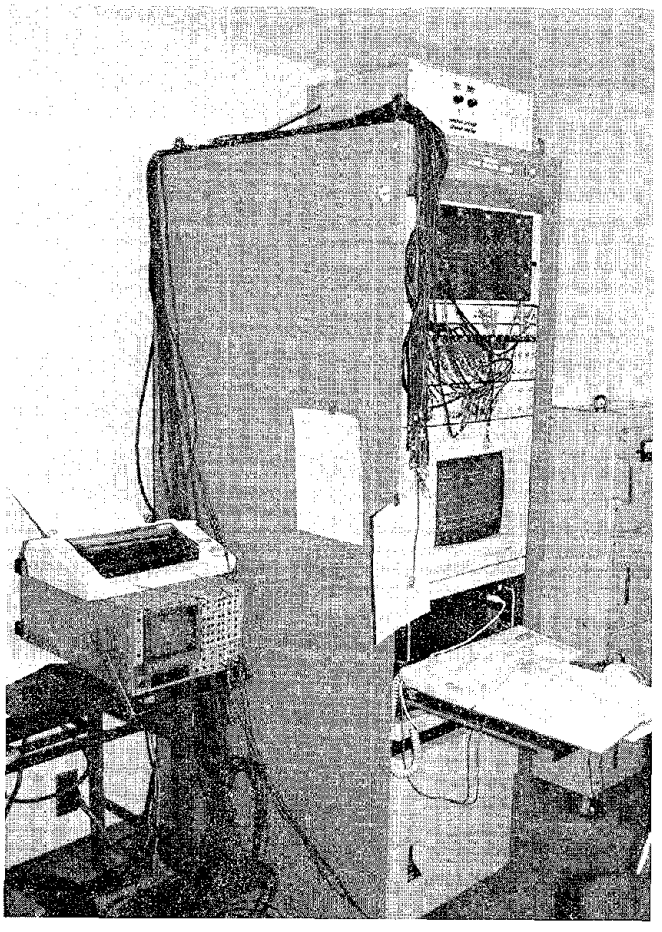

Fig. 2.12 Digital Microcomputer System

LSTTL digital logic channels are available on the computer boards. The analog channels are used to interface with the sensors (conditioners) and with the analog servoloop. The digital logic channels are used to monitor the state-of-the-controller and adjust its operations. An RGB monitor is connected to the system to enable visual monitoring of operations.

2.5 Sensors

The control system has four servovelocity seismometers of type Tokyo Sokushin VSE11, which is shown in Fig. 2.13, for each principal direction of the building with an output range of ±100 cm/sec. The velocity sensors are located on the ground, at the first, at the third, and at the sixth floors of the building. Same sensors can provide acceleration information up to ± 1000 cm/sec^2. Additional transducers are mounted at each floor to monitor building behavior. Each actuator is equipped with a displacement transducer (LVDT) which is shown in Fig. 2.14 having a range of ± 12 mm which is used to adjust the length of the brace via the servovalve loop.

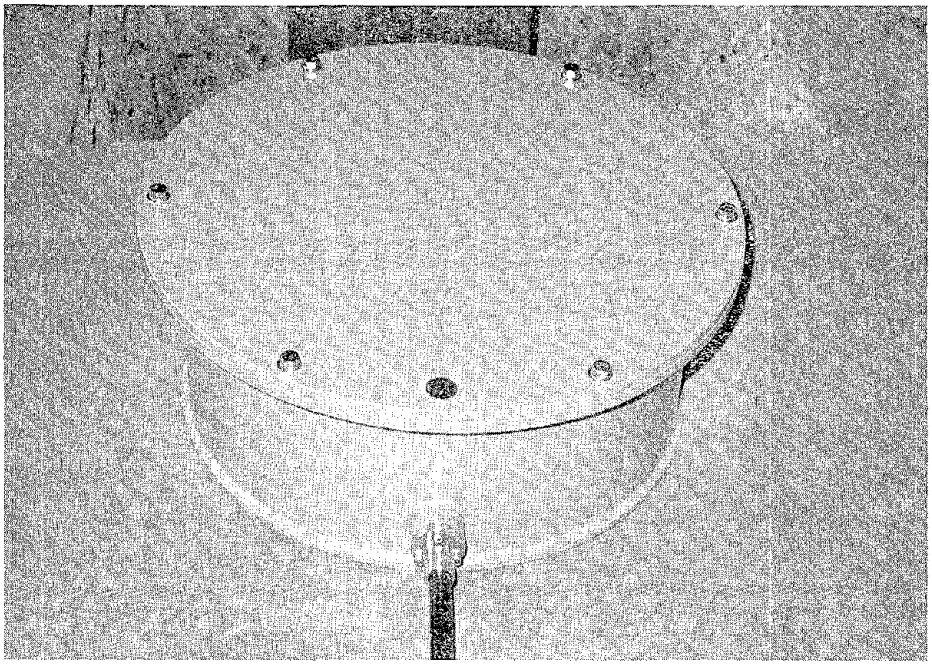

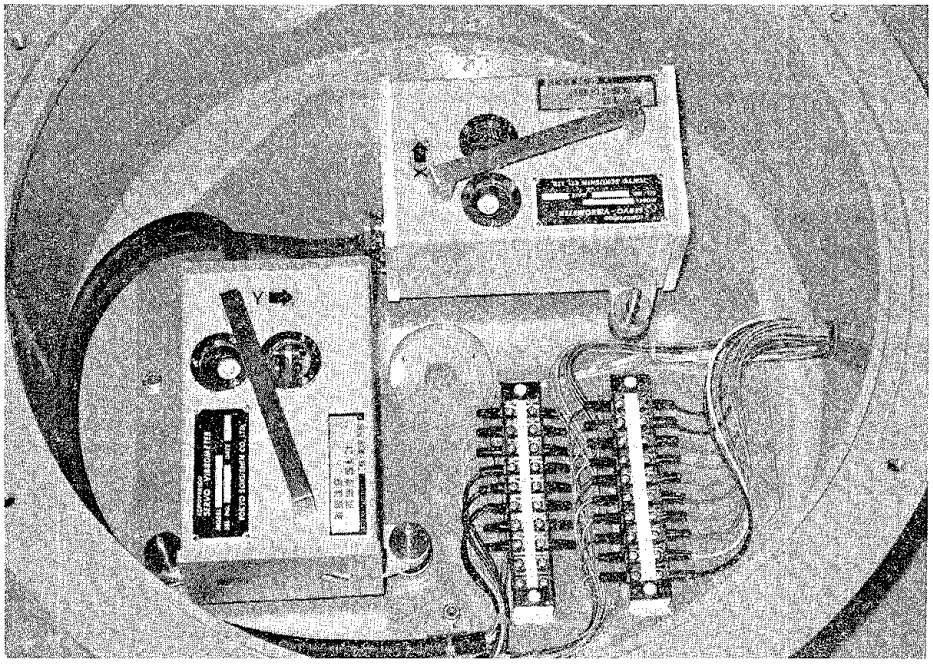

Fig. 2.13 Servovelocity Seismometer

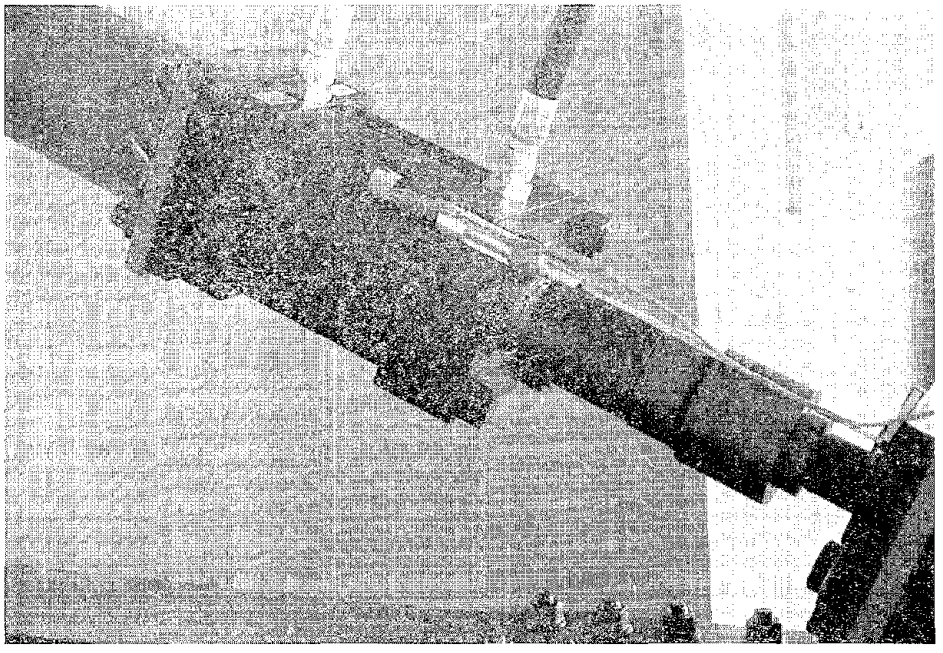

Fig. 2.14 LVDT Installed on Actuator

SECTION 3

CONTROL ALGORITHM DEVELOPMENT

The control algorithms developed for the full-scale test were based on classical linear optimal control laws previously discussed by Chung et al. (1988,1989) and Reinhorn et al. (1989). However, unlike in the laboratory, the use of displacement measurements as feedback state variables in conventional control design is not feasible in the field. Under the constraint that only three velocity sensors are available, two alternative control strategies were developed. They are (1) velocity feedback with observer which provides full-dimensional state feedback with the aid of a state-estimator and (2) three-velocity feedback which treats the full-state as an equivalent reduced-order system. These control algorithms are described below following a brief summary of the classical linear optimal control theory.

3.1 Basic Considerations

The classical linear optimal closed-loop control algorithm which is the basis of the control design is reviewed herein. The equation of motion of a discrete-parameter structure, under earthquake excitation $\ddot{x}_o(t)$ and active control force which is expressed in terms of actuator displacement $u(t)$, is described in the state-space representation as:

$$\dot{\underset{\sim}{z}}(t) = \underset{\sim}{A}\,\underset{\sim}{z}(t) + \underset{\sim}{b}\,u(t) + \underset{\sim}{w}\,\ddot{x}_o(t) \qquad (1)$$

where

$$\underset{\sim}{z}(t) = \begin{bmatrix} \underset{\sim}{x}(t) \\ \dot{\underset{\sim}{x}}(t) \end{bmatrix}, \underset{\sim}{A} = \begin{bmatrix} 0 & I \\ -\underset{\sim}{M}^{-1}\underset{\sim}{K} & -\underset{\sim}{M}^{-1}\underset{\sim}{C}_d \end{bmatrix}, \underset{\sim}{b} = \begin{bmatrix} 0 \\ -\underset{\sim}{M}^{-1}\underset{\sim}{b}_1 \end{bmatrix}, \underset{\sim}{w} = \begin{bmatrix} 0 \\ \underset{\sim}{w}_1 \end{bmatrix} \qquad (2)$$

where $\underset{\sim}{z}(t)$ is the state vector of order $2n$ consisting of vectors $\underset{\sim}{x}(t)$ and $\dot{\underset{\sim}{x}}(t)$

which are the relative displacement and relative velocity vectors of order n, respectively, n being the number of degrees of freedom (DOF) of the structure ($n = 6$ in the present case); $u(t)$ is the actuator displacement that characterizes the control force. Matrices $\underset{\sim}{M}$, $\underset{\sim}{C}_d$ and $\underset{\sim}{K}$ are the mass, damping and stiffness matrices, respectively, which

can be estimated through identification tests. Vector $\underset{\sim}{b}_1$ is the control force location

vector of order n, whose elements are $2k_c \cos \alpha$ for the corresponding floor where the active braces are attached and zero otherwise, k_c being the stiffness of the active brace and α the brace inclination angle from the horizontal; $\underset{\sim}{w}_1$ is a vector of order

with all elements equal to -1 , , indicating the contribution of the ground acceleration.

Based on the classical quadratic performance criterion, $u(t)$ is found by minimizing the integral:

$$J = \frac{1}{2}\int_o^{t_f} \left[\underset{\sim}{z}^T(t)\underset{\sim}{Q}\underset{\sim}{z}(t) + ru^2(t) \right] dt \qquad (3)$$

for the duration t_f of ground excitation. In Eq. (3), $\underset{\sim}{Q}$ is a positive semi-definite weighting matrix for the response and r is a positive weighting factor for the control.

In the present case, matrix $\underset{\sim}{Q}$ is chosen to be:

$$\underset{\sim}{Q} = \begin{bmatrix} K & 0 \\ 0 & 0 \end{bmatrix} \tag{4}$$

so that the first term in Eq. (3) characterizes the potential energy of the structure, and

$$r = 2\beta k_c \tag{5}$$

such that the second term in Eq. (3) characterizes the control energy. β is a control parameter which determines the relative importance between safety and economy; $\beta = \infty$ represents the uncontrolled case. It is noted from the above derivation that β is the only parameter that needs to be specified in the control design.

Under linear feedback control, $u(t)$ is obtained to be linearly related to the state vector $\underset{\sim}{z}(t)$ as (Sage 1977, Chung et al. 1988,1989):

$$u(t) = \underset{\sim}{G}\ \underset{\sim}{z}(t) = r^{-1}\underset{\sim}{b}^T \underset{\sim}{P}\ \underset{\sim}{z}(t) \tag{6}$$

where $\underset{\sim}{G}$ is the feedback gain of order $2n$ and $\underset{\sim}{P}$ is obtained from the approximated time invariant Ricatti matrix question:

$$\underset{\sim}{P}\ \underset{\sim}{A} + \underset{\sim}{A}^T \underset{\sim}{P} - \underset{\sim}{P}\ \underset{\sim}{b}\, r^{-1}\underset{\sim}{b}^T \underset{\sim}{P} + \underset{\sim}{Q} = \underset{\sim}{0} \tag{7}$$

It can be seen from the above that information of all state variables, i.e., displacements and velocities, is required in order to calculate the feedback control force. This requirement, however, is impractical in field applications either because all the state variables are not

accessible for direct measurement or because the available sensing devices are limited. In the present full-scale structural test, only three velocity sensors are provided in each of the principle directions which necessitates modifications.

3.2 Velocity Feedback with Observer

Suppose the state variables of a dynamic system are not fully accessible. In order to apply the state feedback strategy, a state observer can be used if the system is completely observable (Chen 1984).

Consider a dynamical system whose state equation is given by Eq. (1) and the associated output or observation equation is expressed as:

$$\underset{\sim}{y}(t) = \underset{\sim}{C}\,\underset{\sim}{z}(t) \tag{8}$$

where $\underset{\sim}{y}(t)$ is the observed vector of order $m (m \leq 2n)$ and $\underset{\sim}{C}$ is the $mx2n$ measurement matrix. Assuming that $\hat{\underset{\sim}{z}}(t)$ is an estimator of $\underset{\sim}{z}(t)$, then the state observer equation can be written as (Chen 1984, Soong 1989):

$$\dot{\hat{\underset{\sim}{z}}}(t) = \underset{\sim}{A}\,\hat{\underset{\sim}{z}}(t) + \underset{\sim}{b}\,u(t) + \underset{\sim}{w}\,\ddot{x}_o(t) + \underset{\sim}{L}\left(\underset{\sim}{y}(t) - \underset{\sim}{C}\,\hat{\underset{\sim}{z}}(t)\right) \tag{9}$$

where $\underset{\sim}{L}$ is the $2nxm$ observer matrix.

Let $\tilde{\underset{\sim}{z}}(t)$, be the error between the actual state vector $\underset{\sim}{z}(t)$, and the estimated state vector $\hat{\underset{\sim}{z}}(t)$, i.e:

$$\tilde{\underset{\sim}{z}}(t) = \underset{\sim}{z}(t) - \hat{\underset{\sim}{z}}(t) \tag{10}$$

Substituting Eqs. (1) and (9) into Eq. (10), one obtains:

$$\dot{\tilde{\underset{\sim}{z}}}(t) = \left(A - \underset{\sim}{L}\,\underset{\sim}{C}\right)\tilde{\underset{\sim}{z}}(t) \tag{11}$$

It is seen from Eq. (11) that, if the observer matrix $\underset{\sim}{L}$ is properly selected so that the eigenvalues of matrix $\left(\underset{\sim}{A} - \underset{\sim}{L}\,\underset{\sim}{C}\right)$ have negative real parts smaller than $-\sigma$, then all elements of the error vector $\tilde{\underset{\sim}{z}}(t)$ will die out at rates faster than $e^{-\sigma t}$. Consequently, even if there is large error between $\hat{\underset{\sim}{z}}(t_o)$ and $\underset{\sim}{z}(t_o)$ at initial time t_o, the vector $\hat{\underset{\sim}{z}}(t)$ will approach $\underset{\sim}{z}(t)$ rapidly.

Once the full-dimensional state vector is established, the state feedback control can be accomplished by substituting the observed state $\hat{\underset{\sim}{z}}(t)$ for the real state $\underset{\sim}{z}(t)$ in Eq. (6), giving:

$$u(t) = -r^{-1}\underset{\sim}{b}^{T}\underset{\sim}{P}\,\hat{\underset{\sim}{z}}(t) \tag{12}$$

In an effort to reduce on-line computation, an approximation is introduced in solving Eq. (11) by using finite differences. Equation (9) then becomes a difference equation in the discrete-time form:

$$\underset{\sim}{\hat{z}}(t) = \left[\underset{\sim}{I} - \left(\underset{\sim}{A} - \underset{\sim}{L}\,\underset{\sim}{C} + \underset{\sim}{b}\,\underset{\sim}{G}\right)\Delta t\right]^{-1}\left[\underset{\sim}{\hat{z}}(t-\Delta t) + \underset{\sim}{w}\,\Delta t\,\ddot{x}_o(t) + \underset{\sim}{L}\,\Delta t\,\underset{\sim}{y}(t)\right] \qquad (13)$$

It is noted that, in order to predict the state vector at time instant t, , the knowledge of ground acceleration $\ddot{x}_o$ at time t and the estimated state vector at the previous time step are required along with the available output measurements. As a consequence, an increase in on-line computation is inevitable with a potential increase in time delay, which is critical in real time control.

In the present study, two velocity transducers located at the first and third floors are selected for output measurements of the system. To illustrate the effectiveness of the proposed control algorithm, a series of numerical simulations were performed with various β values using the 32% El Centro earthquake as input. The observer matrix is $\underset{\sim}{L}$ determined in a way that the poles of matrix $\left(\underset{\sim}{A} - \underset{\sim}{L}\,\underset{\sim}{C}\right)$ are assigned to be three times of those of matrix $\underset{\sim}{A}$ so that the error term will diminish rapidly. The correlation between the control force requirement with the weighting factor β is shown in Fig. 3.1(a), where the associated control efficiency in terms of reductions in maximum structural relative displacement, maximum absolute acceleration and maximum base shear is given in Fig. 3.1(b). It is seen that, as expected, the smaller the β value, the better the performance. The case of $\beta = 4$ is determined for the design of ABS as will be explained in the next section. As an illustration, time histories of the top floor response and base shear corresponding to $\beta = 4$ are shown in Fig. 3.2. The associated control force requirement is shown in Fig. 3.3(a).

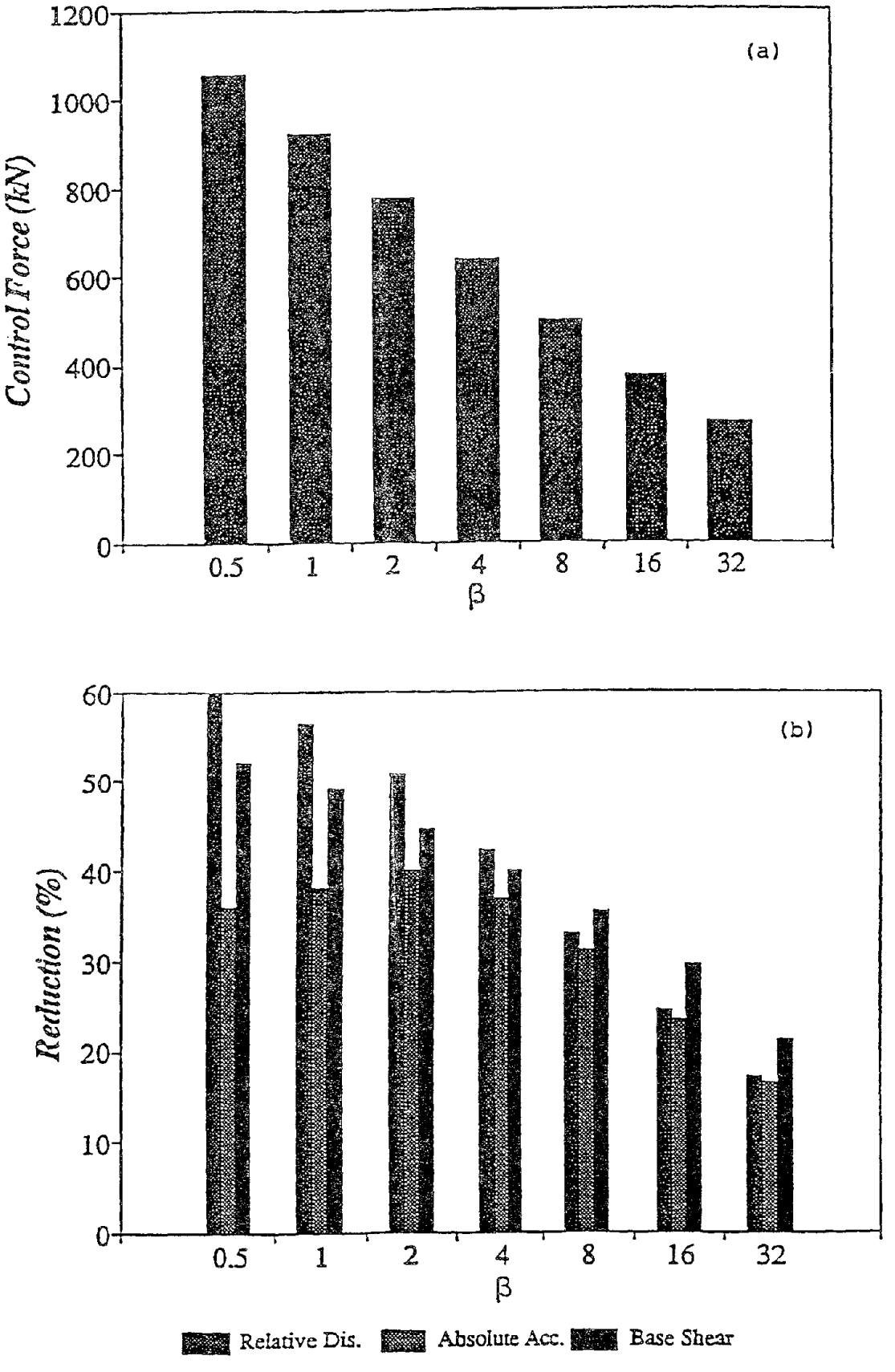

Fig. 3.1 Control Parameters as Functions of (β)

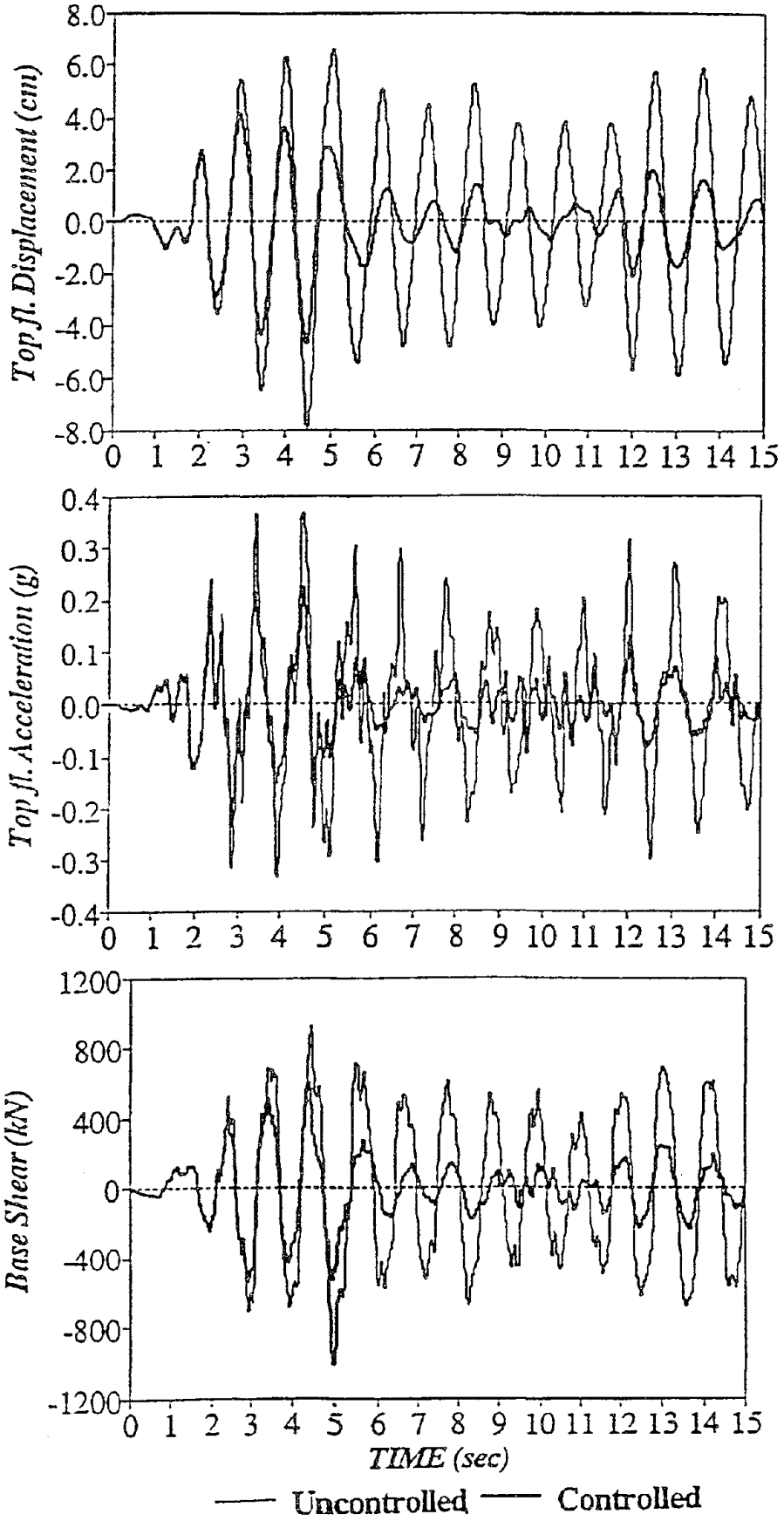

Fig. 3.2 Structural Response under 32% El Centro Earthquake (β = 4)

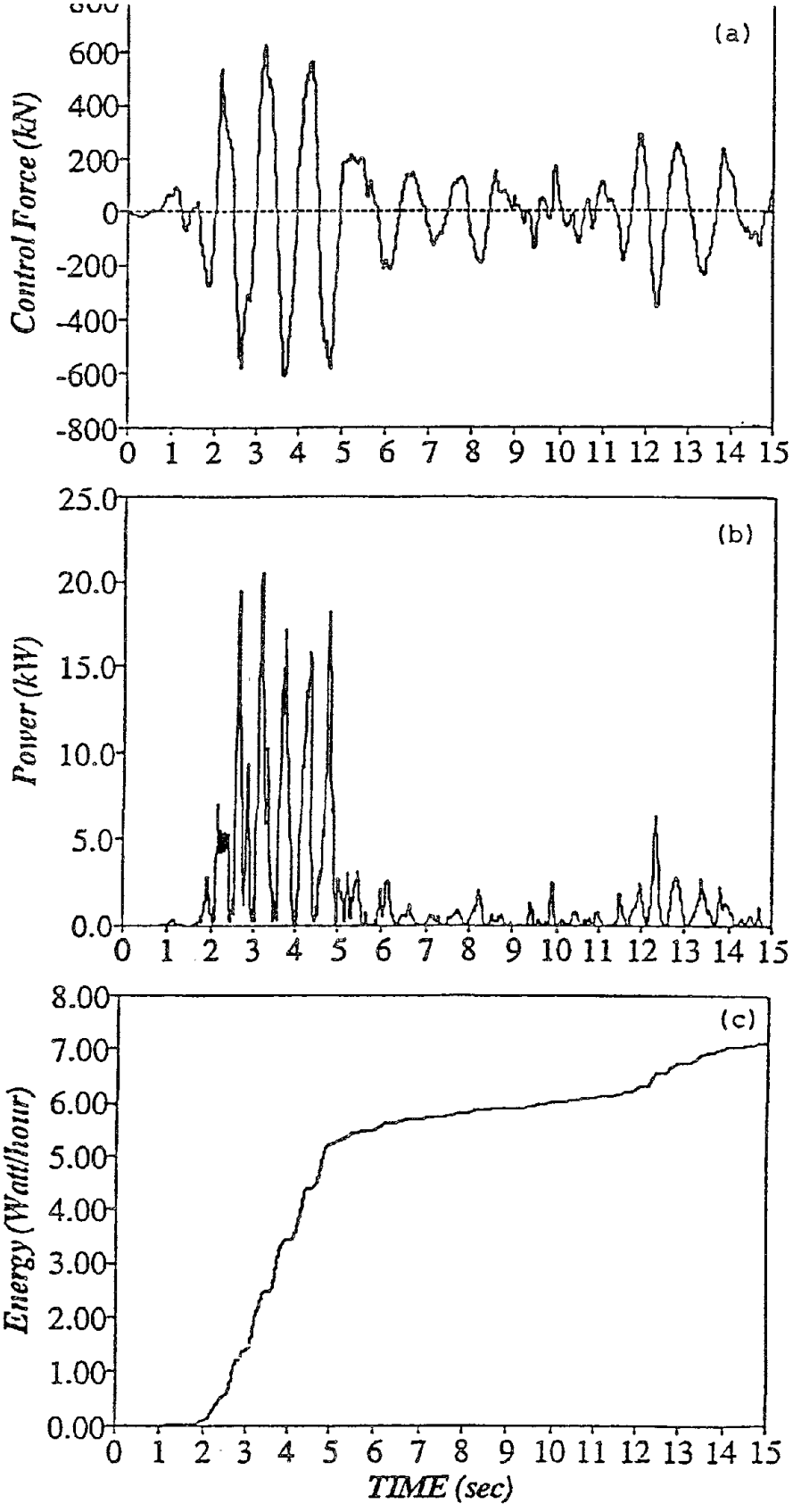

Fig. 3.3 Control Requirements under 32% El Centro Earthquake (β = 4)

3.3 Three-Velocity Feedback Control

Since three velocity sensors are available at the first, third and sixth floors, an alternate control design is one using direct three-velocity feedback. In this development, the full-order system is first reduced to a 3-DOF system and the mode shapes of the reduced order system are constructed from the first three modes of the frequency response functions of relevant floors. It is noted that orthogonality between the mode shapes does not hold here because a part of the modal displacement information has been discarded. A mode smoothing procedure to improve the modal orthogonality is therefore conducted for a more comprehensive dynamic analysis whereby the masses are redistributed to three nodal points and the equivalent stiffness and damping matrices are derived, respectively, by pre- and post-multiplying the diagonal generalized stiffness and damping matrices by the inverse modal matrix. Accordingly, the natural frequencies of the reduced order system are close to the first three modes of the full-order system.

The control design is now developed using velocity information only. The effectiveness of this strategy is confirmed by simulation. The difference between the control efficiency of using both displacement and velocity feedback and that of using velocity feedback alone is insignificant as can be seen in the last two columns of Table 3.1. However, it is interesting to see that less control force is required in the velocity feedback case but more power is required.

Control requirements and structural performance using different control strategies are also compared in Table 3.1. While the control algorithm with observer gives the best result as expected, its implementation requires more on-line computation time, as mentioned earlier, implying greater increase in time delay and reduction in control efficiency.

Table 3.1 Performance Comparisons with Different Control Algorithms

Control Algorithm	uncontrolled	Observer Control	Full-state Feedback Based on 3DOF	Velocity Feedback Based on 3DOF
Top fl. Rel. Disp. Maximun (cm)	7.9769	4.6673	5.0406	5.0480
Reduction (%)		41.5	36.8	36.7
Top fl. Abs. Acc. Maximun (g's)	0.3678	0.2340	0.2555	0.2576
Reduction (%)		36.4	30.5	30.0
Base Shear Maximun (kN)	1019.7	606.6	632.7	650.3
Reduction (%)		40.5	38.0	36.2
Control Force (kN)		629.1	565.5	563.4
Power Requirement (kW)		20.47	24.1	28.8

3.4 Time Delay

In real time control, time delay is contributed mostly by signal processing, on-line computation, and control execution using the hydraulic system. These time delays accumulated in the control loop can cause deterioration of control performance or even system instability if they are not properly compensated (Soong 1990).

Time delay can be determined from the phase lag measured between the signal input and signal output for a given system component. In an identification test, the phase lag angle is determined from the imaginary and real parts of the input and output frequency transfer functions. The delay time for each component of the system is in turn determined by:

$$T_d = \frac{\theta}{360 f} \tag{14}$$

where T_d is the time delay in seconds, θ is the phase lag in degrees and f is the frequency in Hertz.

A preliminary assessment of time delay of the hydraulic actuators used in this test was carried out in the laboratory. Using banded white noise as input, the delay time between the command signal and the achieved actuator response was estimated to be about 12 msec. The required on-line computation time was also estimated in a similar manner to be about 14 msec for the observer control algorithm and 5 msec for the three-velocity feedback algorithm.

Among various time delay compensation methods, phase compensation that was first discussed by Roorda (1980) and verified effective in laboratory experiments (Chung et al. 1988, McGreevy et al. 1988 and Chung et al. 1989) is one of the most attractive strategies. This method is adopted in the present study as briefly described below.

If the displacement feedback force lags the displacement by τ_x in time while velocity feedback force lags the velocity by $\tau_{\dot{x}}$,their corresponding phase lags for the i-th mode are $\omega_i\tau_x$ and $\omega_i\tau_{\dot{x}}$. With the phase shift, the displacement feedback force may be resolved to produce positive active stiffness and negative active damping while the velocity feedback force may be resolved to produce positive active stiffness and positive active damping. Due to the existence of negative active damping, control effects are diminished for the real system as compared to the ideal one. Even worse, time delay will cause instability if the resultant damping force is negative. Since phase lag is proportional to the delay time and modal frequency, the effect of time delay can become serious for higher modes even with small amounts of time delay.

The control force contributed by the i-th mode can be expressed as (Chung et al. 1989):

$$u_i(t) = -g_{1i}\eta_i(t) - g_{2i}\dot{\eta}_i(t) = -g'_{1i}\eta_i(t - \tau_x) - g'_{2i}\dot{\eta}_i(t - \tau_{\dot{x}}) \qquad (15)$$

where g'_{1i} and g'_{2i} are the modified displacement and velocity feedback gains, respectively, with time delay compensation. The modified feedback gain factors are determined so that the same control effect can be achieved.

Due to phase shift, the displacement feedback forces contributed by the mode can be resolved into $(g'_{1i}\cos\omega_i\tau_x)\eta_i$ as a displacement component and $(-g'_{1i}\sin\omega_i\tau_x)\dot{\eta}_i/w_i$ as a velocity component. Similarly, the displacement and velocity components of the velocity feedback force contributed by the i-th mode are, respectively, $(g'_{2i}\sin\omega_i\tau_{\dot{x}})\omega_i\eta_i$ and $(g'_{2i}\cos\omega_i\tau_{\dot{x}})\dot{\eta}_i$. In order to make the real system equivalent to the ideal one, the relationship between feedback gains for the real

system and those for the ideal system can be established such that both systems have the same active stiffness and active damping. Thus, the modified feedback gains are obtained as :

$$[g'_{1i} \;\; g'_{2i}] = [g_{1i} \;\; g_{2i}] \begin{bmatrix} \cos\omega_i\tau_x & -(1/w_i)\sin\omega_i\tau_x \\ \omega_i\sin\omega_i\tau_x & \cos w_i\tau_x \end{bmatrix}^{-1} \qquad (16)$$

For multi-degree-of-freedom systems, the control gain correction due to time delay as indicated in Eq. (16) can be applied to each mode in the modal domain and transformed into the physical domain through modal transformation. More detailed derivation can be found in (Reinhorn and Soong et al. 1989).

SECTION 4

DESIGN OF ACTIVE CONTROL

4.1 Design Earthquakes

For design purposes, the peak velocity of the design earthquakes was taken to be 10 cm/sec based on local seismic records over the past seven years (maximum = 9.5 cm/sec). Accordingly, the scaled (32%) El Centro earthquake with 98 cm/sec^2 (0.1 g) peak acceleration was determined as the design earthquake which corresponds to the criterion of 10 cm/sec maximum velocity. Response analyses were also carried out using a series of recorded earthquake time histories to verify the adequacy of the design specifications. Table 4.1 tabulates the earthquakes considered in the verification of the control system with their maximum accelerations scaled to 0.1 g.

4.2 Analysis and Design

4.2.1 Determination of weighting factor β.

A series of numerical simulations with different β values have been presented in the preceding section. While the best reduction in displacement was observed in the case of $\beta = 0.5$, $\beta = 4$ was used for control system design from the practical standpoint since it gave satisfactory structural performance (approximately 40% reduction) while requiring reasonable amount of control force (665 kN), just within the capacity of the selected actuators. The associated maximum actuator displacement and velocity are $(\pm)$0.5 cm and 6.6 cm/sec, respectively, also within the performance limitation of the specified device. The following analysis for design of the power resource is based on this β value.

Table 4.1 Design Earthquakes

Earthquakes	Component	Scale factor	Duration (sec)	Sampling time (sec)
El Centro	NS	0.32	20	0.02
Hachinohe	NS	0.60	20	0.01
Miyagioki		0.68	30	0.01
Taft	N21E	0.715	20	0.02
Mexico	N90W	0.65	100	0.02
Mexico	S00E	1.115	100	0.02
Pacomia Dam	S16E	0.095	20	0.02
Pacomia Dam	S74W	0.104	20	0.02
Tokyo		1.48	10	0.02

4.2.2 Design of passive power resource.

The required flow rate $\dot{q}(t)$ of the hydraulic cylinders can be determined approximately in terms of the piston area A_p and the actuator velocity $\dot{u}(t)$ as:

$$\dot{q}(t) = A_p \dot{u}(t) \qquad (17)$$

in which $\dot{u}(t)$ is calculated based on the selected β value and the assumed brace stiffness.

Equation (17) is a first-order approximation in which compressibility of the hydraulic fluid and leakage around the valve and piston are neglected, which is adequate only when the load reaction is small. In general, maximum values are the criteria of design specification. The design capacity of the flow rate, however, is not based on the extreme value; it is rather determined in accordance with the average flow rate from an economic point of view. The servo-controlled system pumps the hydraulic oil with a constant speed during the control action. The difference of the oil flow between the required and the supplied is then adjusted through the hydraulic accumulators.

Figure 4.1 illustrates the cumulative flow accumulated during an earthquake, which is obtained by integrating the time history of the flow rate. The slope of this curve represents the instantaneous flow rate required to achieve the control goal. It is observed from interpreting the slope of the curve that system demand is the highest between 2 and 5 seconds and less so over the rest of the time history, a property apparently resulted from the nonstationary nature of the earthquake motion and the control effect contributed in the previous time period. The linear curve represents the cumulative volume of a constant flow which is obtained by minimizing the difference between the demand and supply

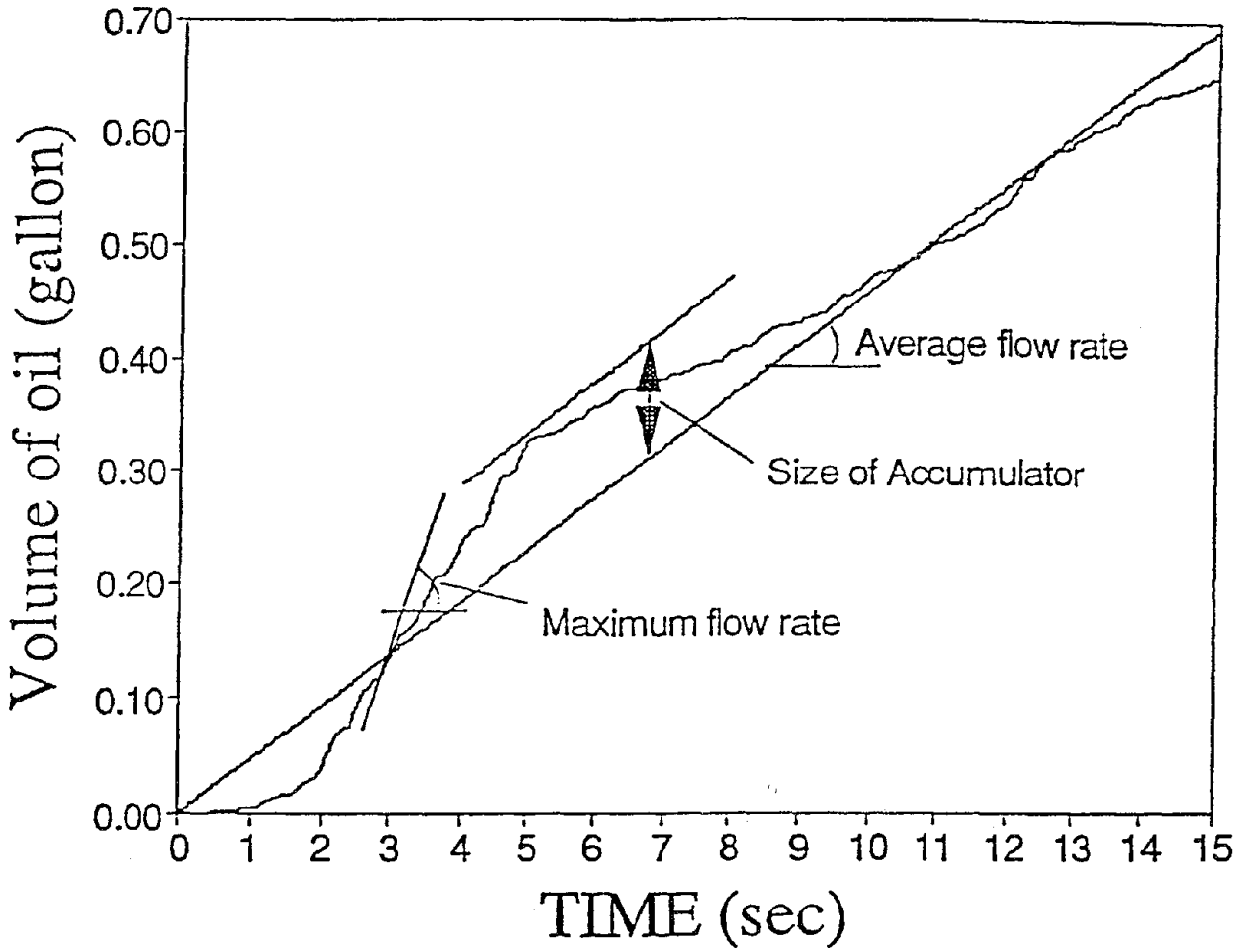

Fig. 4.1 Cumulative Oil Flow During 32% El Centro Earthquake

of oil using the least-square criterion. The largest difference between the cumulative flow and the average flow indicates the minimum volume of the hydraulic accumulator to be considered in design.

A summary of simulated results under representative earthquakes is given in Table 4.2. The ABS design specifications are determined accordingly.

4.3 Verification

From the analytical data shown in Table 4.2, it was found that the design was appropriate for almost all earthquake records used except for the case of Hachinohe earthquake. In that case, it requires a maximum control force of 696.5 kN which is far beyond the design capacity of the system if the same control strategy is to be used. Investigation was made by restricting the output control force within the design capacity of the actuator while using the same feedback gains. Results show less reduction of structural response (about 30% in displacement and 47% otherwise) when the control force is restricted to 333 kN per actuator whereas stability of the mechanical system is preserved.

This situation should also be taken into account in the on-line control practice due to erratic nature of earthquake ground motions.

4.4 Power and Energy

In order to generate the required control forces, large power supply may be required to effectively activate the actuators. Power requirement, $p(t)$, of the hydraulic system can be evaluated in terms of the control force $F(t)$, and actuator velocity $\dot{u}(t)$ as:

$$p(t) = F(t)\dot{u}(t) \tag{18}$$

Energy consumption, $E(t)$, can be obtained from:

Table 4.2 Summary of Response Analysis under Design Earthquakes (B = 4)

Earthquakes	Scale factor		Performance indices			Resource requirement / Actuator						
			Top fl. disp. (cm)	Top fl. acc. (g)	Base shear (kN)	control Force (kN)	Actuator disp. (cm)	Max. flow rate (gpm)	Ave. flow rate (gpm)	Vol.of accum. (gal.)	Total volume of oil (gal.)	Power (Kw)
El Centro	0.32	Unctrl Ctrl Red.(%)	7.98 4.66 41.6	0.37 0.23 36.5	1018.3 618.0 39.5	313.9	0.51	19.72	2.7	0.11	0.74 in 20 s	20.02
Miyagioki	0.68	Unctrl Ctrl Red.(%)	5.30 3.27 36.4	0.43 0.21 50.7	847.6 547.4 35.8	245.3	0.40	15.24	2.0	0.12	0.71 in 30 s	16.08
Mexico (N90W)	0.65	Unctrl Ctrl Red.(%)	9.70 5.80 40.2	0.32 0.18 44.2	1347.9 877.0 35.0	255.1	0.41	6.21	1.2	0.18	1.33 in 100 s	5.65
Mexico (S00E)	1.115	Unctrl Ctrl Red.(%)	9.95 6.99 29.8	0.34 0.24 30.4	1389.1 1000.6 28.2	323.7	0.53	9.36	1.5	0.34	2.13 in 100 s	10.77
Pacomia Dam (S16E)	0.095	Unctrl Ctrl Red.(%)	5.58 3.90 30.1	0.35 0.17 50.7	741.6 500.3 32.7	255.1	0.42	10.94	2.0	0.06	0.47 in 20 s	10.06
Pacomia Dam (S74W)	0.104	Unctrl Ctrl Red.(%)	4.14 2.68 35.1	0.30 0.14 52.6	606.3 406.1 33.0	176.6	0.29	9.35	2.0	0.055	0.44 in 20 s	4.88
Taft (N21E)	0.715	Unctrl Ctrl Red.(%)	7.64 4.36 42.9	0.63 0.30 53.3	1083.0 535.6 50.5	333.5	0.54	18.29	3.0	0.12	0.96 in 20 s	21.48
Tokyo	1.48	Unctrl Ctrl Red.(%)	4.85 3.73 23.2	0.33 0.26 21.1	623.9 406.1 34.6	333.5	0.54	12.63	2.7	0.07	0.37 in 10 s	21.60
Hachinohe	0.60	Unctrl Ctrl Red.(%)	17.93 9.48 47.1	0.79 0.41 48.6	2731.1 1471.5 46.0	696.5	1.13	26.74	6.0	0.17	1.51 in 20 s	59.02
Hachinohe (limited Ctrl force)	0.60	Unctrl Ctrl Red.(%)	17.93 12.65 29.4	0.79 0.69 12.5	2731.1 1660.8 39.2	333.5	0.54	31.04	4.0	0.17	1.21 in 20 s	55.54

$$E(t) = \int_o^t p(\tau)dr = \int_o^t F(\tau)\dot{u}(\tau)d\tau \qquad (19)$$

Figures 6(b) and 6(c) illustrate the time histories of power and energy resources required under the 32% El Centro earthquake.

SECTION 5

EXPERIMENTAL STUDY

5.1 Control Algorithm

As discussed in Sections 3.1 through 3.3, the three-velocity feedback control algorithm is the simplest of those available based on the sensor configuration. It is, thus, used in the experimental study discussed in this section.

Using the three velocity feedback control, the movement of the actuators which provide the control force is calculated by:

$$u_x(t) = G_x^T \dot{x}(t) \qquad \text{and} \qquad u_y(t) = G_y^T \dot{y}(t)$$

in which u_x and u_y are the actuators displacements, G_x and G_y are control gain vectors, and $\dot{x}$ and $\dot{y}$ are vectors of sensed velocities in the $x-$ and $y-$ directions, respectively.

The uncompensated feedback gains used in this case are 0.02166, 0.01031 and 0.00595 for the first, third and sixth floor velocities in the x- direction, respectively. The gains in the y-direction are 0.02476, 0.01400 and 0.00706.

The implementation of this algorithm in real-time requires adjustment of gains to enable quick integer operations. The program is compiled to execute modules that allow for a computational cycle of 4.2 msec.

5.2 Automatic Control Operation

As discussed in Sec. 2.2.3, the hydraulic power for the full-scale active bracing system needs to be continuously available, yet, unlike in a laboratory, it is not practical to have the hydraulic system operating constantly. Consequently, the system had to be designed so that the hydraulic system remains in a ready, but dormant, state, with the control software

capable of bringing the system to full operation. In addition, the hydraulic system had to be capable of almost instantly supplying full power to the active braces, and keeping the braces supplied with power for the duration of the event, even if the hydraulic pump loses power. To accomplish this, the control software monitors the status of the control hardware, and adjusts the state as necessary. These requirements are met by subroutines added in the control program, which monitors system status, starts or stops the control operations.

5.3 System Reliability and Maintenance

While occasional minor glitches in operation of a control system may be acceptable in a laboratory, any problems or errors in the full-scale control system, operating without continuous human guidance and monitoring, have the potential to cause damage or catastrophic failure. To properly protect the system and the structure from damage in the event of a full or partial failure of the control system, fail-safes were added to both the hardware and the software.

The long-term maintenance of the system poses an additional series of challenges. If strict tolerances are not met, the continuous wear can lead to degradation in the system performance, and even to failure. The standard maintenance must include manual inspection and verification of the system components on a regular bases.

As a safety feature, the computer can latch the servovalve commands, such that the actuators are held in a rest position. When the latching command is sent to the controller, all external servovalve commands are immediately disabled, and the actuators are adjusted from their current position to the rest position. During rapid adjustment to the rest position, the actuator displacement decays exponentially, such that neither the structure nor the control system is stressed by the adjustment, and so that the natural frequencies of the structure are not excited. This latching circuit is designed to be activated either by an external signal from the computer, or by the fail-safe circuitry of the controller.

To improve safety and reliability of the entire system, an external electrical circuit was added to the system's fail-safe chain. This circuit is directly connected to the controller, the hydraulic pump, the control computer, and the top floor velocity transducers. The circuit monitors both the signals from the velocity transducers and an analog signal from the control computer. If the velocity signals exceed a preset limit or if the computer sends a large signal, the circuit will trigger the fail-safe interlocks of both the controller and the hydraulic pump. The connection to the hydraulic pump is a redundant safety feature, since when the controller's interlock circuit is triggered, the controller will automatically trigger the pump's interlock circuit.

5.4 Control Software

The design and development of the control software for the full-scale active bracing system posed a variety of challenges. The control program is required to monitor the system and the structure, start and stop the control system operation, and intelligently handle any problems that might occur; moreover, the software must be able to handle these tasks reliably for a long period of time. In addition, the software must be able to perform these tasks efficiently; while the operating speed is not critical during the routine monitoring and maintenance operations, the program must operate extremely fast during the actual control operation. The major features of the control software are shown in a block diagram (Fig. 5.1) outlined in Table 5.1. A detailed description is given below.

(a) *Normal Operation.* During normal operation the control software deals with three operations, i.e., "stand-by," "control," and "shut-down."

(i) During the "*stand-by*" operation the control program monitors both the status of the control system and the motion of the structure. The controller is continually monitored for system interlocks and problems with the hydraulic system, both of which could either reduce the effectiveness of, or prevent altogether, any active control

operation. All of the instruments are constantly monitored for zero drift; any offsets in the zero position of the instruments' signals are removed, first when the program is started and then on a regular basis during the normal operation. The base and top floor instruments are monitored for seismic and wind induced motions, respectively, and the active control system is started if a significant motion is detected. An averaging technique is used to minimize the possibility that signal noise will unnecessarily trigger the control.

(ii) "*Control*" starts when a seismic ground motion or high wind is detected, the control program first turns on the hydraulic power and releases the servovalve command latch, before beginning the controlled operation. During the controlled operation, the program uses the signals from the instruments to calculate control signals according to the previously detailed control algorithms. The program checks both the control signal and the top floor velocity, to see that neither exceeds preset limits. If the control signal exceeds the limit, the output is clipped at the limit level.

(iii) If the top floor velocity exceeds the limit, the software performs an emergency "*shutdown*." In addition, the program monitors the controller for any problems. If a problem is detected in the system, the program will either attempt to correct the problem, if possible, or will perform an emergency shutdown of the system. When the motions of both the ground and the structure have returned to reasonable levels, the program will latch the servovalve command, turn off the hydraulic power, and return to the normal waiting state until the next event is detected.

(b) *System Self-Maintenance.* Besides the normal operating routines, the control program contains several routines for testing and verifying the integrity of the system. A self excitation test is used to verify that the control system is working properly, and to check the efficiency of the control. A self identification test is used for verifying the natural

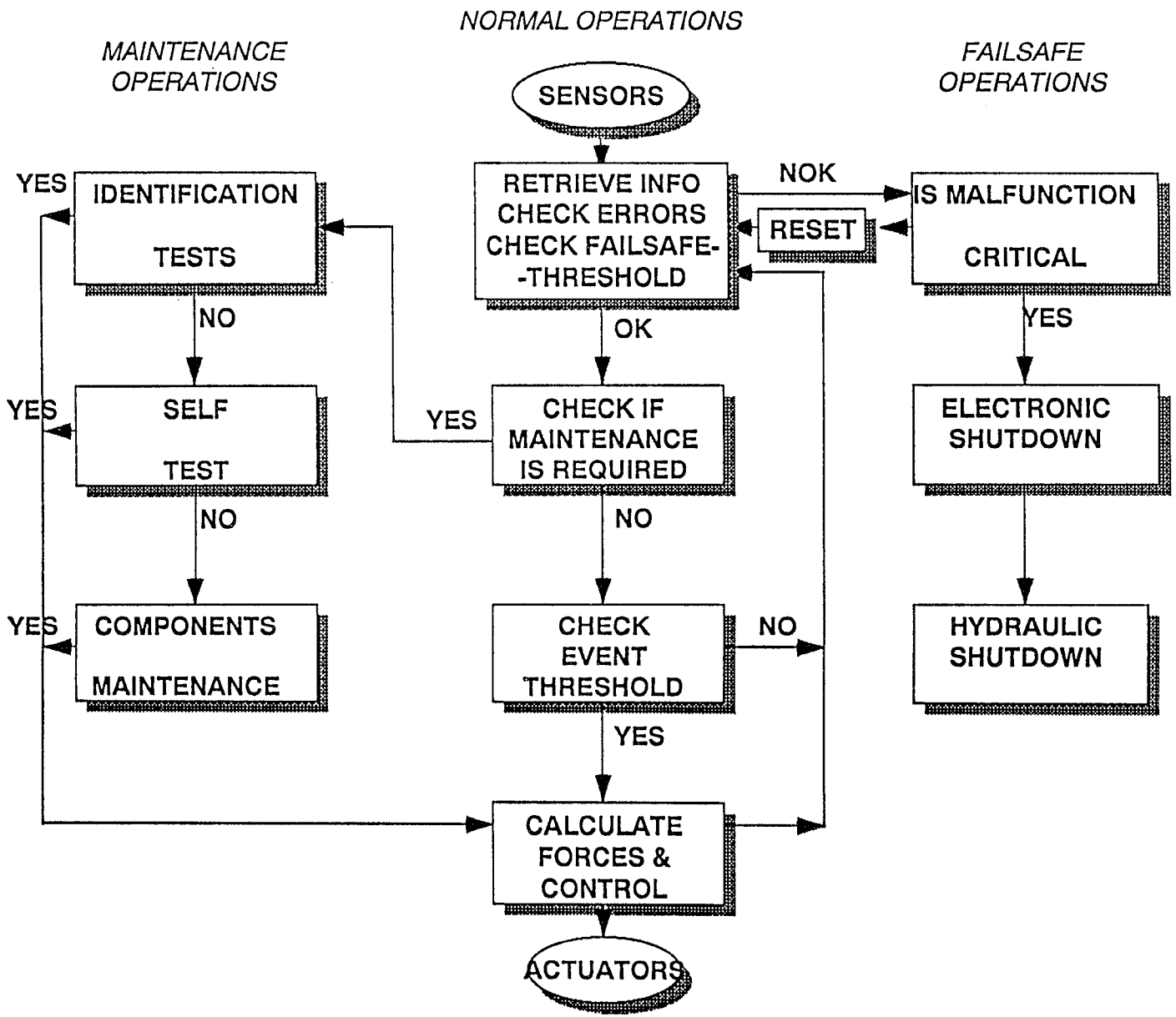

Fig. 5.1 Block Diagram of Control System Software

Table 5.1 Control System Software

Module / purpose (1)	Notes (2)
Normal operations	
Monitor ground and individual floor velocities	
Adjust instrument offsets	
Start / stop control	The software can identify signal noise to eliminate false starts.
• Turn hydraulic power on / off	
• Release / lock servovalve commands	
Generate control signal	
Monitor system status	See system/software reliability
System maintenance	
Self excitation test	
Self identification test	
Emergency stop test	
System / software reliability	
Servovalve command locked when control is off	Command locked at zero
Traps and properly handles software errors	Critical errors cause an emergency stop
Monitor status of computer hardware	Uses intelligent error handling
Monitor status of digital controller (Monitor hydraulics and electronics through controller)	Uses intelligent error handling
Monitor top floor velocity	Large velocity causes emergency stop
Intelligent error handling	
◦ Recovery from certain non-critical errors	
◦ System protected from some operator errors	
◦ Excessive errors trigger emergency stop	
Emergency stop	Actuators are smoothly returned to the resting positions, such that the natural frequencies of the structure are not excited.
◦ Redundant interlock triggers	
Digital signal to controller	
Analog signal to remote relay/trigger	
◦ Servovalve command instantly locked	
◦ Hydraulic power stopped	
◦ Control signal "ramped" to zero	

frequencies of the structure and comparing the uncontrolled response of the structure to the controlled response from the self excitation test. A third test is used to verify that the emergency stop procedures and the fail-safe systems are working properly.

(c) *Safety and Reliability.* To protect the integrity of the control system, the software contains many features designed to improve safety and reliability. As a general safety feature, the servovalve command is kept latched, with the actuators in the rest positions, whenever the program is not running either the control or a test routine. In addition, the control is started automatically daily to prevent stick of the sensitive servovalves. Besides extensive debugging and beta testing, the software is programmed so that a defect in the program code or the occurrence of an unpreventable software error during operation will not cause an outright failure of the program. Instead, when such an error is detected, the program will trap the error and attempt an emergency shutdown of the system. Finally, the program extensively monitors the status of the system hardware. The software constantly checks the computer's data acquisition boards for any problems. The program can clear most of the data acquisition board errors; however, if an excessive number of errors occur, or if an error cannot be cleared, the program will perform an emergency shutdown. The software monitors the status of the controller in a similar way, and monitors the top floor velocity as mentioned above.

When the control program detects a problem anywhere in the system hardware or software, it will determine if the error is critical or not. If the error can be identified as a non-critical error, an attempt is made to correct the problem. If the program is unable to correct the error, or if an excessive number of correctable errors occur, the system is immediately halted through an emergency shutdown. The emergency stop sequence consists of sending two redundant interlock triggers; a digital signal to the controller, and an analog signal to the external fail-safe circuit. The servovalve command is latched, and the hydraulic

power stopped. As an added redundant safety feature, the program will return the analog control signal to zero through an exponential decay similar to the servovalve command latch.

SECTION 6

SYSTEM PERFORMANCE

The building structure was subjected to a series of excitations to identify its dynamic properties and to verify the performance of individual components as well as of the overall system. For the identification studies, the structure was monitored during ambient vibrations created by heavy traffic and during self excitation tests. Free vibrations and forced vibrations were generated using the 6 mton AMD located at the top of the test structure operated in reverse action of its usual function. Note that the presence of the AMD in the same test structure allows also a performance comparison with the active bracing system as further explained. The "actual test" of the system was observed during three strong ground motions that occurred on April 10, April 14, and May 11, 1992. The three earthquakes of magnitude 4.9 5.0, and 5.6 (respectively) had peak accelerations of approximately 10 cm/sec^2 (approximately 1% of gravity).

6.1 Identification of Dynamic Properties

The dynamic properties of the uncontrolled system are determined from frequency response functions obtained from ambient vibration tests or sweep tests produced with the bracing system. The dynamic properties, listed in Table 6.1, did not change during the observation period of 20 months except for small variations within the measurement accuracies. It is interesting to note the lower damping ratios in the y-direction as compared with the ratios in the x-direction. It should be remembered that the x-direction is reflecting the strong axis of the columns and that connections are different in both directions. The mode shapes were orthonormalized for the computation of the control gain coefficients. The difference between the orthonormalized and the unmodified

Table 6.1 Uncontrolled Dynamic Properties of Structure

Direction (1)	Mode (2)	(3)	I (4)	II (5)	III (6)	IV (7)	V (8)	VI (9)
	Frequency	Hz	0.98	2.88	4.93	7.18	9.79	13.23
	Damping	%	1.0%	2.0%	4.0%	8.0%	(>10%)	(>10%)
		6	0.0264	-0.0248	0.0181	-0.0130	-0.0019	0.0001
		5	0.0224	-0.0030	-0.0204	0.0287	0.0003	0.0006
X	Modal	4	0.0185	0.0163	-0.0176	-0.0252	0.0130	-0.0051
	Shapes	3	0.0125	0.0230	0.0104	-0.0000	-0.0264	0.0161
		2	0.0069	0.0170	0.0212	0.0119	0.0102	-0.0267
		1	0.0022	0.0063	0.0117	0.0063	0.0279	0.0274
	Participation Factors		50.82	19.94	13.40	4.97	13.20	7.09
	Frequency		0.69	1.91	3.18	4.39	5.81	8.30
	Damping		0.5%	0.3%	0.7%	1.5%	(>15%)	(>15%)
		6	0.0268	-0.0234	0.0210	0.0065	0.0001	-0.0004
		5	0.0230	-0.0040	-0.0275	0.0196	-0.0077	0.0029
Y	Modal	4	0.0183	0.0187	-0.0088	-0.0196	0.0227	-0.0097
	Shapes	3	0.0114	0.0229	0.0085	-0.0095	-0.0262	0.0158
		2	0.0063	0.0171	0.0190	0.0265	0.0030	-0.0186
		1	0.0018	0.0043	0.0068	0.0122	0.0219	0.0325
	Participation Factors		50.01	20.34	10.88	20.42	7.90	12.84

(...) Values in parantheses could not be precisely verified due to excessive noise.

normal modes is almost negligible in the lower four modes and more substantial in the higher two. However, this difference is less important in these higher modes since natural damping in these modes is relatively high.

6.2 Free and Forced Vibration Response

The AMD was activated in both directions using harmonic excitations that produced vibrations in the building. Free vibration observations were obtained from measurements of the structural response made after abruptly stopping the mass damper movement. Typical excitations of the AMD are shown in Fig. 6.1. The responses of the sixth floor shown in Fig. 6.2 indicate large increases in damping, more pronounced in the decay in the y-direction, and a successful brake in the buildup in the resonant response [Fig. 6.2(e) and (f)]. The performance of the structure, summarized in Table 6.2, shows a substantial increase in the equivalent damping ratio [Col.(7) and (8)] and a substantial reduction of the resonant amplitude [Col. (5) and (6)]. Control results from nonresonant forced vibrations indicated good amplitude reductions in all affected modes.

6.3 Response to Earthquakes

The structures response was recorded while the control system was automatically activated during the earthquake episodes mentioned earlier. The ground motion was simultaneously recorded (as shown in Fig. 6.3) and is used with an analytical model to estimate the probable response of the structure in the uncontrolled mode. The analytical model was carefully calibrated prior to its use for earthquake response estimates by comparing the structural response in various tests with the ones computed (Aizawa et al 1990, Wang, et al 1992). Some typical response histories of the sixth floor are shown in Fig. 6.4 for the controlled (observed) and the uncontrolled (estimated) cases. The peak response and the RMS are tabulated in Table 6.3 for the sixth floor and for the base of the structure.

Table 6.2 Characteristics of Harmonic Loading Tests

Vibration Source	Control Status	Response Frequency (Hz)		Maximum Velocity (cm/sec)		Equivalent Damping (%)	
		X	Y	X	Y	X	Y
(1)	(2)	(3)	(4)	(5)	(6)	(7)	(8)
Free Vibrations	OFF	0.98	0.68	6.26	5.64	1.04	0.55
	ON	0.98	0.68	6.86	6.86	3.34	3.47
Resonant Force Vibrations	OFF	0.95	0.70	(12.78)	(23.42)	1.04	0.55
	ON	0.95	0.70	3.98	3.84	3.34	3.47
Nonresonant Force Vibrations	OFF	0.80	0.80	2.57	2.57	1.04	0.55
	ON	0.80	0.80	1.22	1.71	3.34	3.47
	OFF	2.00	2.00	0.63	2.53	1.04	0.55
	ON	2.00	2.00	0.52	0.89	3.34	3.47

( ) Estimated values (actual values exceed allowable in structure)

Table 6.3 Peak and RMS Response During Earthquakes

Response	Floor	X Direction						Y Direction					
		April 10,92		April 14,92		May 11,92		April 10,92		April 14,92		May 11, 92	
		Control		Control		Control		Control		Control		Control	
		ON	OFF	ON	OFF	ON	OFF	ON	OFF	ON	OFF	ON	OFF
(1)	(2)	(3)	(4)	(5)	(6)	(7)	(8)	(9)	(10)	(11)	(12)	(13)	(14)
(a) Peak response													
Acceleration (cm/sec/sec)	6	11.36	15.30	15.25	19.50	19.13	30.52	15.66	15.46	11.50	15.03	17.82	22.28
	3	13.95	10.91	12.70	14.40	16.58	19.17	16.47	19.28	22.98	40.29	15.18	19.17
	Base	7.36	7.36	8.93	8.93	7.57	7.57	11.77	11.77	9.24	9.24	9.94	9.94
Velocity (cm/sec)	6	0.74	1.16	1.06	1.66	2.82	n/a	1.27	1.55	1.53	1.58	2.15	n/a
	3	0.60	0.73	0.75	1.15	1.33	n/a	1.26	1.15	0.96	1.78	1.74	n/a
	1	0.54	0.61	0.87	0.92	0.29	n/a	0.42	0.81	0.48	0.69	0.30	n/a
	Base	0.23	0.23	0.37	0.37	0.64	n/a	0.74	0.74	0.49	0.49	0.62	n/a
Displacement (mm)	6	1.00	1.51	1.45	1.97	3.67	6.07	1.70	1.70	1.96	2.44	3.45	4.70
	3	0.50	0.82	0.86	1.05	2.26	2.96	1.00	1.10	1.15	1.28	1.83	2.23
	Base	0.30	0.30	0.40	0.40	0.94	0.94	0.78	0.78	0.55	0.55	0.79	0.79
Control Force (kN)		64.0		82.7		177.7		143.2		88.6		107.4	
Control Force/Weight		1.07%		1.38%		2.96%		2.39%		1.48%		1.79%	
(b) RMS response													
Acceleration (cm/sec/sec)	6	1.89	3.39	2.28	3.51	3.75	6.79	1.97	4.67	1.91	4.14	3.46	5.68
	3	3.17	2.66	3.51	3.01	2.86	5.37	2.96	4.57	3.52	5.13	3.22	5.37
	Base	1.04	1.04	1.30	1.30	1.28	1.28	1.02	1.02	1.11	1.11	1.17	1.17
Velocity (cm/sec)	6	0.19	n/a	0.26	n/a	0.53	n/a	0.20	n/a	0.25	n/a	0.55	n/a
	3	0.12	n/a	1.44	n/a	0.27	n/a	0.16	n/a	0.17	n/a	0.30	n/a
	1	0.11	n/a	0.15	n/a	0.05	n/a	0.10	n/a	0.10	n/a	0.06	n/a
	Base	0.04	n/a	0.06	n/a	0.10	n/a	0.05	n/a	0.06	n/a	0.11	n/a
Displacement (mm)	6	0.29	0.77	0.42	0.69	0.85	1.62	0.33	1.08	0.46	0.86	1.09	1.31
	3	0.15	0.36	0.21	0.33	0.43	0.77	0.25	0.52	0.26	0.41	0.51	0.62
	Base	0.11	0.11	0.12	0.12	0.18	0.18	0.06	0.06	0.08	0.08	0.17	0.17
Control Force (kN)		17.2		21.7		39.1		16.3		16.9		46.5	
Control Force/Weight		0.29%		0.36%		0.65%		0.27%		0.28%		0.77%	

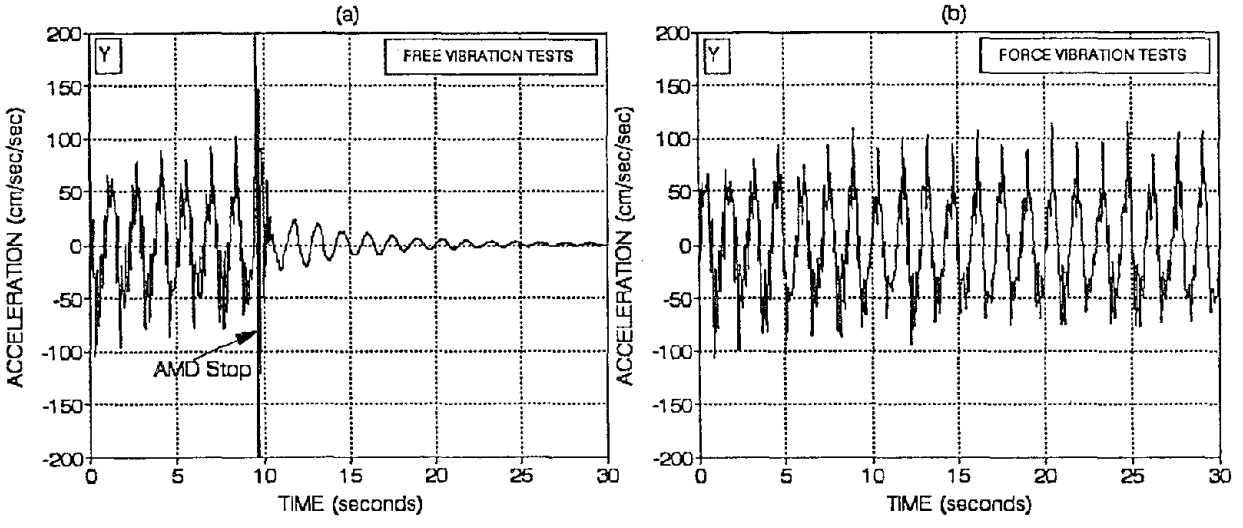

Fig. 6.1 Typical Acceleration of AMD During Harmonic Loading Tests

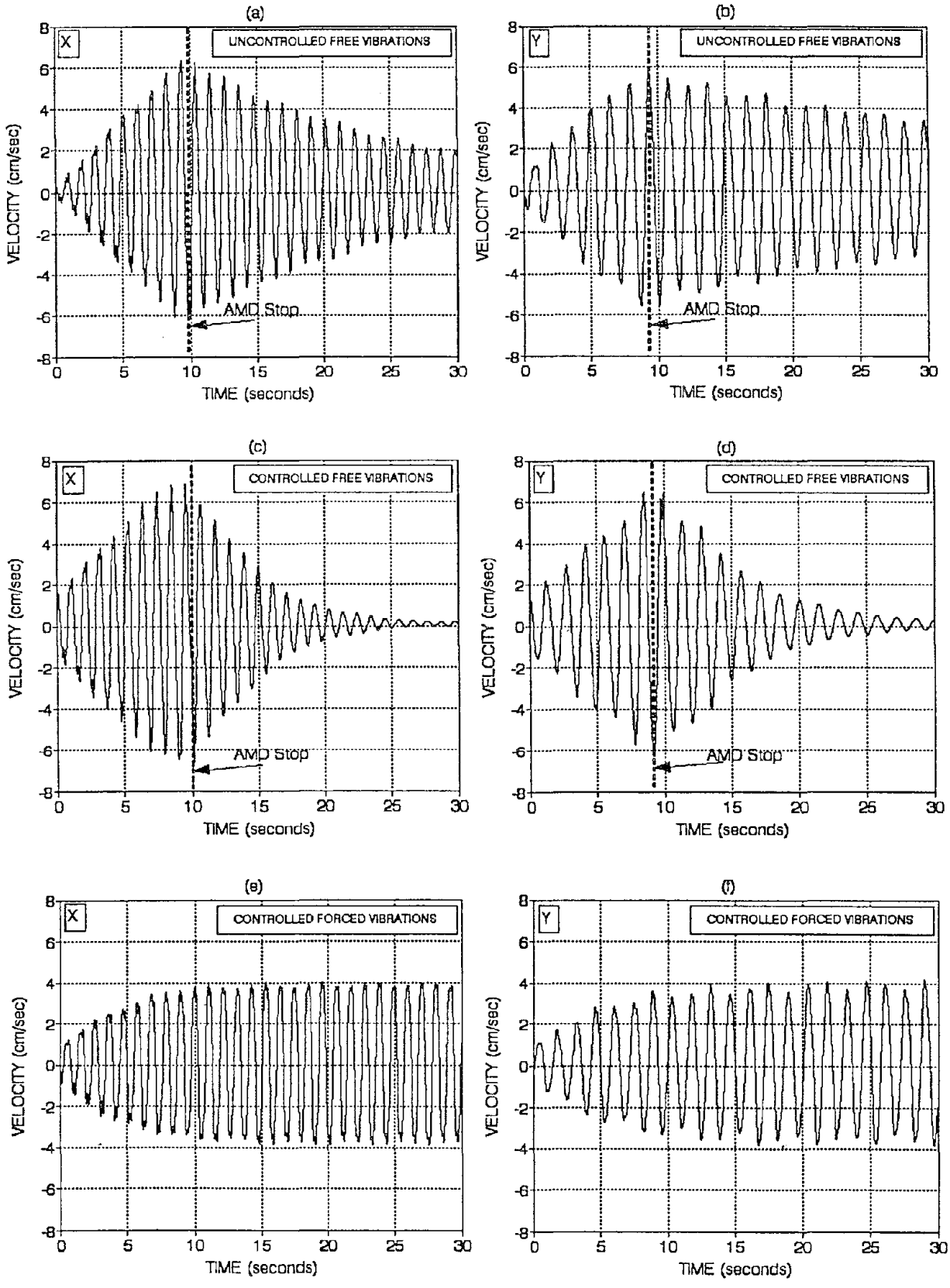

Fig. 6.2 Sixth Floor Response During Harmonic Loading Tests

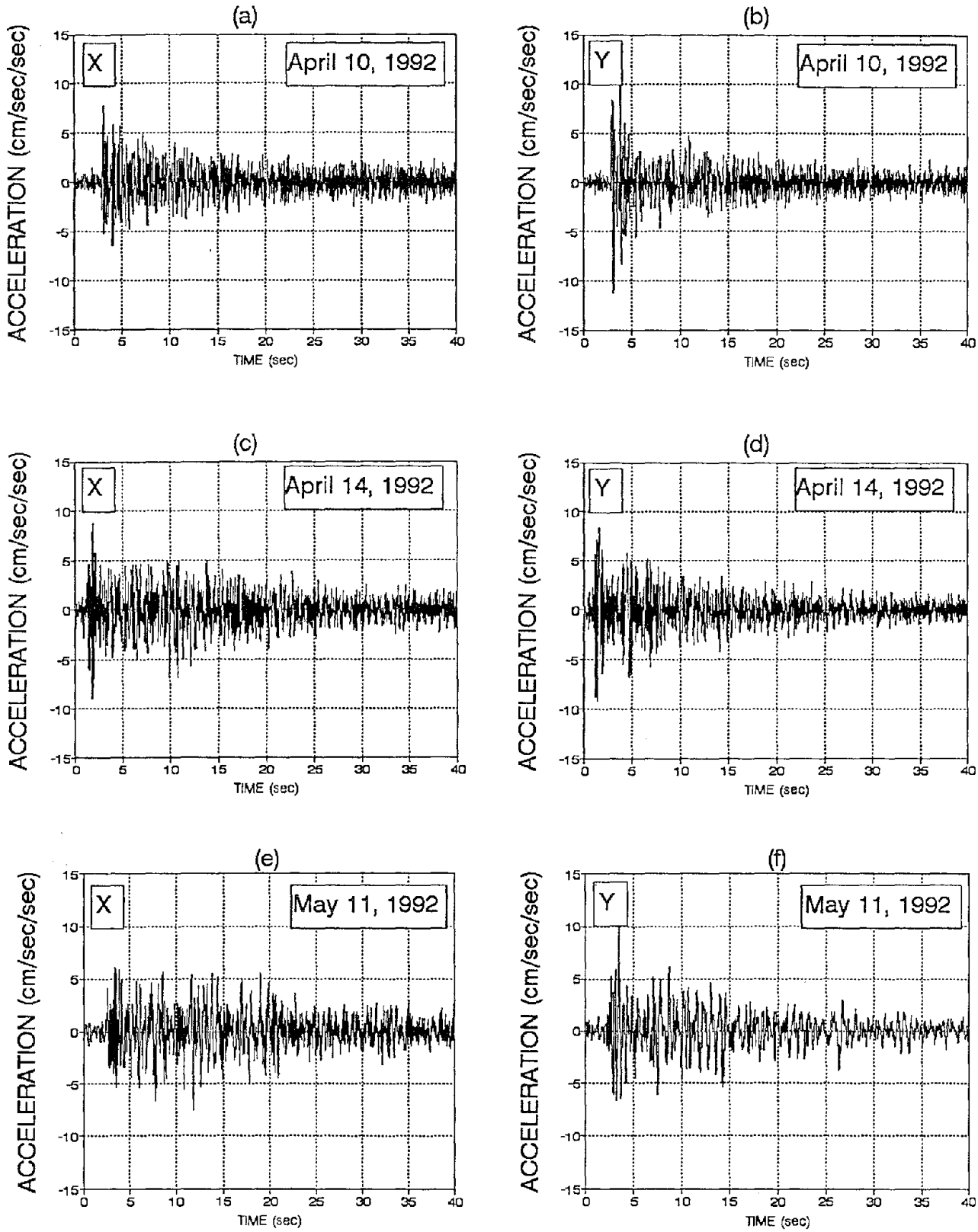

Fig. 6.3 Ground Accelerations During Earthquakes

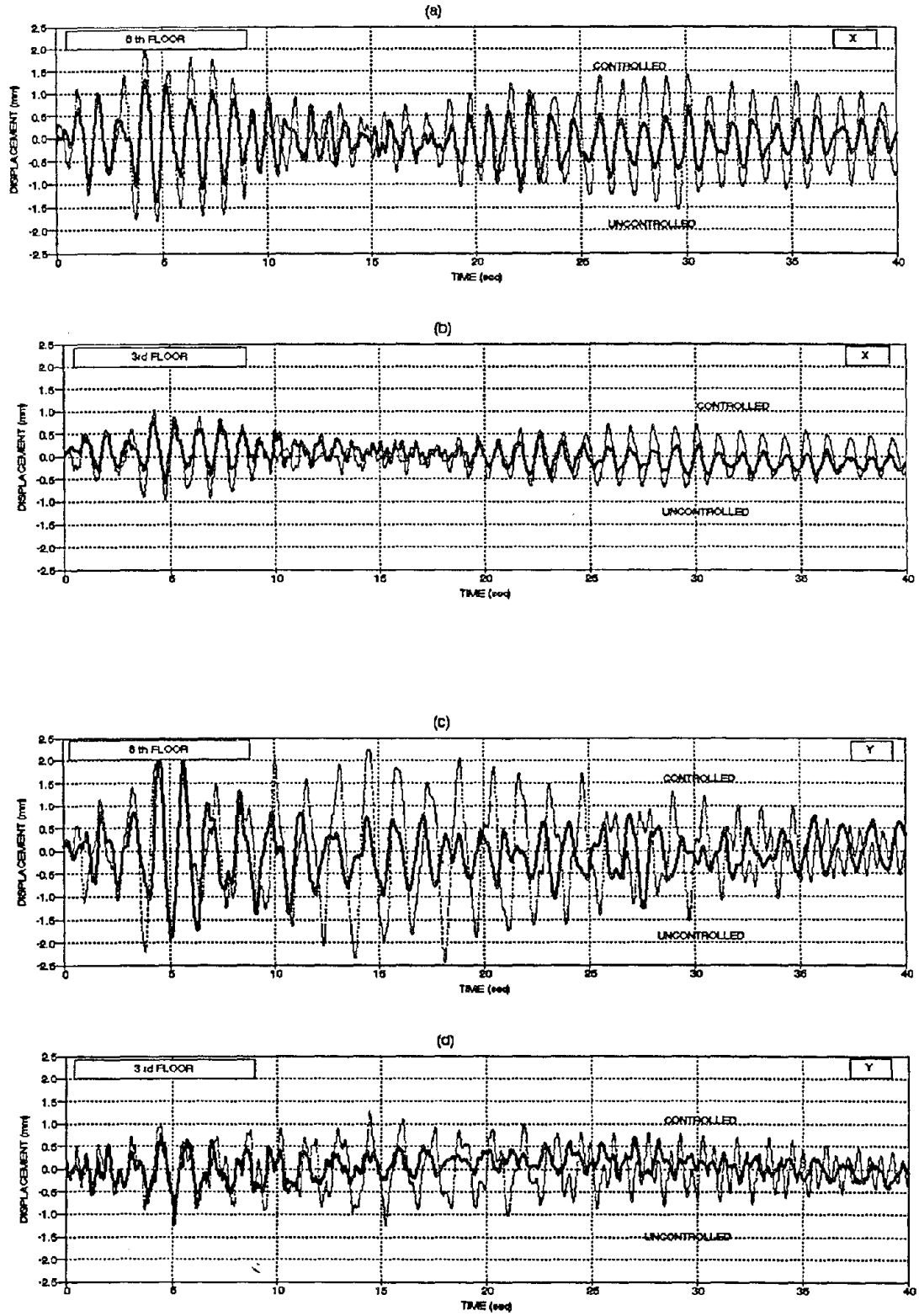

Fig. 6.4 Comparison of Controlled (Observed) vs. Uncontrolled (Estimated) Responses

The **peak responses** are generally reduced in the x-direction, but are less affected in the y-direction. The **RMS responses** are, however, reduced in all cases which indicate an overall reduction of vibration amplitudes throughout the motion.

The reason for small or no reduction of peaks in the y-direction is the inability of the control algorithm used to reduce substantially the first amplitude, which is the largest. Alternative control algorithms can handle this problem. It should be noted also, that the RMS is more indicative of the energy transferred into the structure, and therefore energy reductions obtained with active control are substantial.

The transfer functions of the structural response with respect to the excitation input are indicative of the change of dynamic properties during control as shown in Fig. 6.5. The controlled response has lower peaks and wider distributions around the peak, indicating damping increase. The active bracing system produces a somewhat uniform reduction of modal responses as indicated in the transfer functions in Fig. 6.5. The controlled peaks are somewhat shifted from the uncontrolled ones, although the control algorithm used is supposed to affect only the damping and not the stiffness. This shift is likely due to the imperfect compensation of time delay, which creates "leaks" in the stiffness components and, therefore, the frequency shifts.

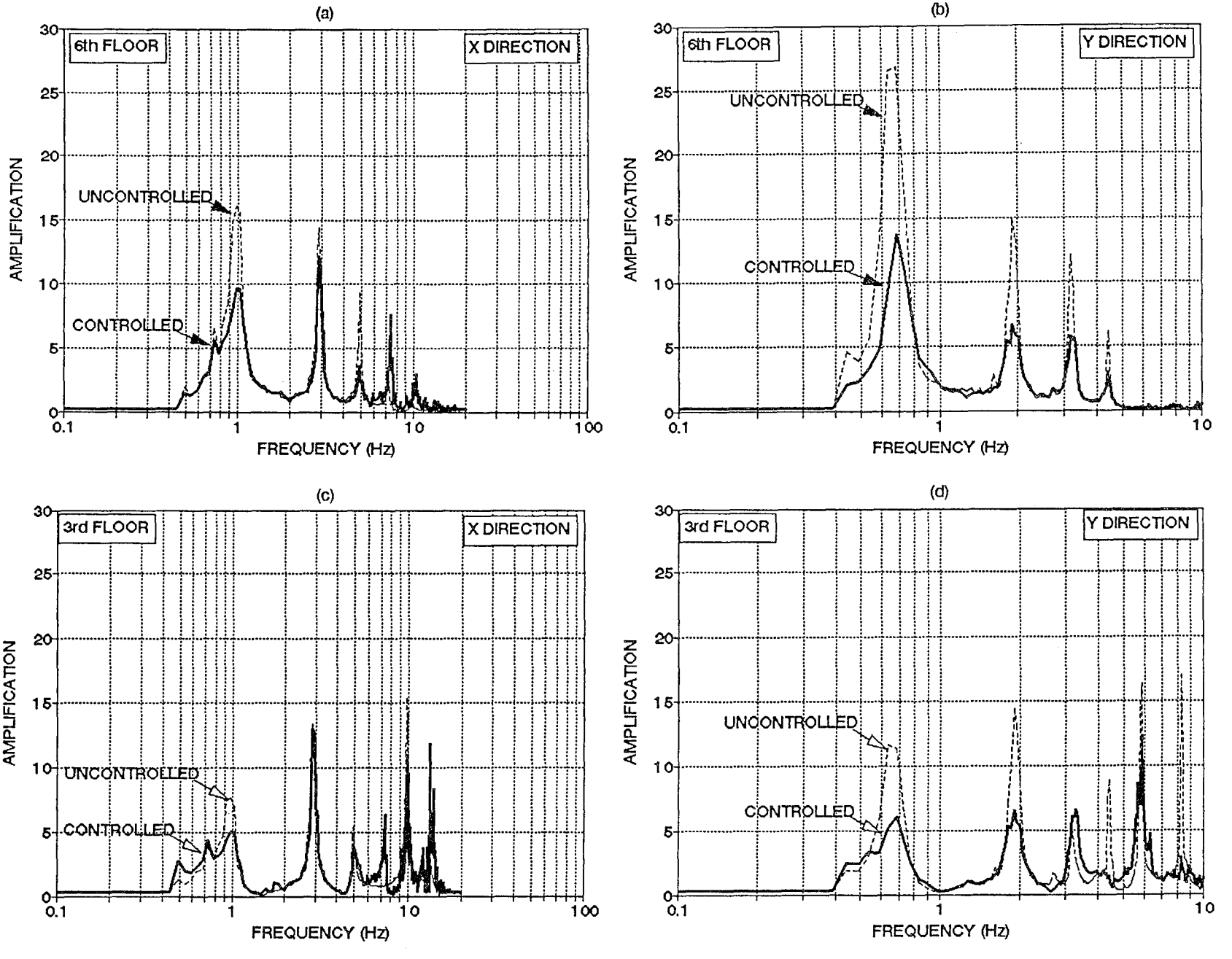

Fig. 6.5 Acceleration Transfer Functions With and Without Active Braces

SECTION 7

ANALYTICAL PREDICTION OF OBSERVED RESPONSE

The analytical model was calibrated based on initial observations during the identification studies. Two models were used: (i) A discrete model based on modal time analysis (Soong et al 1991) and (ii) an approximated continuous model (Wang et al 1992). Both models produced similar results for the simulations used for the design of the bracing system. The approximated continuous model was used to predict the uncontrolled and the controlled responses of the sixth floor of the structure during the nonresonant forced vibration tests as shown in Fig. 7.1. Some discrepancies occur at the beginning of the motion presented. These discrepancies are due to the transient response, which appears in the analysis, while the observed structural response was recorded during the steady state.

The actual earthquake response was predicted using the time step analysis and the identified properties of the system. The control forces were estimated using the uncompensated gains. The analysis was performed using the recorded acceleration time histories shown in Fig. 6.3. The time histories of the analytical and observed responses are compared in Fig. 7.2 for the April 14th earthquake. The differences in the maximum peaks are less than 10%, while the RMS differences are less than 2%. Considering inherent imperfections in the structural system, the analytical predictions seem to be adequate for interpreting the structural response and for designing new systems.

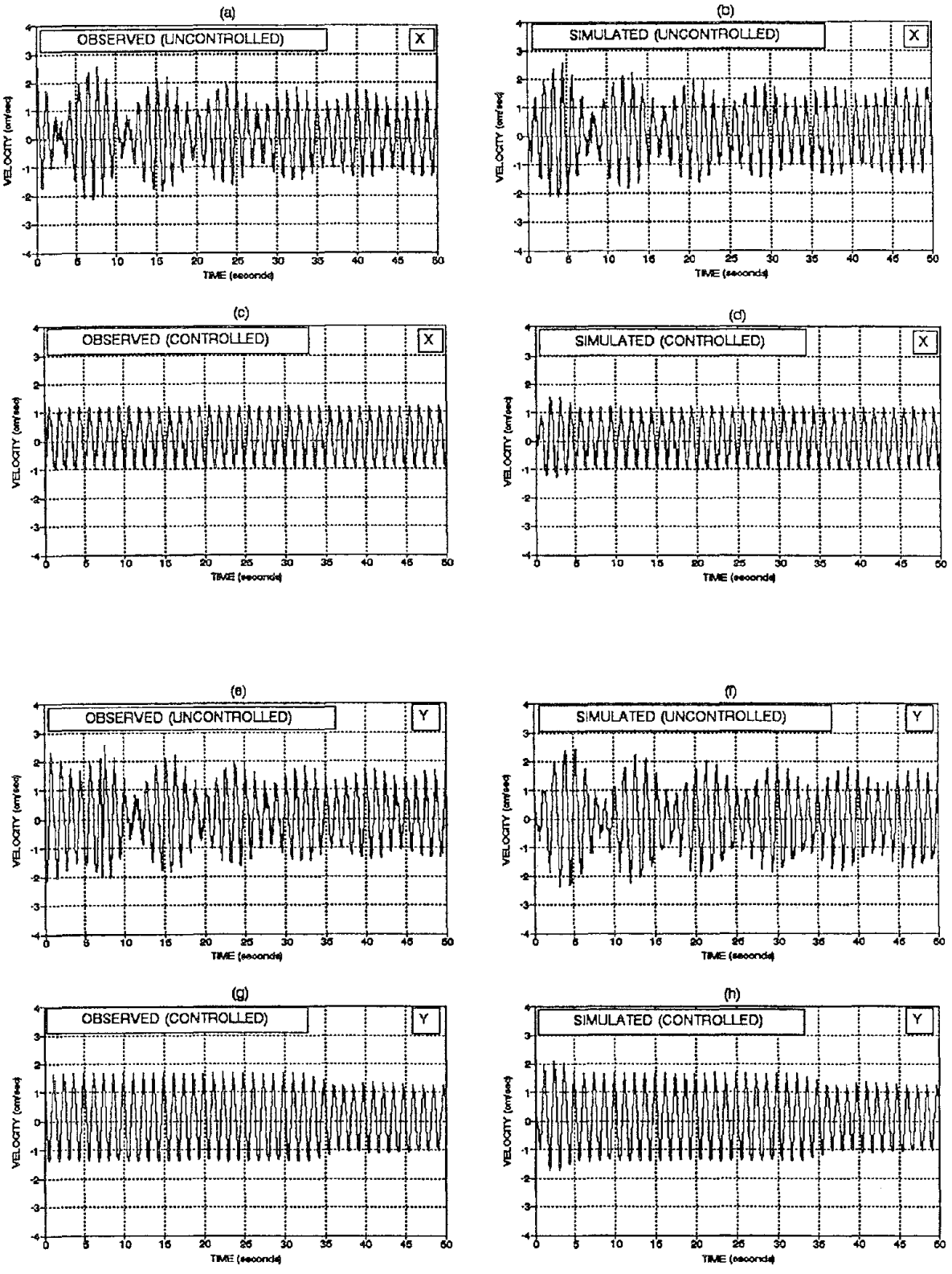

Fig. 7.1 Comparison of Analytical and Observed Responses During Harmonic Loading Tests

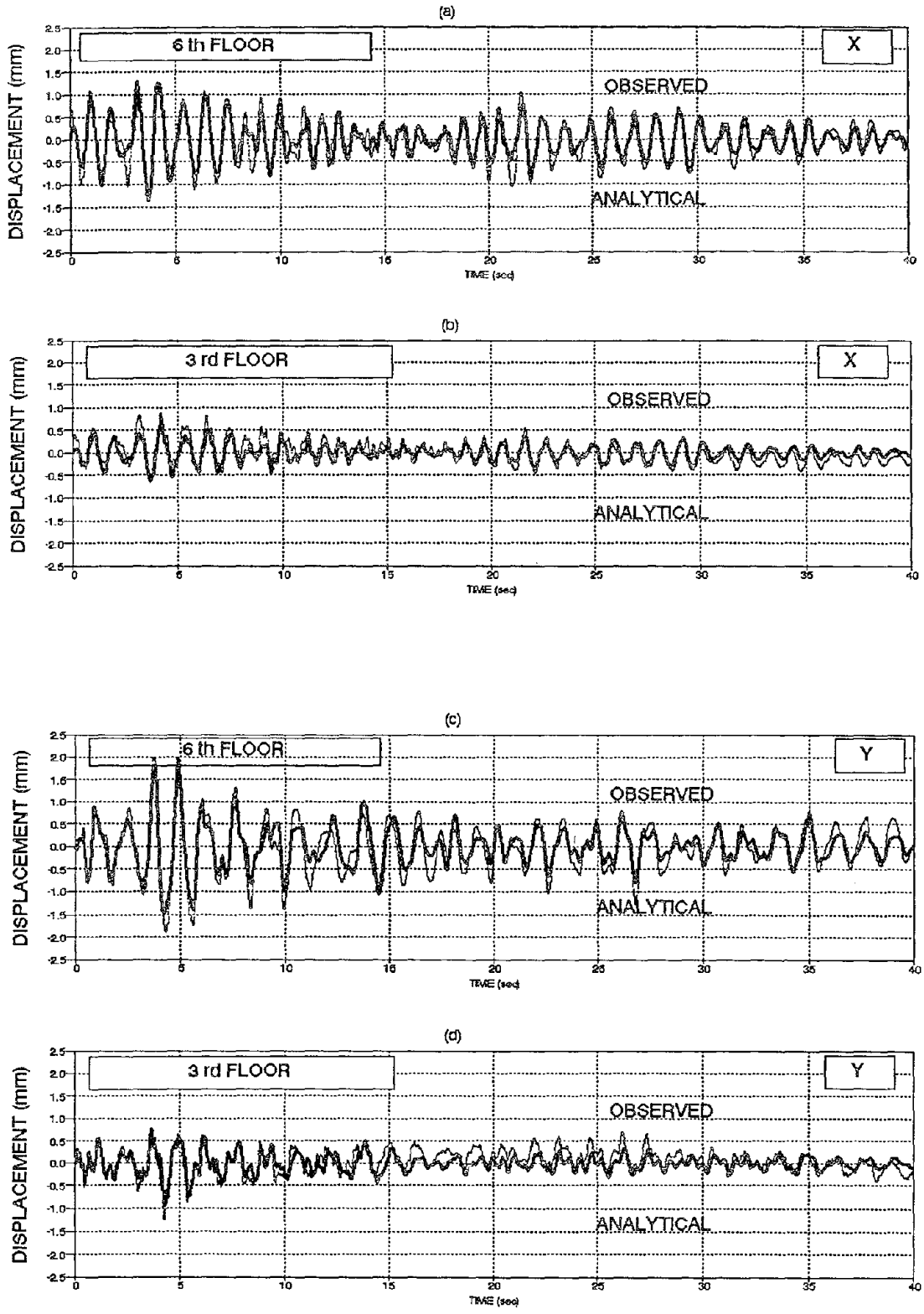

Fig. 7.2 Comparison of Analytical and Observed Responses During April 14 Earthquake

SECTION 8

COMPARISON OF PERFORMANCES OF ABS AND AMD

As a active control devise, an Active Mass Damper system (AMD) has been installed on the top floor of the same test building with ABS (Fig. 2.1) to compare their performances. The top view of the AMD system is shown in Fig. 8.1. A complete description of the AMD system and some observed results are given by Aizawa, S., et al. (1990). In the AMD system, a six-ton moving mass is suspended (T=3.1secs) so that it can respond instantaneously. The structural response can be controlled in two directions by the two electrohydraulic servo actuators, which are installed along orthogonal directions.

While both systems were installed in the same building, the structural control is performed by only one at a time. The control effect of the AMD system was examined during the Izu-Oshima earthquake on October 14, 1989 and on February 20, 1990. The observation results are shown in Fig. 8.2. The structural response in the frequency domain is shown in Fig. 8.3.

Summarizing the observation results for both control systems, a rough performance comparison of AMD and ABS is shown in Table 8.1.

Table 8.1 - Comparison of AMD and ABS

		AMD	ABS
Average Reduction of Peak Structural Response	Displacement	56%	29%
	Acceleration	22%	26%
Maximum Actuator Movement (cm)		10.51	0.194

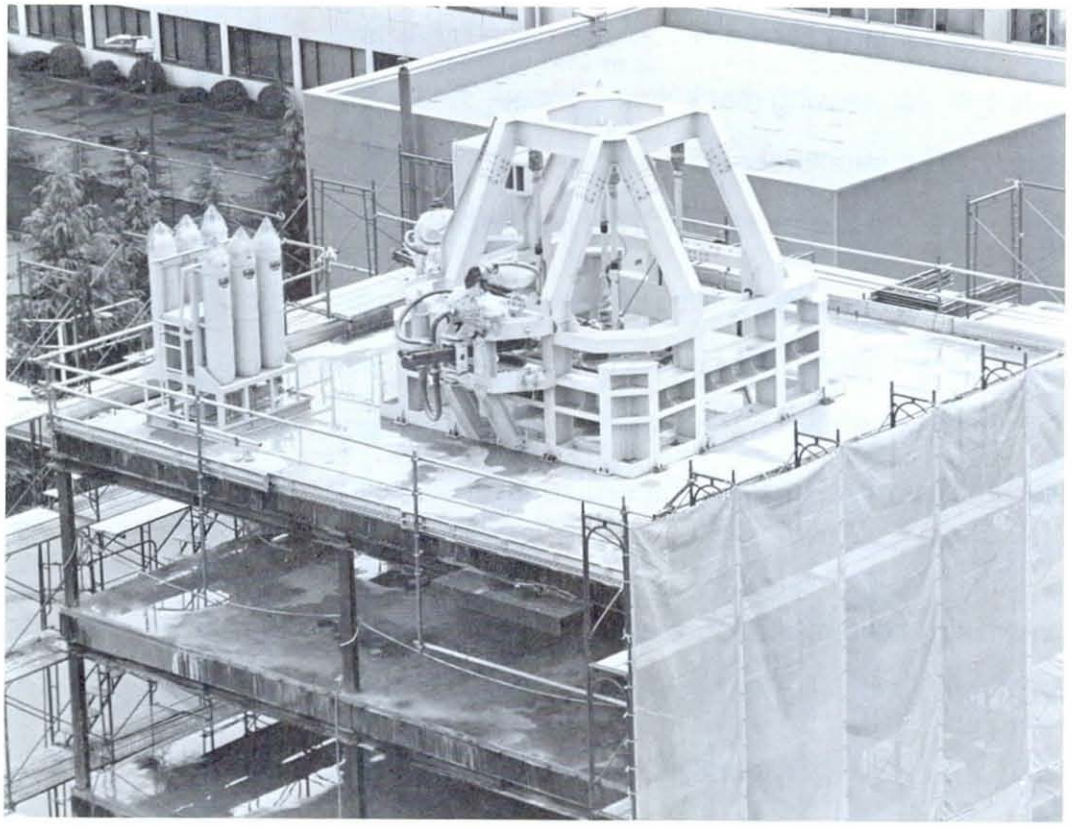

Fig. 8.1 Full-Scale AMD

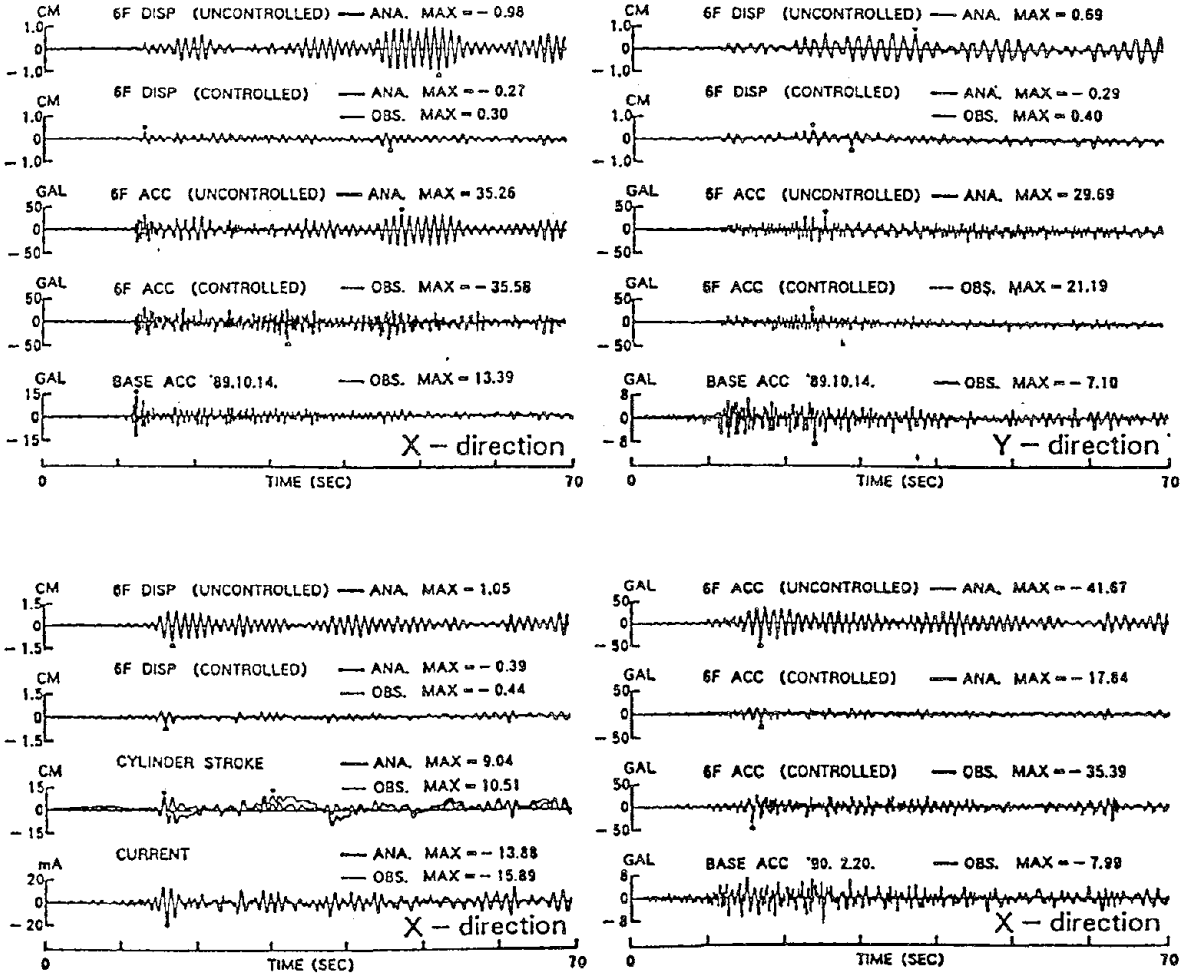

Fig. 8.2 Observation Results of AMD

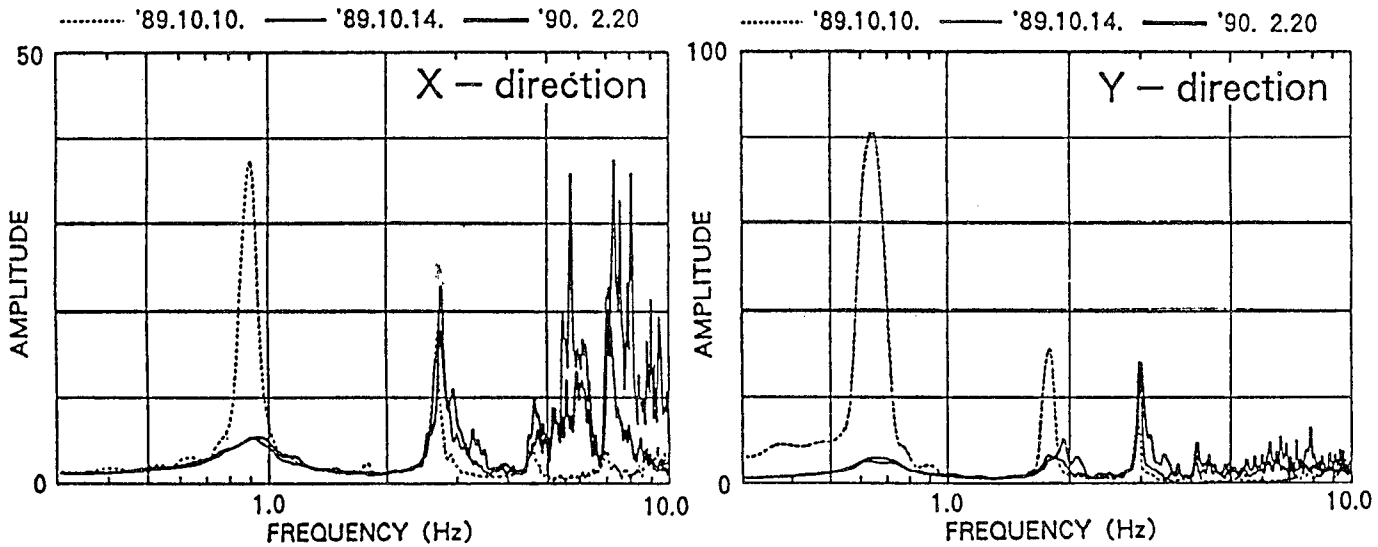

Fig. 8.3 Acceleration Transfer Functions With and Without Active Mass Damper (From Aizawa et al, 1990)

Note that the AMD system has a better reduction of displacement response and a lesser reduction of accelerations. This implies a more comfortable response using the ABS and lesser base shear

using the AMD. The maximum actuator movement is an indicator of the required input energy. It is very large for the AMD system and is quite small for the ABS indicating substantially less energy needed by the ABS. Comparing the response transfer functions shown in Fig. 6.5 and Fig. 8.3, it is noted that the AMD reduces the structural response substantially in the first and second modes in the y-direction and only in the first mode in the x-direction (Fig. 8.3). The ABS system reduces the structural response in all modes, as can be observed in Fig. 6.5. The main reasons of this behavior are (i) the ABS has better ability to redistribute earthquake energy in higher modes and suppress their influence, as noted also by Yang (1982) and (ii) the AMD constructed in this building was designed to suppress only the lower modes. A change in the control algorithm can produce even better performance in the higher modes for the ABS.

SECTION 9

CONCLUDING REMARKS

The design, installation, and operational characteristics of a full-scale ABS for earthquake resistance of a building have been presented in this report. The control algorithms were developed based on the classic optimal closed-loop control theory. As required by sensor limitations, two modified control algorithms were used. They are (1) velocity feedback with observer, and (2) three-velocity feedback. Both alternatives have been proven to be effective through numerical verification.

Based on the recognition that it is more efficient to control a structure by applying a force rather than a moment, (Yang et al. 1978, Reinhorn et al. 1989), horizontal control forces were applied to the first floor through the action of diagonal active braces. While it is conceivable that extra column axial forces are introduced by the vertical component of the bracing forces when the control system is activated, the $P - \Delta$ effect, which is a problem in structures with large deformations, be less pronounced since the braces are connected to the first floor where the displacement is relatively small.

While several active mass dampers have been implemented in full-scale structures over the last few years, the active bracing system reported here represents the *first* full-scale active system of this type developed and tested under actual ground motions. The results presented in this report demonstrate that:

(a) The concept of an active tendon or bracing system, originated almost 20 years ago, has led to the successful development of the device for civil engineering structural control.

(b) The success of the full-scale ABS performance is the culmination of numerous analytical studies and carefully planned laboratory experiments involving model structures.

(c) The ABS can be implemented with existing technology under practical constraints such as power requirements and under stringent demand of reliability.

(d) The use of ABS in existing structures can be a practical solution for retrofit as demonstrated by this full-scale experiment. Note that the active braces were added only after the structure was completed.

(e) The full-scale ABS performs, by and large, as expected, and its performance can be adequately predicted through simplified analytical and simulation procedures.

(f) The experience gained through the development of this system can serve as an invaluable resource for the development of active structural control systems in the future.

SECTION 10

REFERENCES

Aizawa, S., Hayamizu, Y., Higashino, M., Soga, Y., Yamamoto, M., and Haniuda, N. (1990). "Experimental Study of Dual Axis Active Mass Damper." Proceedings of the U.S. National Workshop on Structural Control Research, (Housner, G.W. and Masri, S.F., eds), University of Southern California, Los Angeles, 68-72.

Chen, C.T. (1984) *Linear System Theory and Design*, Holt, Rinehart and Winston, NY.

Chung, L.L., Lin, R.C., Soong, T.T. and Reinhorn, A.M. (1988), "Experimental Study of Active Control of MDOF Structures Under Seismic Excitations," Report NCEER-88-0025, National Center for Earthquake Engineering Research, Buffalo, NY.

Chung, L.L., Lin, R.C., Soong, T.T. and Reinhorn, A.M. (1989), "Experimental Study of Active Control for MDOF Seismic Structures," ASCE J. Engr. Mech. Div., Vol. 115, No. 8, pp. 1609-1627.

Chung, L.L., Reinhorn, A.M. and Soong, T.T.(1988), "Experiments on Active Control of Seismic Structures," ASCE J. Engr. Mech. Div., Vol. 114, No. 2, pp. 241-256.

Clough, R.W. and Penzien, J. (1975), Dynamics of Structures, McGraw-Hill, NY.

McGreevy, S., Soong, T.T. and Reinhorn, A.M. (1988), "An Experimental Study of Time Delay Compensation in Active Structural Control," Proceedings of 6th International Modal Analysis Conference and Exhibits, Vol. I, pp. 733-739, Orlando, FL.

Reinhorn, A.M. and Soong T.T., et al. (1989), "1:4 Scale Model Studies of Active Tendon Systems and Active Mass Dampers for Aseismic Protection," Report NCEER-89-0026, National Center for Earthquake Engineering Research, Buffalo, NY.

Reinhorn, A.M., Soong, T.T., Riley, M.A., Lin, R.C., Aizawa, S., and Higashino, M., (1992). "Full Scale Implementation of Active Control - Part II: Installation and Performance," ASCE/J. of Structural Engineering, (in print).

Roorda, J. (1980), "Experiments in Feedback Control of Structures, in *Structural Control*, H.H.E. Leipholz (ed.), North Holland, Amsterdam, pp. 629-661.

Soong, T.T. (1990), *Active Structural Control: Theory and Practice*, Longman, London and Wiley, NY.

Soong, T.T., Reinhorn, A.M., Wang, Y.P. and Lin, R.C. (1991). "Full Scale Implementation of Active Control - Part I: Design and Simulation," ASCE/Journal of Structural Engineering, ASCE, Vol. 117, No.11, 3516-3536.

Wang, Y.P., Reinhorn, A.M. and Soong, T.T. (1992). "Development of Design Spectra for Actively Controlled Wall Frame Buildings," ASCE/Journal of Engineering Mechanics, ASCE, Vol. 118 No. 6, 1201-1220.

Yang, J.N. (1982). "Control of Tall Buildings Under Earthquake Excitations," ASCE/Journal of Engineering Mechanics Division, 18 No.1, 50-68.

Yang, J.N. and Giannopoulos, F. (1978), "Active Tendon Control of Structures," ASCE/Journal of Engineering Mechanics Division., Vol. 104, No. EM3, pp. 551-568.

APPENDIX I

EARTHQUAKE OBSERVATIONS - - TIME HISTORIES

OF OBSERVED MOTIONS AND ESTIMATED RESPONSES

Table A1 provided the description of the three earthquakes that considered in this report. This is followed by the display of a more complete set of the structural response time histories (observed and simulated) related to this earthquakes.

Table A1 - Actual Earthquakes During the Operation Period of ABS

Time of Occurrence	Epicenter Location	Depth (KM)	Magnitude
April 10, 1992 (23:31)	North latitude 35° 14'/ East longitude 139° 38'	89	4.9
April 14, 1992 (12:03)	North latitude 36° 10'/ East longitude 139° 50'	62	5.0
May 11, 1992 (19:07)	North latitude 36° 32'/ East longitude 140° 32'	56	5.6

1. Earthquake on April 10, 1992:

1) Response of 6th Floor in X-Direction

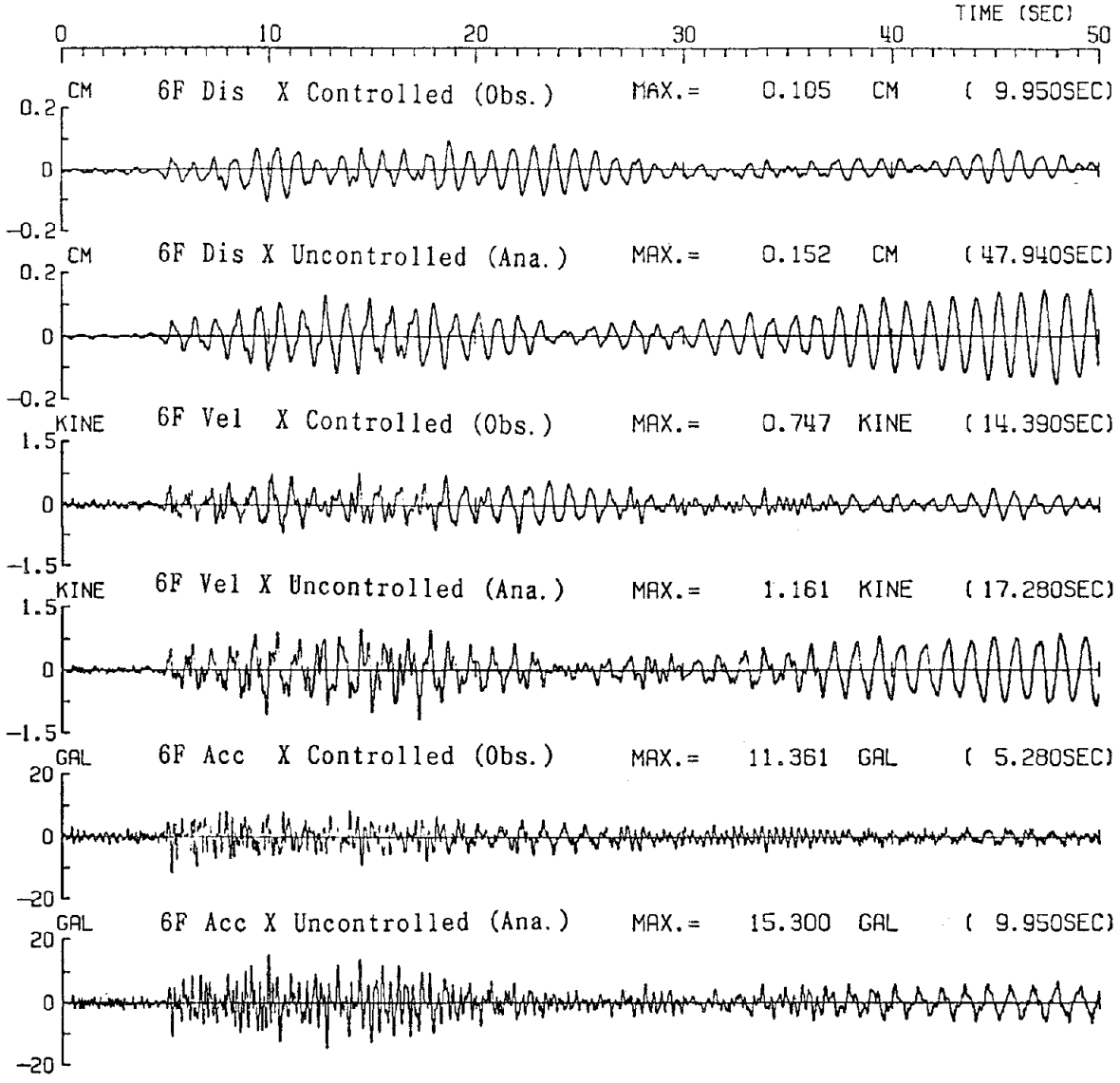

2) Responses of 6th Floor in Y-Direction

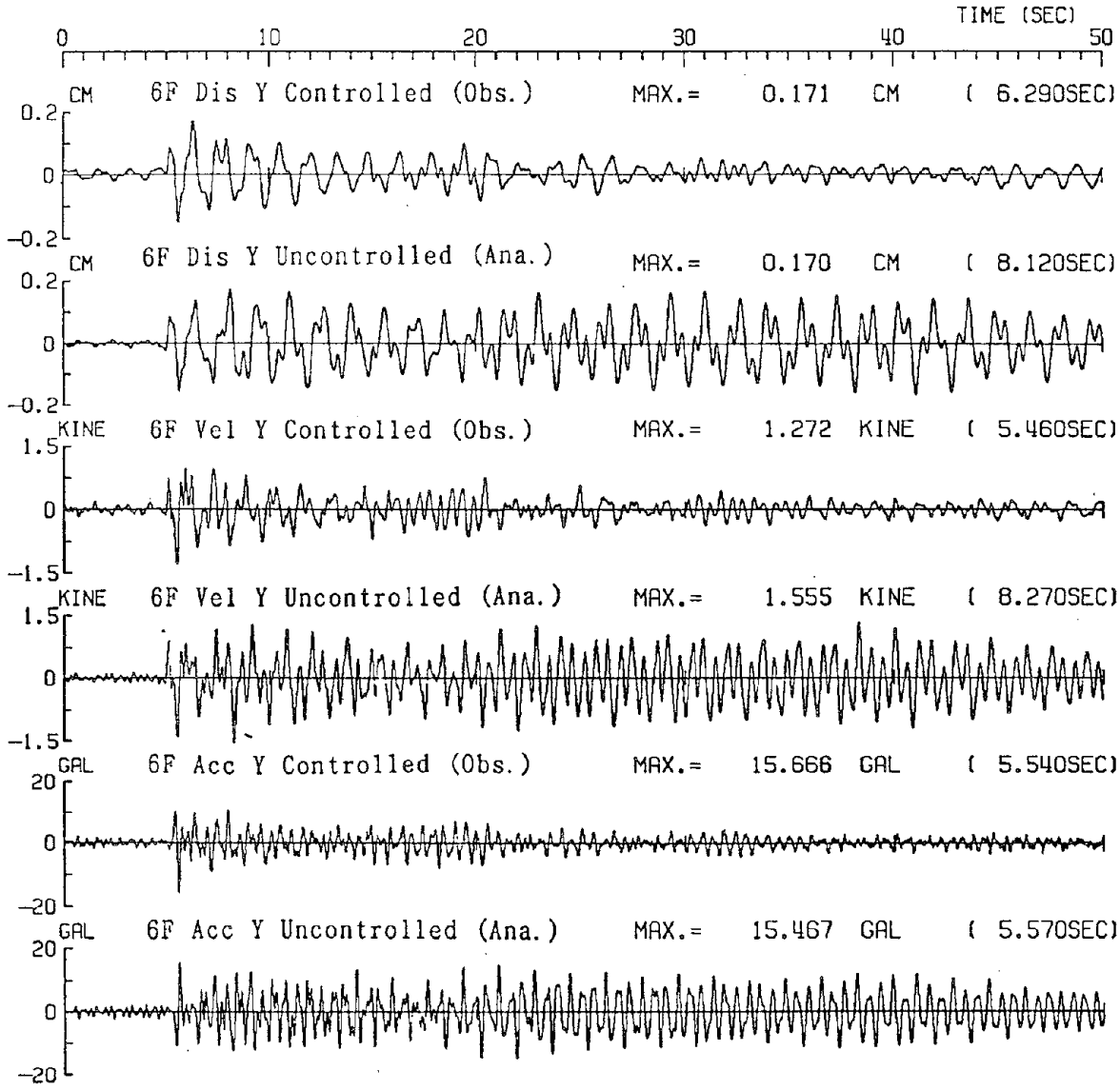

3) Responses of 3rd Floor in X-Direction

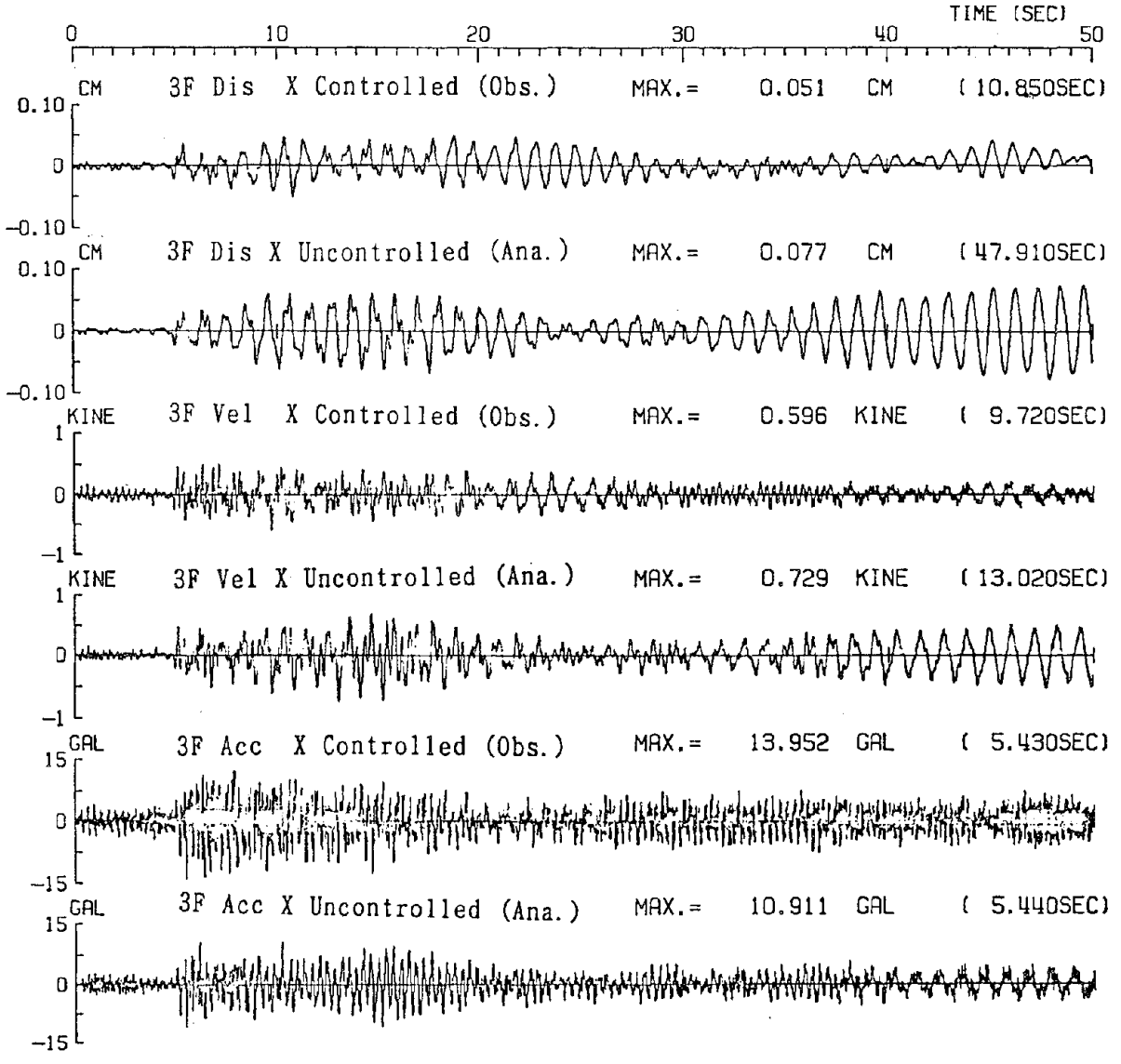

4) Responses of 3rd Floor in Y-Direction

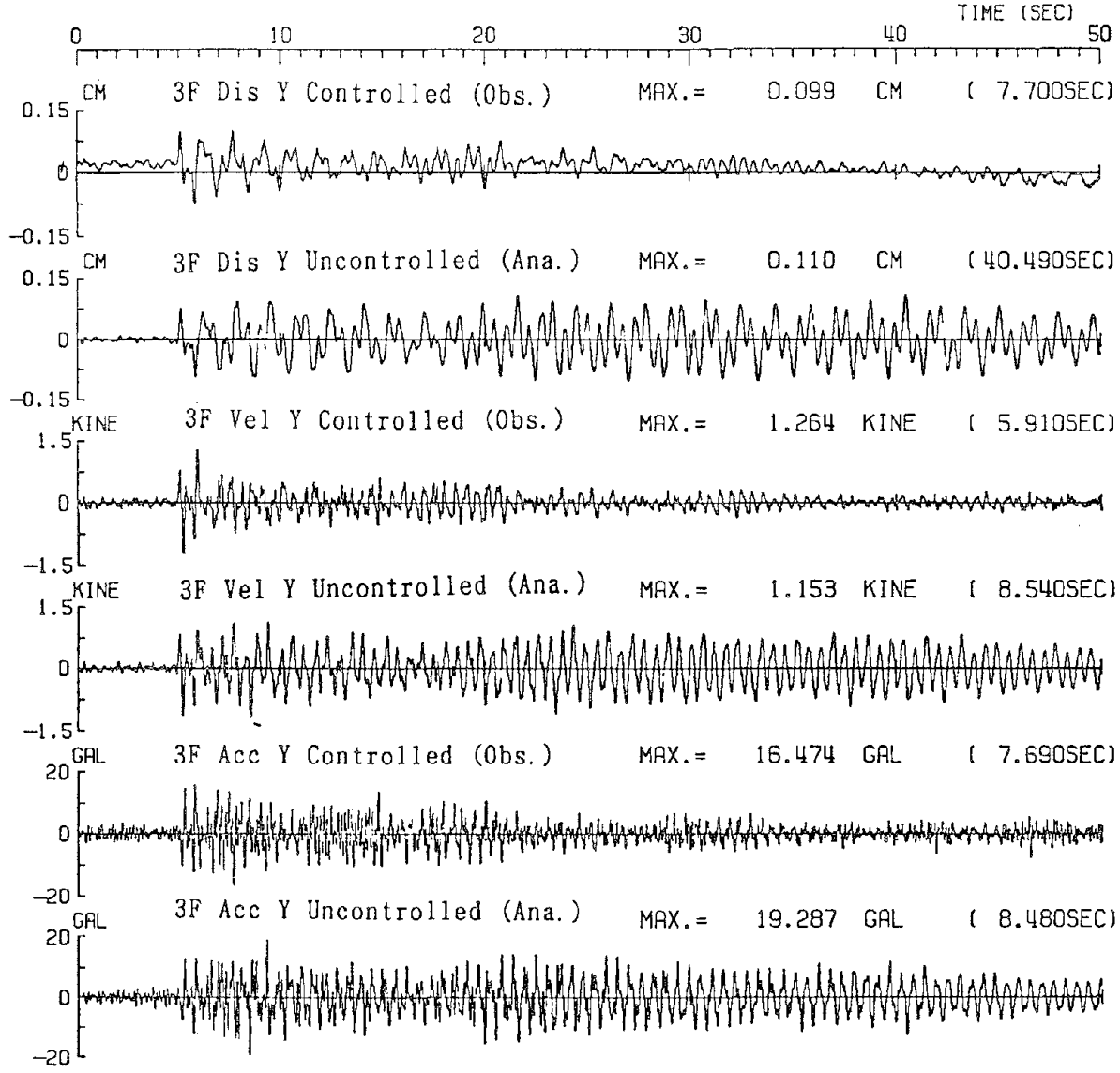

2. Earthquake on April 14, 1992:

1) Response of 6th Floor in X-Direction

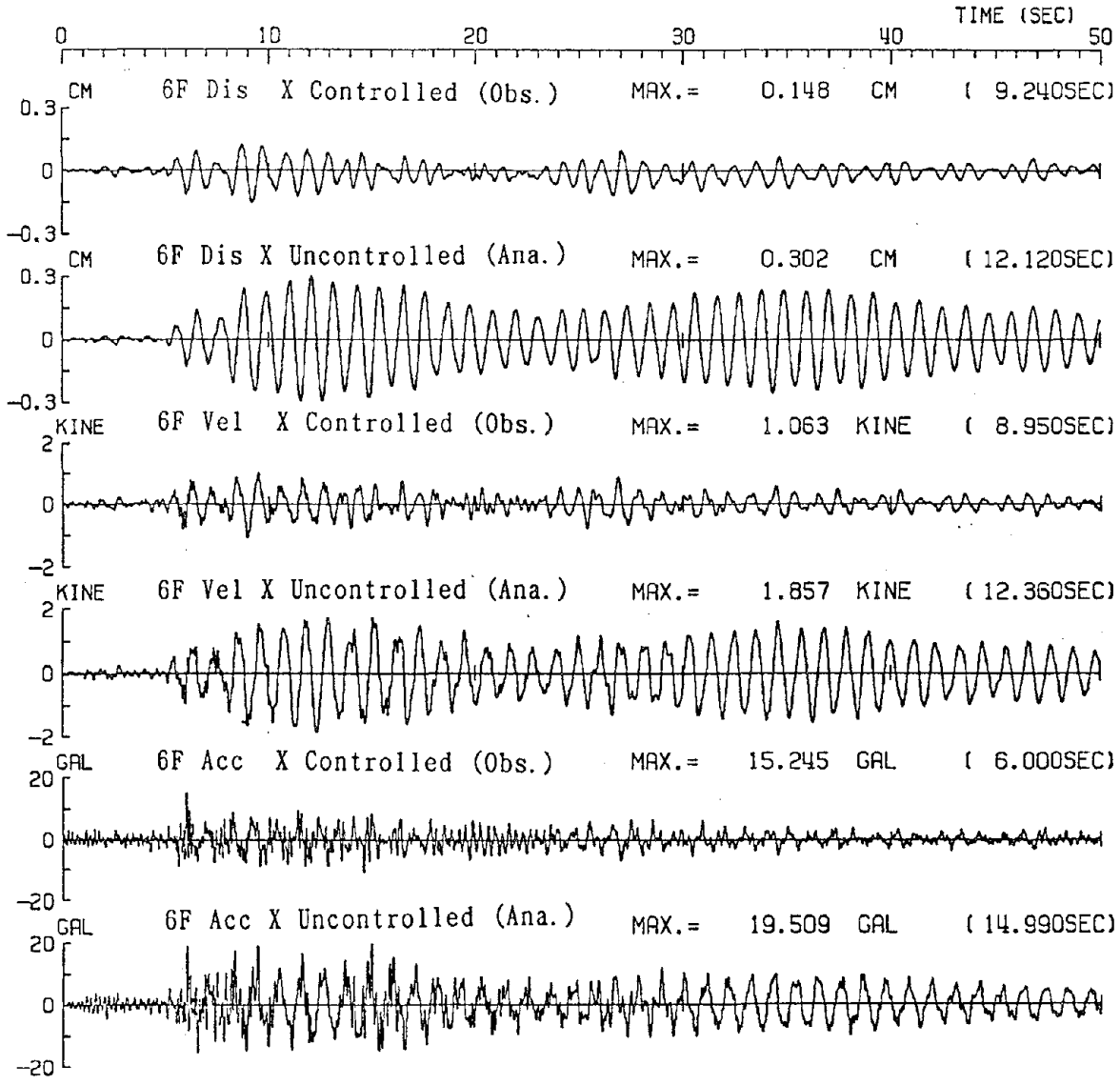

2) Response of 6th Floor in Y-Direction

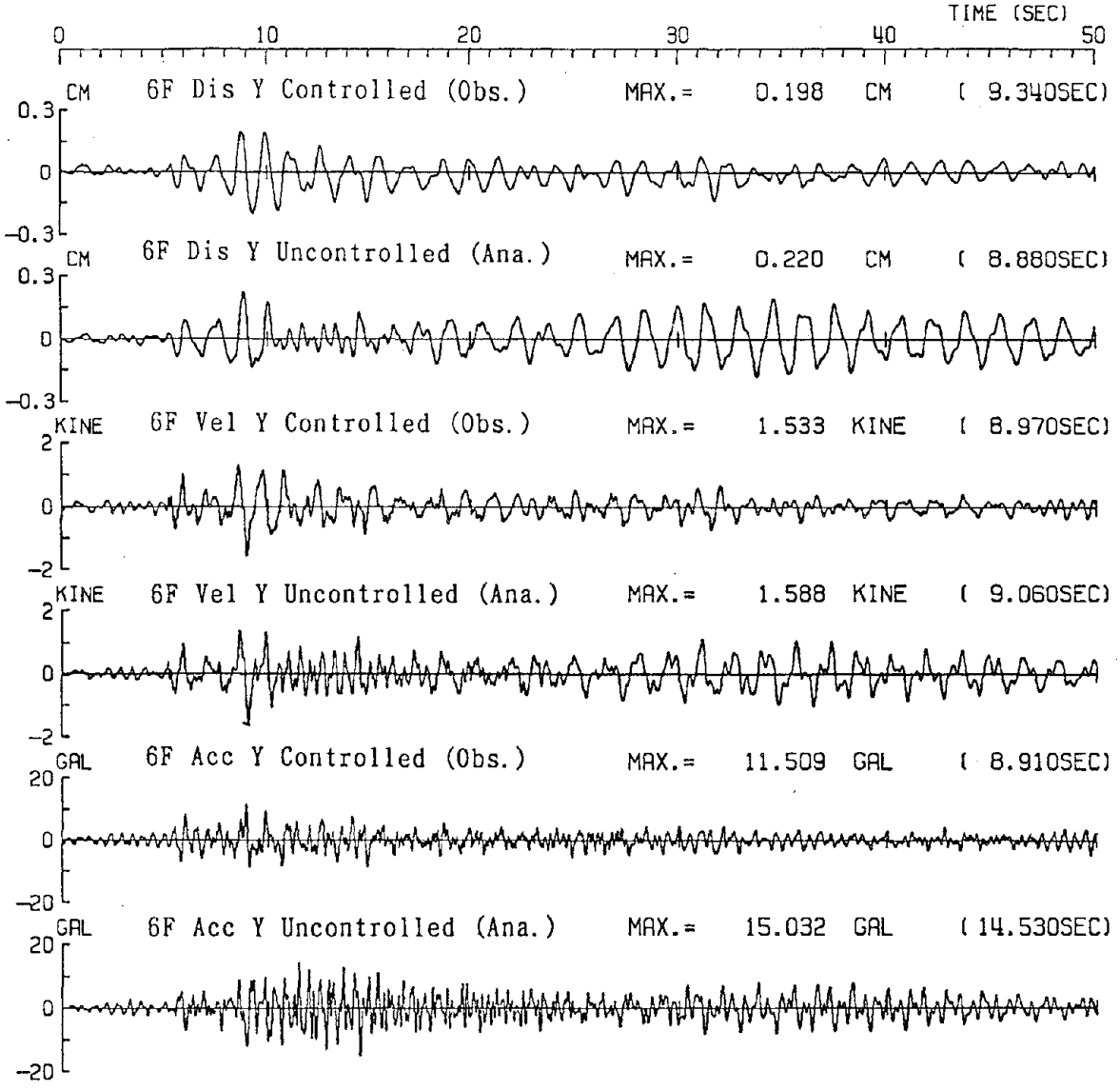

3) Responses of 3rd Floor in X-Direction

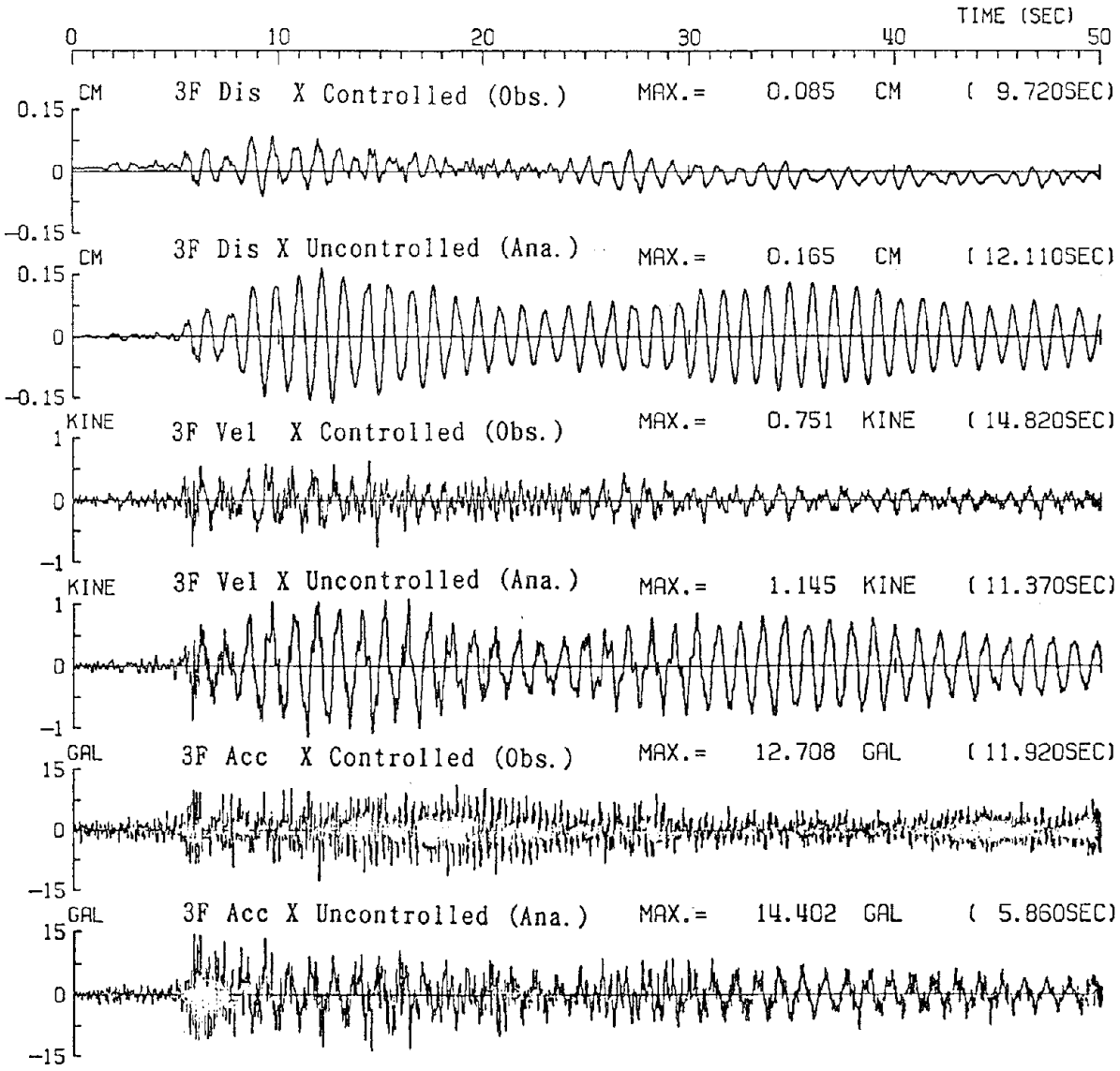

4) Response of 3rd Floor in Y-Direction

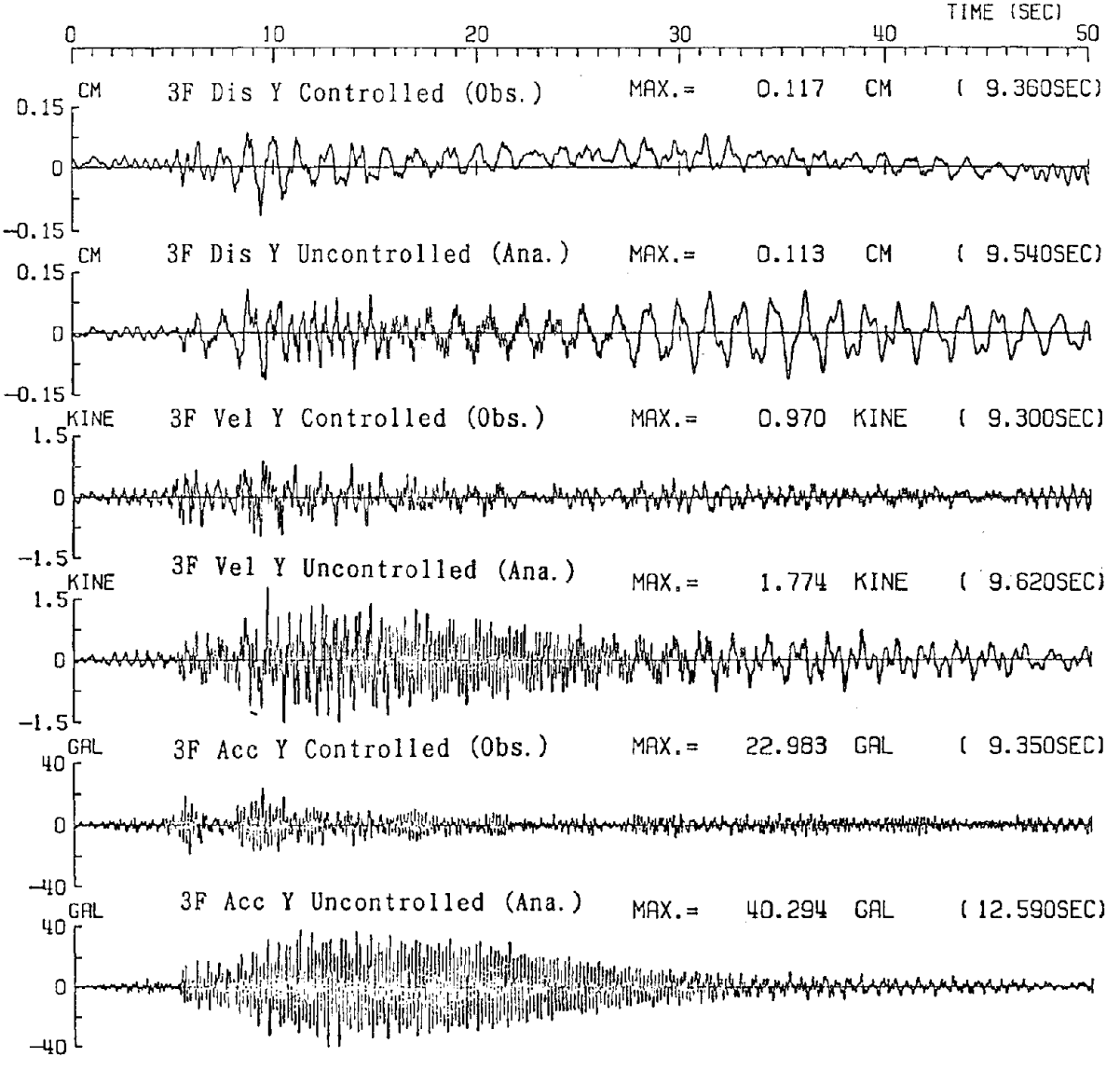

3. Earthquake on May 11, 1992:

1) Response of 6th Floor in X-Direction

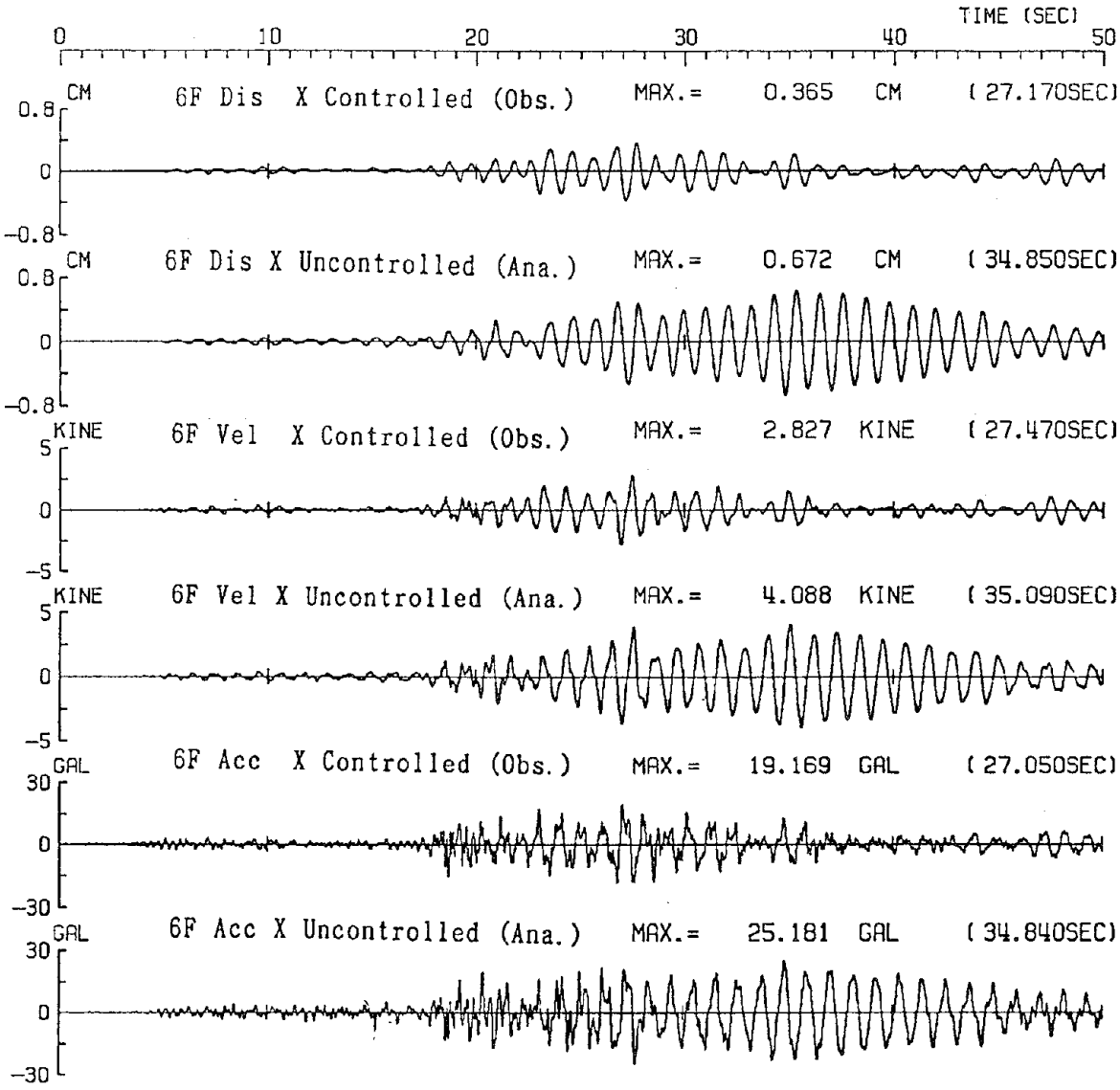

2) Response of 6th Floor in Y-Direction

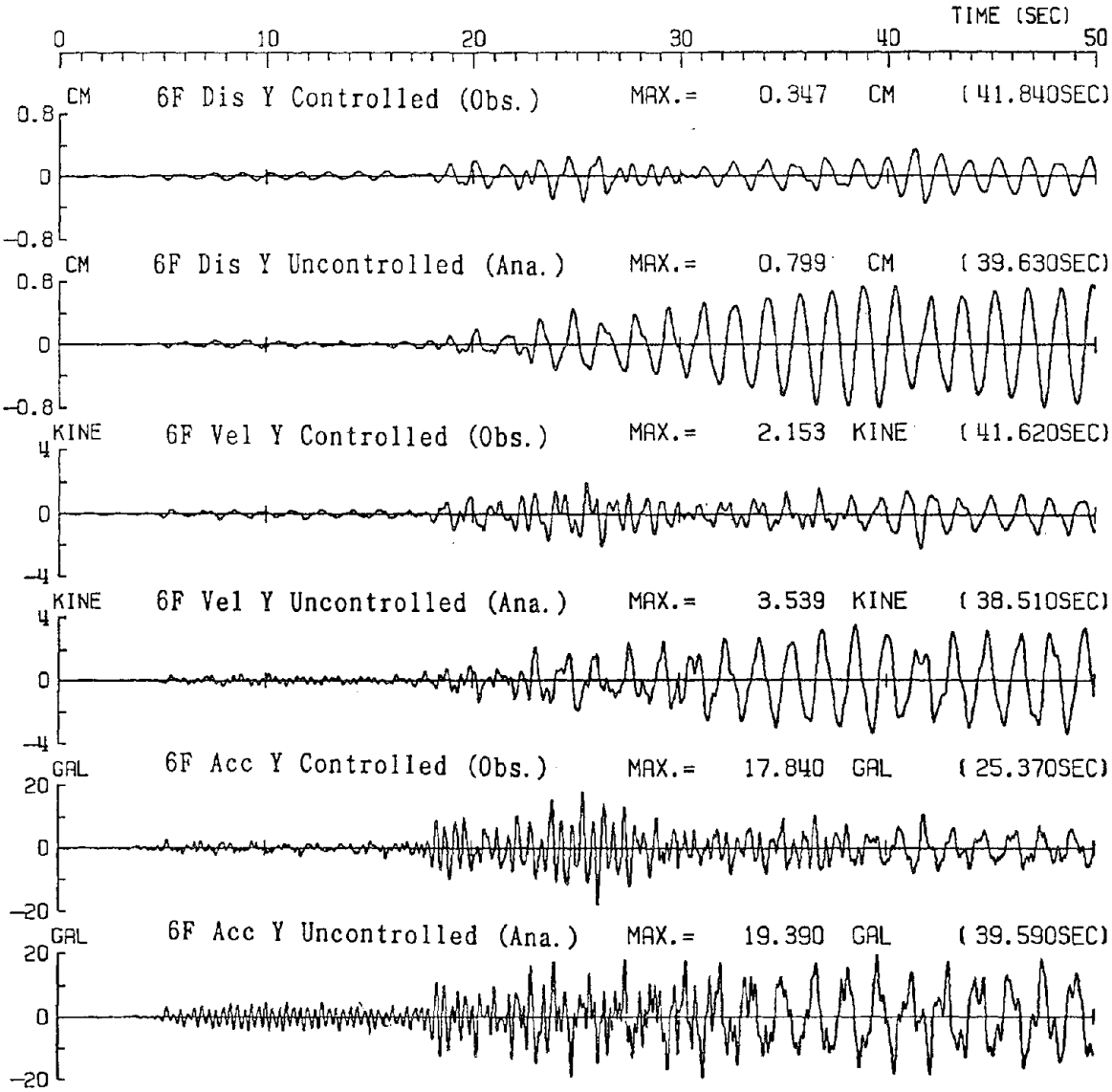

3) Responses of 3rd Floor in X-Direction

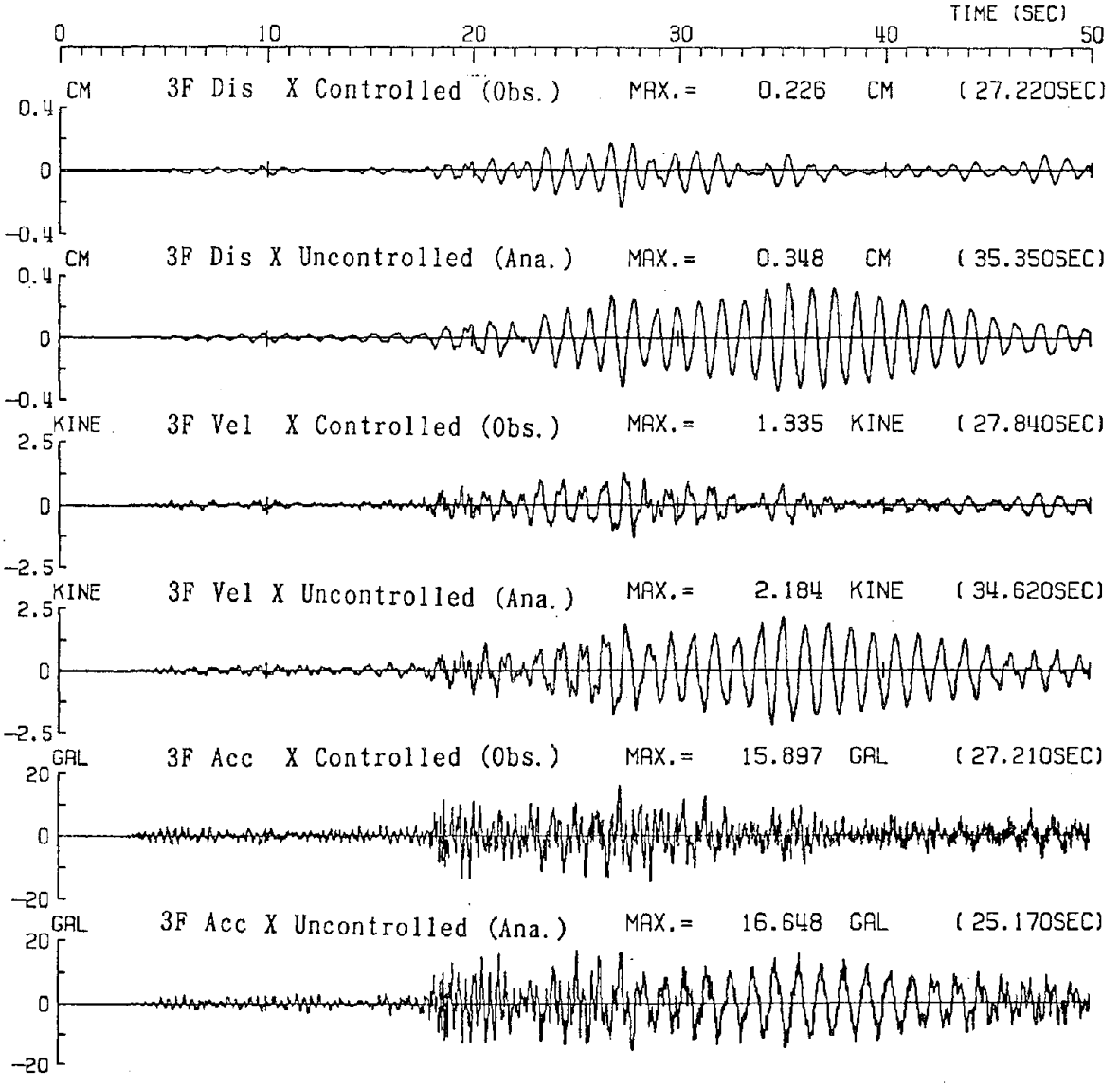

4) Response of 3rd Floor in Y-Direction

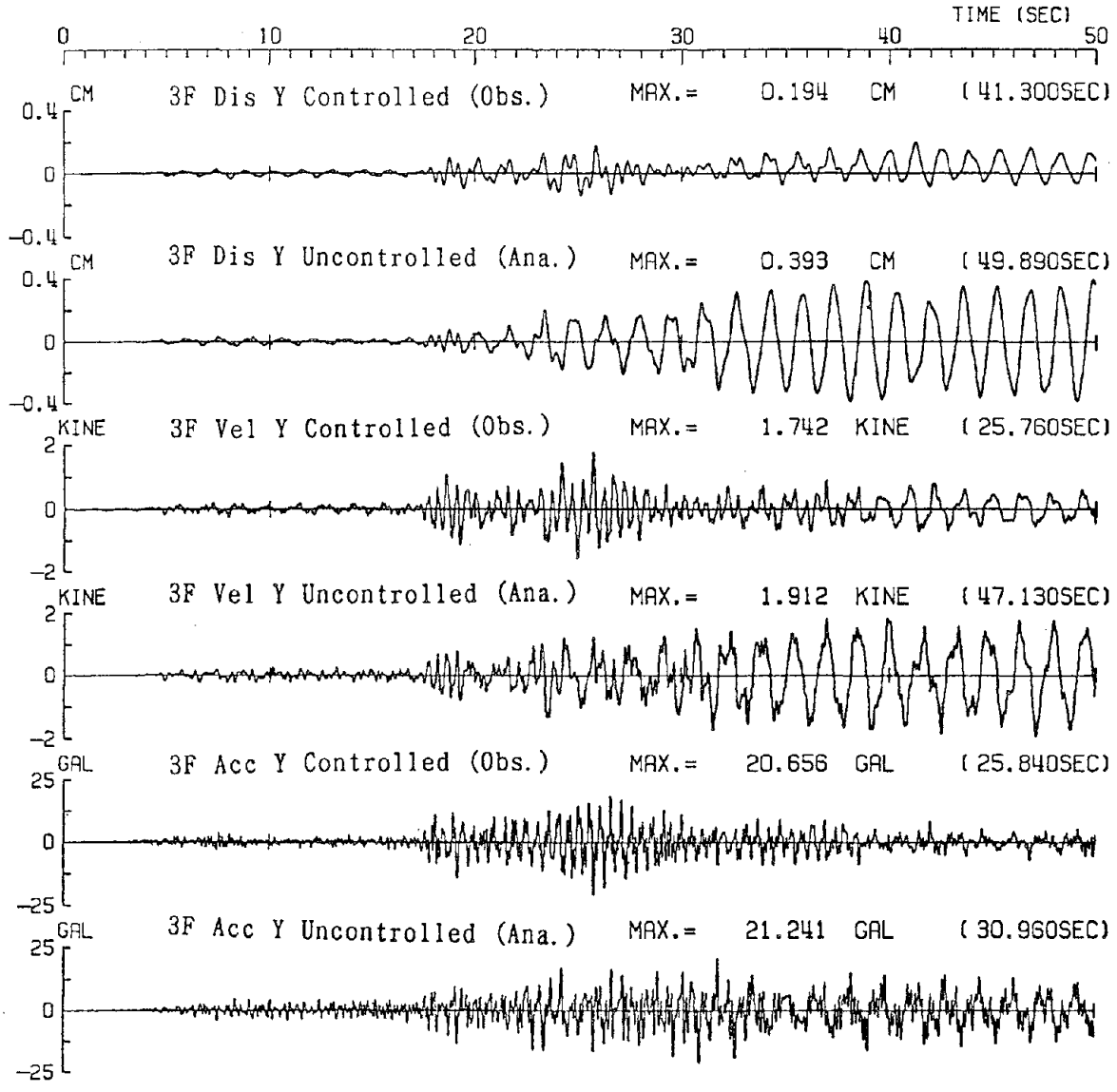

NATIONAL CENTER FOR EARTHQUAKE ENGINEERING RESEARCH
LIST OF TECHNICAL REPORTS

The National Center for Earthquake Engineering Research (NCEER) publishes technical reports on a variety of subjects related to earthquake engineering written by authors funded through NCEER. These reports are available from both NCEER's Publications Department and the National Technical Information Service (NTIS). Requests for reports should be directed to the Publications Department, National Center for Earthquake Engineering Research, State University of New York at Buffalo, Red Jacket Quadrangle, Buffalo, New York 14261. Reports can also be requested through NTIS, 5285 Port Royal Road, Springfield, Virginia 22161. NTIS accession numbers are shown in parenthesis, if available.

NCEER-87-0001 "First-Year Program in Research, Education and Technology Transfer," 3/5/87, (PB88-134275/AS).

NCEER-87-0002 "Experimental Evaluation of Instantaneous Optimal Algorithms for Structural Control," by R.C. Lin, T.T. Soong and A.M. Reinhorn, 4/20/87, (PB88-134341/AS).

NCEER-87-0003 "Experimentation Using the Earthquake Simulation Facilities at University at Buffalo," by A.M. Reinhorn and R.L. Ketter, to be published.

NCEER-87-0004 "The System Characteristics and Performance of a Shaking Table," by J.S. Hwang, K.C. Chang and G.C. Lee, 6/1/87, (PB88-134259/AS). This report is available only through NTIS (see address given above).

NCEER-87-0005 "A Finite Element Formulation for Nonlinear Viscoplastic Material Using a Q Model," by O. Gyebi and G. Dasgupta, 11/2/87, (PB88-213764/AS).

NCEER-87-0006 "Symbolic Manipulation Program (SMP) - Algebraic Codes for Two and Three Dimensional Finite Element Formulations," by X. Lee and G. Dasgupta, 11/9/87, (PB88-219522/AS).

NCEER-87-0007 "Instantaneous Optimal Control Laws for Tall Buildings Under Seismic Excitations," by J.N. Yang, A. Akbarpour and P. Ghaemmaghami, 6/10/87, (PB88-134333/AS).

NCEER-87-0008 "IDARC: Inelastic Damage Analysis of Reinforced Concrete Frame - Shear-Wall Structures," by Y.J. Park, A.M. Reinhorn and S.K. Kunnath, 7/20/87, (PB88-134325/AS).

NCEER-87-0009 "Liquefaction Potential for New York State: A Preliminary Report on Sites in Manhattan and Buffalo," by M. Budhu, V. Vijayakumar, R.F. Giese and L. Baumgras, 8/31/87, (PB88-163704/AS). This report is available only through NTIS (see address given above).

NCEER-87-0010 "Vertical and Torsional Vibration of Foundations in Inhomogeneous Media," by A.S. Veletsos and K.W. Dotson, 6/1/87, (PB88-134291/AS).

NCEER-87-0011 "Seismic Probabilistic Risk Assessment and Seismic Margins Studies for Nuclear Power Plants," by Howard H.M. Hwang, 6/15/87, (PB88-134267/AS).

NCEER-87-0012 "Parametric Studies of Frequency Response of Secondary Systems Under Ground-Acceleration Excitations," by Y. Yong and Y.K. Lin, 6/10/87, (PB88-134309/AS).

NCEER-87-0013 "Frequency Response of Secondary Systems Under Seismic Excitation," by J.A. HoLung, J. Cai and Y.K. Lin, 7/31/87, (PB88-134317/AS).

NCEER-87-0014 "Modelling Earthquake Ground Motions in Seismically Active Regions Using Parametric Time Series Methods," by G.W. Ellis and A.S. Cakmak, 8/25/87, (PB88-134283/AS).

NCEER-87-0015 "Detection and Assessment of Seismic Structural Damage," by E. DiPasquale and A.S. Cakmak, 8/25/87, (PB88-163712/AS).

NCEER-87-0016 "Pipeline Experiment at Parkfield, California," by J. Isenberg and E. Richardson, 9/15/87, (PB88-163720/AS). This report is available only through NTIS (see address given above).

NCEER-87-0017 "Digital Simulation of Seismic Ground Motion," by M. Shinozuka, G. Deodatis and T. Harada, 8/31/87, (PB88-155197/AS). This report is available only through NTIS (see address given above).

NCEER-87-0018 "Practical Considerations for Structural Control: System Uncertainty, System Time Delay and Truncation of Small Control Forces," J.N. Yang and A. Akbarpour, 8/10/87, (PB88-163738/AS).

NCEER-87-0019 "Modal Analysis of Nonclassically Damped Structural Systems Using Canonical Transformation," by J.N. Yang, S. Sarkani and F.X. Long, 9/27/87, (PB88-187851/AS).

NCEER-87-0020 "A Nonstationary Solution in Random Vibration Theory," by J.R. Red-Horse and P.D. Spanos, 11/3/87, (PB88-163746/AS).

NCEER-87-0021 "Horizontal Impedances for Radially Inhomogeneous Viscoelastic Soil Layers," by A.S. Veletsos and K.W. Dotson, 10/15/87, (PB88-150859/AS).

NCEER-87-0022 "Seismic Damage Assessment of Reinforced Concrete Members," by Y.S. Chung, C. Meyer and M. Shinozuka, 10/9/87, (PB88-150867/AS). This report is available only through NTIS (see address given above).

NCEER-87-0023 "Active Structural Control in Civil Engineering," by T.T. Soong, 11/11/87, (PB88-187778/AS).

NCEER-87-0024 "Vertical and Torsional Impedances for Radially Inhomogeneous Viscoelastic Soil Layers," by K.W. Dotson and A.S. Veletsos, 12/87, (PB88-187786/AS).

NCEER-87-0025 "Proceedings from the Symposium on Seismic Hazards, Ground Motions, Soil-Liquefaction and Engineering Practice in Eastern North America," October 20-22, 1987, edited by K.H. Jacob, 12/87, (PB88-188115/AS).

NCEER-87-0026 "Report on the Whittier-Narrows, California, Earthquake of October 1, 1987," by J. Pantelic and A. Reinhorn, 11/87, (PB88-187752/AS). This report is available only through NTIS (see address given above).

NCEER-87-0027 "Design of a Modular Program for Transient Nonlinear Analysis of Large 3-D Building Structures," by S. Srivastav and J.F. Abel, 12/30/87, (PB88-187950/AS).

NCEER-87-0028 "Second-Year Program in Research, Education and Technology Transfer," 3/8/88, (PB88-219480/AS).

NCEER-88-0001 "Workshop on Seismic Computer Analysis and Design of Buildings With Interactive Graphics," by W. McGuire, J.F. Abel and C.H. Conley, 1/18/88, (PB88-187760/AS).

NCEER-88-0002 "Optimal Control of Nonlinear Flexible Structures," by J.N. Yang, F.X. Long and D. Wong, 1/22/88, (PB88-213772/AS).

NCEER-88-0003 "Substructuring Techniques in the Time Domain for Primary-Secondary Structural Systems," by G.D. Manolis and G. Juhn, 2/10/88, (PB88-213780/AS).

NCEER-88-0004 "Iterative Seismic Analysis of Primary-Secondary Systems," by A. Singhal, L.D. Lutes and P.D. Spanos, 2/23/88, (PB88-213798/AS).

NCEER-88-0005 "Stochastic Finite Element Expansion for Random Media," by P.D. Spanos and R. Ghanem, 3/14/88, (PB88-213806/AS).

NCEER-88-0006 "Combining Structural Optimization and Structural Control," by F.Y. Cheng and C.P. Pantelides, 1/10/88, (PB88-213814/AS).

NCEER-88-0007 "Seismic Performance Assessment of Code-Designed Structures," by H.H-M. Hwang, J-W. Jaw and H-J. Shau, 3/20/88, (PB88-219423/AS).

NCEER-88-0008 "Reliability Analysis of Code-Designed Structures Under Natural Hazards," by H.H-M. Hwang, H. Ushiba and M. Shinozuka, 2/29/88, (PB88-229471/AS).

NCEER-88-0009 "Seismic Fragility Analysis of Shear Wall Structures," by J-W Jaw and H.H-M. Hwang, 4/30/88, (PB89-102867/AS).

NCEER-88-0010 "Base Isolation of a Multi-Story Building Under a Harmonic Ground Motion - A Comparison of Performances of Various Systems," by F-G Fan, G. Ahmadi and I.G. Tadjbakhsh, 5/18/88, (PB89-122238/AS).

NCEER-88-0011 "Seismic Floor Response Spectra for a Combined System by Green's Functions," by F.M. Lavelle, L.A. Bergman and P.D. Spanos, 5/1/88, (PB89-102875/AS).

NCEER-88-0012 "A New Solution Technique for Randomly Excited Hysteretic Structures," by G.Q. Cai and Y.K. Lin, 5/16/88, (PB89-102883/AS).

NCEER-88-0013 "A Study of Radiation Damping and Soil-Structure Interaction Effects in the Centrifuge," by K. Weissman, supervised by J.H. Prevost, 5/24/88, (PB89-144703/AS).

NCEER-88-0014 "Parameter Identification and Implementation of a Kinematic Plasticity Model for Frictional Soils," by J.H. Prevost and D.V. Griffiths, to be published.

NCEER-88-0015 "Two- and Three- Dimensional Dynamic Finite Element Analyses of the Long Valley Dam," by D.V. Griffiths and J.H. Prevost, 6/17/88, (PB89-144711/AS).

NCEER-88-0016 "Damage Assessment of Reinforced Concrete Structures in Eastern United States," by A.M. Reinhorn, M.J. Seidel, S.K. Kunnath and Y.J. Park, 6/15/88, (PB89-122220/AS).

NCEER-88-0017 "Dynamic Compliance of Vertically Loaded Strip Foundations in Multilayered Viscoelastic Soils," by S. Ahmad and A.S.M. Israil, 6/17/88, (PB89-102891/AS).

NCEER-88-0018 "An Experimental Study of Seismic Structural Response With Added Viscoelastic Dampers," by R.C. Lin, Z. Liang, T.T. Soong and R.H. Zhang, 6/30/88, (PB89-122212/AS). This report is available only through NTIS (see address given above).

NCEER-88-0019 "Experimental Investigation of Primary - Secondary System Interaction," by G.D. Manolis, G. Juhn and A.M. Reinhorn, 5/27/88, (PB89-122204/AS).

NCEER-88-0020 "A Response Spectrum Approach For Analysis of Nonclassically Damped Structures," by J.N. Yang, S. Sarkani and F.X. Long, 4/22/88, (PB89-102909/AS).

NCEER-88-0021 "Seismic Interaction of Structures and Soils: Stochastic Approach," by A.S. Veletsos and A.M. Prasad, 7/21/88, (PB89-122196/AS).

NCEER-88-0022 "Identification of the Serviceability Limit State and Detection of Seismic Structural Damage," by E. DiPasquale and A.S. Cakmak, 6/15/88, (PB89-122188/AS). This report is available only through NTIS (see address given above).

NCEER-88-0023 "Multi-Hazard Risk Analysis: Case of a Simple Offshore Structure," by B.K. Bhartia and E.H. Vanmarcke, 7/21/88, (PB89-145213/AS).

NCEER-88-0024 "Automated Seismic Design of Reinforced Concrete Buildings," by Y.S. Chung, C. Meyer and M. Shinozuka, 7/5/88, (PB89-122170/AS). This report is available only through NTIS (see address given above).

NCEER-88-0025 "Experimental Study of Active Control of MDOF Structures Under Seismic Excitations," by L.L. Chung, R.C. Lin, T.T. Soong and A.M. Reinhorn, 7/10/88, (PB89-122600/AS).

NCEER-88-0026 "Earthquake Simulation Tests of a Low-Rise Metal Structure," by J.S. Hwang, K.C. Chang, G.C. Lee and R.L. Ketter, 8/1/88, (PB89-102917/AS).

NCEER-88-0027 "Systems Study of Urban Response and Reconstruction Due to Catastrophic Earthquakes," by F. Kozin and H.K. Zhou, 9/22/88, (PB90-162348/AS).

NCEER-88-0028 "Seismic Fragility Analysis of Plane Frame Structures," by H.H-M. Hwang and Y.K. Low, 7/31/88, (PB89-131445/AS).

NCEER-88-0029 "Response Analysis of Stochastic Structures," by A. Kardara, C. Bucher and M. Shinozuka, 9/22/88, (PB89-174429/AS).

NCEER-88-0030 "Nonnormal Accelerations Due to Yielding in a Primary Structure," by D.C.K. Chen and L.D. Lutes, 9/19/88, (PB89-131437/AS).

NCEER-88-0031 "Design Approaches for Soil-Structure Interaction," by A.S. Veletsos, A.M. Prasad and Y. Tang, 12/30/88, (PB89-174437/AS). This report is available only through NTIS (see address given above).

NCEER-88-0032 "A Re-evaluation of Design Spectra for Seismic Damage Control," by C.J. Turkstra and A.G. Tallin, 11/7/88, (PB89-145221/AS).

NCEER-88-0033 "The Behavior and Design of Noncontact Lap Splices Subjected to Repeated Inelastic Tensile Loading," by V.E. Sagan, P. Gergely and R.N. White, 12/8/88, (PB89-163737/AS).

NCEER-88-0034 "Seismic Response of Pile Foundations," by S.M. Mamoon, P.K. Banerjee and S. Ahmad, 11/1/88, (PB89-145239/AS).

NCEER-88-0035 "Modeling of R/C Building Structures With Flexible Floor Diaphragms (IDARC2)," by A.M. Reinhorn, S.K. Kunnath and N. Panahshahi, 9/7/88, (PB89-207153/AS).

NCEER-88-0036 "Solution of the Dam-Reservoir Interaction Problem Using a Combination of FEM, BEM with Particular Integrals, Modal Analysis, and Substructuring," by C-S. Tsai, G.C. Lee and R.L. Ketter, 12/31/88, (PB89-207146/AS).

NCEER-88-0037 "Optimal Placement of Actuators for Structural Control," by F.Y. Cheng and C.P. Pantelides, 8/15/88, (PB89-162846/AS).

NCEER-88-0038 "Teflon Bearings in Aseismic Base Isolation: Experimental Studies and Mathematical Modeling," by A. Mokha, M.C. Constantinou and A.M. Reinhorn, 12/5/88, (PB89-218457/AS). This report is available only through NTIS (see address given above).

NCEER-88-0039 "Seismic Behavior of Flat Slab High-Rise Buildings in the New York City Area," by P. Weidlinger and M. Ettouney, 10/15/88, (PB90-145681/AS).

NCEER-88-0040 "Evaluation of the Earthquake Resistance of Existing Buildings in New York City," by P. Weidlinger and M. Ettouney, 10/15/88, to be published.

NCEER-88-0041 "Small-Scale Modeling Techniques for Reinforced Concrete Structures Subjected to Seismic Loads," by W. Kim, A. El-Attar and R.N. White, 11/22/88, (PB89-189625/AS).

NCEER-88-0042 "Modeling Strong Ground Motion from Multiple Event Earthquakes," by G.W. Ellis and A.S. Cakmak, 10/15/88, (PB89-174445/AS).

NCEER-88-0043 "Nonstationary Models of Seismic Ground Acceleration," by M. Grigoriu, S.E. Ruiz and E. Rosenblueth, 7/15/88, (PB89-189617/AS).

NCEER-88-0044 "SARCF User's Guide: Seismic Analysis of Reinforced Concrete Frames," by Y.S. Chung, C. Meyer and M. Shinozuka, 11/9/88, (PB89-174452/AS).

NCEER-88-0045 "First Expert Panel Meeting on Disaster Research and Planning," edited by J. Pantelic and J. Stoyle, 9/15/88, (PB89-174460/AS).

NCEER-88-0046 "Preliminary Studies of the Effect of Degrading Infill Walls on the Nonlinear Seismic Response of Steel Frames," by C.Z. Chrysostomou, P. Gergely and J.F. Abel, 12/19/88, (PB89-208383/AS).

NCEER-88-0047 "Reinforced Concrete Frame Component Testing Facility - Design, Construction, Instrumentation and Operation," by S.P. Pessiki, C. Conley, T. Bond, P. Gergely and R.N. White, 12/16/88, (PB89-174478/AS).

NCEER-89-0001 "Effects of Protective Cushion and Soil Compliancy on the Response of Equipment Within a Seismically Excited Building," by J.A. HoLung, 2/16/89, (PB89-207179/AS).

NCEER-89-0002 "Statistical Evaluation of Response Modification Factors for Reinforced Concrete Structures," by H.H-M. Hwang and J-W. Jaw, 2/17/89, (PB89-207187/AS).

NCEER-89-0003 "Hysteretic Columns Under Random Excitation," by G-Q. Cai and Y.K. Lin, 1/9/89, (PB89-196513/AS).

NCEER-89-0004 "Experimental Study of 'Elephant Foot Bulge' Instability of Thin-Walled Metal Tanks," by Z-H. Jia and R.L. Ketter, 2/22/89, (PB89-207195/AS).

NCEER-89-0005 "Experiment on Performance of Buried Pipelines Across San Andreas Fault," by J. Isenberg, E. Richardson and T.D. O'Rourke, 3/10/89, (PB89-218440/AS).

NCEER-89-0006 "A Knowledge-Based Approach to Structural Design of Earthquake-Resistant Buildings," by M. Subramani, P. Gergely, C.H. Conley, J.F. Abel and A.H. Zaghw, 1/15/89, (PB89-218465/AS).

NCEER-89-0007 "Liquefaction Hazards and Their Effects on Buried Pipelines," by T.D. O'Rourke and P.A. Lane, 2/1/89, (PB89-218481).

NCEER-89-0008 "Fundamentals of System Identification in Structural Dynamics," by H. Imai, C-B. Yun, O. Maruyama and M. Shinozuka, 1/26/89, (PB89-207211/AS).

NCEER-89-0009 "Effects of the 1985 Michoacan Earthquake on Water Systems and Other Buried Lifelines in Mexico," by A.G. Ayala and M.J. O'Rourke, 3/8/89, (PB89-207229/AS).

NCEER-89-R010 "NCEER Bibliography of Earthquake Education Materials," by K.E.K. Ross, Second Revision, 9/1/89, (PB90-125352/AS).

NCEER-89-0011 "Inelastic Three-Dimensional Response Analysis of Reinforced Concrete Building Structures (IDARC-3D), Part I - Modeling," by S.K. Kunnath and A.M. Reinhorn, 4/17/89, (PB90-114612/AS).

NCEER-89-0012 "Recommended Modifications to ATC-14," by C.D. Poland and J.O. Malley, 4/12/89, (PB90-108648/AS).

NCEER-89-0013 "Repair and Strengthening of Beam-to-Column Connections Subjected to Earthquake Loading," by M. Corazao and A.J. Durrani, 2/28/89, (PB90-109885/AS).

NCEER-89-0014 "Program EXKAL2 for Identification of Structural Dynamic Systems," by O. Maruyama, C-B. Yun, M. Hoshiya and M. Shinozuka, 5/19/89, (PB90-109877/AS).

NCEER-89-0015 "Response of Frames With Bolted Semi-Rigid Connections, Part I - Experimental Study and Analytical Predictions," by P.J. DiCorso, A.M. Reinhorn, J.R. Dickerson, J.B. Radziminski and W.L. Harper, 6/1/89, to be published.

NCEER-89-0016 "ARMA Monte Carlo Simulation in Probabilistic Structural Analysis," by P.D. Spanos and M.P. Mignolet, 7/10/89, (PB90-109893/AS).

NCEER-89-P017 "Preliminary Proceedings from the Conference on Disaster Preparedness - The Place of Earthquake Education in Our Schools," Edited by K.E.K. Ross, 6/23/89.

NCEER-89-0017 "Proceedings from the Conference on Disaster Preparedness - The Place of Earthquake Education in Our Schools," Edited by K.E.K. Ross, 12/31/89, (PB90-207895). This report is available only through NTIS (see address given above).

NCEER-89-0018 "Multidimensional Models of Hysteretic Material Behavior for Vibration Analysis of Shape Memory Energy Absorbing Devices, by E.J. Graesser and F.A. Cozzarelli, 6/7/89, (PB90-164146/AS).

NCEER-89-0019 "Nonlinear Dynamic Analysis of Three-Dimensional Base Isolated Structures (3D-BASIS)," by S. Nagarajaiah, A.M. Reinhorn and M.C. Constantinou, 8/3/89, (PB90-161936/AS). This report is available only through NTIS (see address given above).

NCEER-89-0020 "Structural Control Considering Time-Rate of Control Forces and Control Rate Constraints," by F.Y. Cheng and C.P. Pantelides, 8/3/89, (PB90-120445/AS).

NCEER-89-0021 "Subsurface Conditions of Memphis and Shelby County," by K.W. Ng, T-S. Chang and H-H.M. Hwang, 7/26/89, (PB90-120437/AS).

NCEER-89-0022 "Seismic Wave Propagation Effects on Straight Jointed Buried Pipelines," by K. Elhmadi and M.J. O'Rourke, 8/24/89, (PB90-162322/AS).

NCEER-89-0023 "Workshop on Serviceability Analysis of Water Delivery Systems," edited by M. Grigoriu, 3/6/89, (PB90-127424/AS).

NCEER-89-0024 "Shaking Table Study of a 1/5 Scale Steel Frame Composed of Tapered Members," by K.C. Chang, J.S. Hwang and G.C. Lee, 9/18/89, (PB90-160169/AS).

NCEER-89-0025 "DYNA1D: A Computer Program for Nonlinear Seismic Site Response Analysis - Technical Documentation," by Jean H. Prevost, 9/14/89, (PB90-161944/AS). This report is available only through NTIS (see address given above).

NCEER-89-0026 "1:4 Scale Model Studies of Active Tendon Systems and Active Mass Dampers for Aseismic Protection," by A.M. Reinhorn, T.T. Soong, R.C. Lin, Y.P. Yang, Y. Fukao, H. Abe and M. Nakai, 9/15/89, (PB90-173246/AS).

NCEER-89-0027 "Scattering of Waves by Inclusions in a Nonhomogeneous Elastic Half Space Solved by Boundary Element Methods," by P.K. Hadley, A. Askar and A.S. Cakmak, 6/15/89, (PB90-145699/AS).

NCEER-89-0028 "Statistical Evaluation of Deflection Amplification Factors for Reinforced Concrete Structures," by H.H.M. Hwang, J-W. Jaw and A.L. Ch'ng, 8/31/89, (PB90-164633/AS).

NCEER-89-0029 "Bedrock Accelerations in Memphis Area Due to Large New Madrid Earthquakes," by H.H.M. Hwang, C.H.S. Chen and G. Yu, 11/7/89, (PB90-162330/AS).

NCEER-89-0030 "Seismic Behavior and Response Sensitivity of Secondary Structural Systems," by Y.Q. Chen and T.T. Soong, 10/23/89, (PB90-164658/AS).

NCEER-89-0031 "Random Vibration and Reliability Analysis of Primary-Secondary Structural Systems," by Y. Ibrahim, M. Grigoriu and T.T. Soong, 11/10/89, (PB90-161951/AS).

NCEER-89-0032 "Proceedings from the Second U.S. - Japan Workshop on Liquefaction, Large Ground Deformation and Their Effects on Lifelines, September 26-29, 1989," Edited by T.D. O'Rourke and M. Hamada, 12/1/89, (PB90-209388/AS).

NCEER-89-0033 "Deterministic Model for Seismic Damage Evaluation of Reinforced Concrete Structures," by J.M. Bracci, A.M. Reinhorn, J.B. Mander and S.K. Kunnath, 9/27/89.

NCEER-89-0034 "On the Relation Between Local and Global Damage Indices," by E. DiPasquale and A.S. Cakmak, 8/15/89, (PB90-173865).

NCEER-89-0035 "Cyclic Undrained Behavior of Nonplastic and Low Plasticity Silts," by A.J. Walker and H.E. Stewart, 7/26/89, (PB90-183518/AS).

NCEER-89-0036 "Liquefaction Potential of Surficial Deposits in the City of Buffalo, New York," by M. Budhu, R. Giese and L. Baumgrass, 1/17/89, (PB90-208455/AS).

NCEER-89-0037 "A Deterministic Assessment of Effects of Ground Motion Incoherence," by A.S. Veletsos and Y. Tang, 7/15/89, (PB90-164294/AS).

NCEER-89-0038 "Workshop on Ground Motion Parameters for Seismic Hazard Mapping," July 17-18, 1989, edited by R.V. Whitman, 12/1/89, (PB90-173923/AS).

NCEER-89-0039 "Seismic Effects on Elevated Transit Lines of the New York City Transit Authority," by C.J. Costantino, C.A. Miller and E. Heymsfield, 12/26/89, (PB90-207887/AS).

NCEER-89-0040 "Centrifugal Modeling of Dynamic Soil-Structure Interaction," by K. Weissman, Supervised by J.H. Prevost, 5/10/89, (PB90-207879/AS).

NCEER-89-0041 "Linearized Identification of Buildings With Cores for Seismic Vulnerability Assessment," by I-K. Ho and A.E. Aktan, 11/1/89, (PB90-251943/AS).

NCEER-90-0001 "Geotechnical and Lifeline Aspects of the October 17, 1989 Loma Prieta Earthquake in San Francisco," by T.D. O'Rourke, H.E. Stewart, F.T. Blackburn and T.S. Dickerman, 1/90, (PB90-208596/AS).

NCEER-90-0002 "Nonnormal Secondary Response Due to Yielding in a Primary Structure," by D.C.K. Chen and L.D. Lutes, 2/28/90, (PB90-251976/AS).

NCEER-90-0003 "Earthquake Education Materials for Grades K-12," by K.E.K. Ross, 4/16/90, (PB91-113415/AS).

NCEER-90-0004 "Catalog of Strong Motion Stations in Eastern North America," by R.W. Busby, 4/3/90, (PB90-251984)/AS.

NCEER-90-0005 "NCEER Strong-Motion Data Base: A User Manual for the GeoBase Release (Version 1.0 for the Sun3)," by P. Friberg and K. Jacob, 3/31/90 (PB90-258062/AS).

NCEER-90-0006 "Seismic Hazard Along a Crude Oil Pipeline in the Event of an 1811-1812 Type New Madrid Earthquake," by H.H.M. Hwang and C-H.S. Chen, 4/16/90(PB90-258054).

NCEER-90-0007 "Site-Specific Response Spectra for Memphis Sheahan Pumping Station," by H.H.M. Hwang and C.S. Lee, 5/15/90, (PB91-108811/AS).

NCEER-90-0008 "Pilot Study on Seismic Vulnerability of Crude Oil Transmission Systems," by T. Ariman, R. Dobry, M. Grigoriu, F. Kozin, M. O'Rourke, T. O'Rourke and M. Shinozuka, 5/25/90, (PB91-108837/AS).

NCEER-90-0009 "A Program to Generate Site Dependent Time Histories: EQGEN," by G.W. Ellis, M. Srinivasan and A.S. Cakmak, 1/30/90, (PB91-108829/AS).

NCEER-90-0010 "Active Isolation for Seismic Protection of Operating Rooms," by M.E. Talbott, Supervised by M. Shinozuka, 6/8/9, (PB91-110205/AS).

NCEER-90-0011 "Program LINEARID for Identification of Linear Structural Dynamic Systems," by C-B. Yun and M. Shinozuka, 6/25/90, (PB91-110312/AS).

NCEER-90-0012 "Two-Dimensional Two-Phase Elasto-Plastic Seismic Response of Earth Dams," by A.N. Yiagos, Supervised by J.H. Prevost, 6/20/90, (PB91-110197/AS).

NCEER-90-0013 "Secondary Systems in Base-Isolated Structures: Experimental Investigation, Stochastic Response and Stochastic Sensitivity," by G.D. Manolis, G. Juhn, M.C. Constantinou and A.M. Reinhorn, 7/1/90, (PB91-110320/AS).

NCEER-90-0014 "Seismic Behavior of Lightly-Reinforced Concrete Column and Beam-Column Joint Details," by S.P. Pessiki, C.H. Conley, P. Gergely and R.N. White, 8/22/90, (PB91-108795/AS).

NCEER-90-0015 "Two Hybrid Control Systems for Building Structures Under Strong Earthquakes," by J.N. Yang and A. Danielians, 6/29/90, (PB91-125393/AS).

NCEER-90-0016 "Instantaneous Optimal Control with Acceleration and Velocity Feedback," by J.N. Yang and Z. Li, 6/29/90, (PB91-125401/AS).

NCEER-90-0017 "Reconnaissance Report on the Northern Iran Earthquake of June 21, 1990," by M. Mehrain, 10/4/90, (PB91-125377/AS).

NCEER-90-0018 "Evaluation of Liquefaction Potential in Memphis and Shelby County," by T.S. Chang, P.S. Tang, C.S. Lee and H. Hwang, 8/10/90, (PB91-125427/AS).

NCEER-90-0019 "Experimental and Analytical Study of a Combined Sliding Disc Bearing and Helical Steel Spring Isolation System," by M.C. Constantinou, A.S. Mokha and A.M. Reinhorn, 10/4/90, (PB91-125385/AS).

NCEER-90-0020 "Experimental Study and Analytical Prediction of Earthquake Response of a Sliding Isolation System with a Spherical Surface," by A.S. Mokha, M.C. Constantinou and A.M. Reinhorn, 10/11/90, (PB91-125419/AS).

NCEER-90-0021 "Dynamic Interaction Factors for Floating Pile Groups," by G. Gazetas, K. Fan, A. Kaynia and E. Kausel, 9/10/90, (PB91-170381/AS).

NCEER-90-0022 "Evaluation of Seismic Damage Indices for Reinforced Concrete Structures," by S. Rodriguez-Gomez and A.S. Cakmak, 9/30/90, PB91-171322/AS).

NCEER-90-0023 "Study of Site Response at a Selected Memphis Site," by H. Desai, S. Ahmad, E.S. Gazetas and M.R. Oh, 10/11/90, (PB91-196857/AS).

NCEER-90-0024 "A User's Guide to Strongmo: Version 1.0 of NCEER's Strong-Motion Data Access Tool for PCs and Terminals," by P.A. Friberg and C.A.T. Susch, 11/15/90, (PB91-171272/AS).

NCEER-90-0025 "A Three-Dimensional Analytical Study of Spatial Variability of Seismic Ground Motions," by L-L. Hong and A.H.-S. Ang, 10/30/90, (PB91-170399/AS).

NCEER-90-0026 "MUMOID User's Guide - A Program for the Identification of Modal Parameters," by S. Rodriguez-Gomez and E. DiPasquale, 9/30/90, (PB91-171298/AS).

NCEER-90-0027 "SARCF-II User's Guide - Seismic Analysis of Reinforced Concrete Frames," by S. Rodriguez-Gomez, Y.S. Chung and C. Meyer, 9/30/90, (PB91-171280/AS).

NCEER-90-0028 "Viscous Dampers: Testing, Modeling and Application in Vibration and Seismic Isolation," by N. Makris and M.C. Constantinou, 12/20/90 (PB91-190561/AS).

NCEER-90-0029 "Soil Effects on Earthquake Ground Motions in the Memphis Area," by H. Hwang, C.S. Lee, K.W. Ng and T.S. Chang, 8/2/90, (PB91-190751/AS).

NCEER-91-0001 "Proceedings from the Third Japan-U.S. Workshop on Earthquake Resistant Design of Lifeline Facilities and Countermeasures for Soil Liquefaction, December 17-19, 1990," edited by T.D. O'Rourke and M. Hamada, 2/1/91, (PB91-179259/AS).

NCEER-91-0002 "Physical Space Solutions of Non-Proportionally Damped Systems," by M. Tong, Z. Liang and G.C. Lee, 1/15/91, (PB91-179242/AS).

NCEER-91-0003 "Seismic Response of Single Piles and Pile Groups," by K. Fan and G. Gazetas, 1/10/91, (PB92-174994/AS).

NCEER-91-0004 "Damping of Structures: Part 1 - Theory of Complex Damping," by Z. Liang and G. Lee, 10/10/91, (PB92-197235/AS).

NCEER-91-0005 "3D-BASIS - Nonlinear Dynamic Analysis of Three Dimensional Base Isolated Structures: Part II," by S. Nagarajaiah, A.M. Reinhorn and M.C. Constantinou, 2/28/91, (PB91-190553/AS).

NCEER-91-0006 "A Multidimensional Hysteretic Model for Plasticity Deforming Metals in Energy Absorbing Devices," by E.J. Graesser and F.A. Cozzarelli, 4/9/91.

NCEER-91-0007 "A Framework for Customizable Knowledge-Based Expert Systems with an Application to a KBES for Evaluating the Seismic Resistance of Existing Buildings," by E.G. Ibarra-Anaya and S.J. Fenves, 4/9/91, (PB91-210930/AS).

NCEER-91-0008 "Nonlinear Analysis of Steel Frames with Semi-Rigid Connections Using the Capacity Spectrum Method," by G.G. Deierlein, S-H. Hsieh, Y-J. Shen and J.F. Abel, 7/2/91, (PB92-113828/AS).

NCEER-91-0009 "Earthquake Education Materials for Grades K-12," by K.E.K. Ross, 4/30/91, (PB91-212142/AS).

NCEER-91-0010 "Phase Wave Velocities and Displacement Phase Differences in a Harmonically Oscillating Pile," by N. Makris and G. Gazetas, 7/8/91, (PB92-108356/AS).

NCEER-91-0011 "Dynamic Characteristics of a Full-Size Five-Story Steel Structure and a 2/5 Scale Model," by K.C. Chang, G.C. Yao, G.C. Lee, D.S. Hao and Y.C. Yeh," 7/2/91.

NCEER-91-0012 "Seismic Response of a 2/5 Scale Steel Structure with Added Viscoelastic Dampers," by K.C. Chang, T.T. Soong, S-T. Oh and M.L. Lai, 5/17/91 (PB92-110816/AS).

NCEER-91-0013 "Earthquake Response of Retaining Walls; Full-Scale Testing and Computational Modeling," by S. Alampalli and A-W.M. Elgamal, 6/20/91, to be published.

NCEER-91-0014 "3D-BASIS-M: Nonlinear Dynamic Analysis of Multiple Building Base Isolated Structures," by P.C. Tsopelas, S. Nagarajaiah, M.C. Constantinou and A.M. Reinhorn, 5/28/91, (PB92-113885/AS).

NCEER-91-0015 "Evaluation of SEAOC Design Requirements for Sliding Isolated Structures," by D. Theodossiou and M.C. Constantinou, 6/10/91, (PB92-114602/AS).

NCEER-91-0016 "Closed-Loop Modal Testing of a 27-Story Reinforced Concrete Flat Plate-Core Building," by H.R. Somaprasad, T. Toksoy, H. Yoshiyuki and A.E. Aktan, 7/15/91, (PB92-129980/AS).

NCEER-91-0017 "Shake Table Test of a 1/6 Scale Two-Story Lightly Reinforced Concrete Building," by A.G. El-Attar, R.N. White and P. Gergely, 2/28/91.

NCEER-91-0018 "Shake Table Test of a 1/8 Scale Three-Story Lightly Reinforced Concrete Building," by A.G. El-Attar, R.N. White and P. Gergely, 2/28/91.

NCEER-91-0019 "Transfer Functions for Rigid Rectangular Foundations," by A.S. Veletsos, A.M. Prasad and W.H. Wu, 7/31/91, to be published.

NCEER-91-0020 "Hybrid Control of Seismic-Excited Nonlinear and Inelastic Structural Systems," by J.N. Yang, Z. Li and A. Danielians, 8/1/91.

NCEER-91-0021 "The NCEER-91 Earthquake Catalog: Improved Intensity-Based Magnitudes and Recurrence Relations for U.S. Earthquakes East of New Madrid," by L. Seeber and J.G. Armbruster, 8/28/91, (PB92-176742/AS).

NCEER-91-0022 "Proceedings from the Implementation of Earthquake Planning and Education in Schools: The Need for Change - The Roles of the Changemakers," by K.E.K. Ross and F. Winslow, 7/23/91, (PB92-129998/AS).

NCEER-91-0023 "A Study of Reliability-Based Criteria for Seismic Design of Reinforced Concrete Frame Buildings," by H.H.M. Hwang and H-M. Hsu, 8/10/91.

NCEER-91-0024 "Experimental Verification of a Number of Structural System Identification Algorithms," by R.G. Ghanem, H. Gavin and M. Shinozuka, 9/18/91, (PB92-176577/AS).

NCEER-91-0025 "Probabilistic Evaluation of Liquefaction Potential," by H.H.M. Hwang and C.S. Lee," 11/25/91.

NCEER-91-0026 "Instantaneous Optimal Control for Linear, Nonlinear and Hysteretic Structures - Stable Controllers," by J.N. Yang and Z. Li, 11/15/91, (PB92-163807/AS).

NCEER-91-0027 "Experimental and Theoretical Study of a Sliding Isolation System for Bridges," by M.C. Constantinou, A. Kartoum, A.M. Reinhorn and P. Bradford, 11/15/91, (PB92-176973/AS).

NCEER-92-0001 "Case Studies of Liquefaction and Lifeline Performance During Past Earthquakes, Volume 1: Japanese Case Studies," Edited by M. Hamada and T. O'Rourke, 2/17/92, (PB92-197243/AS).

NCEER-92-0002 "Case Studies of Liquefaction and Lifeline Performance During Past Earthquakes, Volume 2: United States Case Studies," Edited by T. O'Rourke and M. Hamada, 2/17/92, (PB92-197250/AS).

NCEER-92-0003 "Issues in Earthquake Education," Edited by K. Ross, 2/3/92.

NCEER-92-0004 "Proceedings from the First U.S. - Japan Workshop on Earthquake Protective Systems for Bridges," 2/4/92, to be published.

NCEER-92-0005 "Seismic Ground Motion from a Haskell-Type Source in a Multiple-Layered Half-Space," A.P. Theoharis, G. Deodatis and M. Shinozuka, 1/2/92, to be published.

NCEER-92-0006 "Proceedings from the Site Effects Workshop," Edited by R. Whitman, 2/29/92, (PB92-197201/AS).

NCEER-92-0007 "Engineering Evaluation of Permanent Ground Deformations Due to Seismically-Induced Liquefaction," by M.H. Baziar, R. Dobry and A-W.M. Elgamal, 3/24/92.

NCEER-92-0008 "A Procedure for the Seismic Evaluation of Buildings in the Central and Eastern United States," by C.D. Poland and J.O. Malley, 4/2/92.

NCEER-92-0009 "Experimental and Analytical Study of a Hybrid Isolation System Using Friction Controllable Sliding Bearings," by Q. Feng, S. Fujii and M. Shinozuka, 2/15/92, to be published.

NCEER-92-0010 "Seismic Resistance of Slab-Column Connections in Existing Non-Ductile Flat-Plate Buildings," by A.J. Durrani and Y. Du, 5/18/92.

NCEER-92-0011 "The Hysteretic and Dynamic Behavior of Brick Masonry Walls Upgraded by Ferrocement Coatings Under Cyclic Loading and Strong Simulated Ground Motion," by H. Lee and S.P. Prawel, 5/11/92, to be published.

NCEER-92-0012 "Study of Wire Rope Systems for Seismic Protection of Equipment in Buildings," by G.F. Demetriades, M.C. Constantinou and A.M. Reinhorn, 5/20/92.

NCEER-92-0013 "Shape Memory Structural Dampers: Material Properties, Design and Seismic Testing," by P.R. Witting and F.A. Cozzarelli, 5/26/92.

NCEER-92-0014 "Longitudinal Permanent Ground Deformation Effects on Buried Continuous Pipelines," by M.J. O'Rourke, and C. Nordberg, 6/15/92.

NCEER-92-0015 "A Simulation Method for Stationary Gaussian Random Functions Based on the Sampling Theorem," by M. Grigoriu and S. Balopoulou, 6/11/92.

NCEER-92-0016 "Gravity-Load-Designed Reinforced Concrete Buildings," by G.W. Hoffmann, S.K. Kunnath, J.B. Mander and A.M. Reinhorn, 7/15/92, to be published.

NCEER-92-0017 "Observations on Water System and Pipeline Performance in the Limón Area of Costa Rica Due to the April 22, 1991 Earthquake," by M. O'Rourke and D. Ballantyne, 6/30/92.

NCEER-92-0018 "Fourth Edition of Earthquake Education Materials for Grades K-12," Edited by K.E.K. Ross, 8/10/92.

NCEER-92-0019 "Proceedings from the Fourth Japan-U.S. Workshop on Earthquake Resistant Design of Lifeline Facilities and Countermeasures for Soil Liquefaction," Edited by M. Hamada and T.D. O'Rourke, 8/12/92.

NCEER-92-0020 "Active Bracing System: A Full Scale Implementation of Active Control," by A.M. Reinhorn, T.T. Soong, R.C. Lin, M.A. Riley, Y.P. Wang, S. Aizawa and M. Higashino, 8/14/92.